June, 2010

Vol.9, No.2

Journal of Pipeline Engineering

incorporating

The Journal of Pipeline Integrity

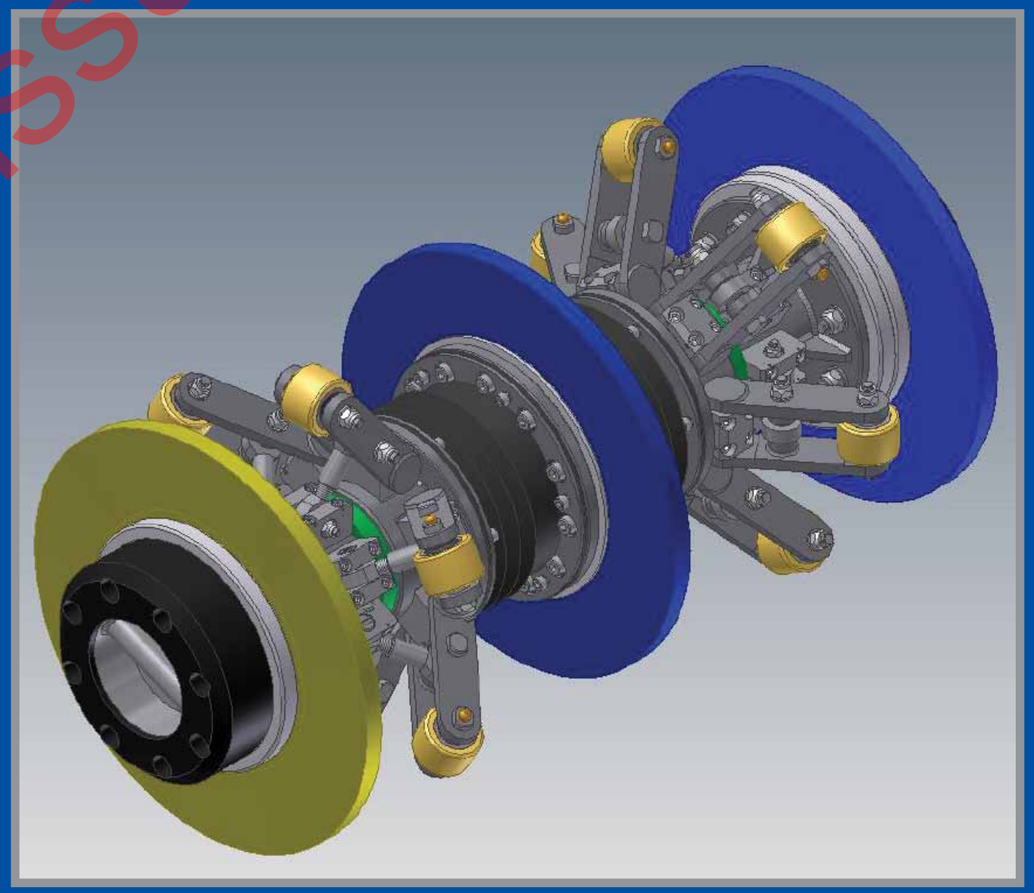

Great Southern Press

Clarion Technical Publishers

The Journal of Pipeline Engineering

incorporating

The Journal of Pipeline Integrity

Volume 9, No 2 • Second Quarter, 2010

Contents

❖ ❖ ❖

OUR COVER PHOTO shows one of the designs considered for the multi-diameter bi-directional pigging operation on the Alve pipeline in Norway. The project to design a pig suitable for this 10-12 in diameter pipeline is described on pages 117-128.

THE Journal of Pipeline Engineering (incorporating the Journal of Pipeline Integrity) is an independent, international, quarterly journal, devoted to the subject of promoting the science of pipeline engineering – and maintaining and improving pipeline integrity – for oil, gas, and products pipelines. The editorial content is original papers on all aspects of the subject. Papers sent to the Journal should not be submitted elsewhere while under editorial consideration.

Authors wishing to submit papers should send them to the Editor, The Journal of Pipeline Engineering, PO Box 21, Beaconsfield, HP9 1NS, UK or to Clarion Technical Publishers, 3401 Louisiana, Suite 255, Houston, TX 77002, USA.

Instructions for authors are available on request: please contact the Editor at the address given below. All contributions will be reviewed for technical content and general presentation.

The Journal of Pipeline Engineering aims to publish papers of quality within six months of manuscript acceptance.

Notes

1. **Disclaimer**: While every effort is made to check the accuracy of the contributions published in The Journal of Pipeline Engineering, Great Southern Press Ltd and Clarion Technical Publishers do not accept responsibility for the views expressed which, although made in good faith, are those of the authors alone.

3. **Information for subscribers**: The Journal of Pipeline Engineering (incorporating the Journal of Pipeline Integrity) is published four times each year. The subscription price for 2010 is US$350 per year (inc. airmail postage). Members of the Professional Institute of Pipeline Engineers can subscribe for the special rate of US$175/year (inc. airmail postage). Subscribers receive free on-line access to all issues of the Journal during the period of their subscription.

4. **Back issues**: Single issues from current and past volumes are available for US$87.50 per copy.

5. **Publisher**: The Journal of Pipeline Engineering is published by Great Southern Press Ltd (UK and Australia) and Clarion Technical Publishers (USA):

Great Southern Press, PO Box 21, Beaconsfield HP9 1NS, UK
tel: +44 (0)1494 675139
fax: +44 (0)1494 670155
email: jtiratsoo@gs-press.com
web: www.j-pipe-eng.com
www.pipelinesinternational.com

Editor: John Tiratsoo
email: jtiratsoo@j-pipe-eng.com

Clarion Technical Publishers, 3401 Louisiana, Suite 255, Houston TX 77002, USA
tel: +1 713 521 5929
fax: +1 713 521 9255
web: www.clarion.org

Associate publisher: BJ Lowe
email: bjlowe@clarion.org

6. ISSN 1753 2116

❖ ❖ ❖

Editorial

European oil pipeline integrity: third-party up, corrosion down

THE latest report by the European oil pipelines management group of CONCAWE* – the European association for the environment, health, and safety in refining and distribution – shows that in 2007 there were nine spillage incidents on the network operated by the association's members, of which two were attributed to corrosion and seven to third-party interference.

The association has collected data on spillagesΩ from European cross-country oil pipelines since 1971, and has published annual reports over this period. CONCAWE gathers comprehensive information from the approximately-70 operating companies and joint-ventures that make up its membership, and publishes it in a statistical form that, albeit non-attributable and clearly anonymous, nevertheless provides an important insight into the industry and its increasing integrity over the decades. Outside the US, there are no such publicly-available data for either oil or gas transmission pipelines, and so the CONCAWE annual reports are of significant value in establishing trends and providing historical analyses on which to base future decisions. The association is acknowledged for its assistance with this introduction to the report and brief discussion of its findings.

The geographical region covered by the CONCAWE reports began as that defined by OECD Western Europe, which at the time included 19 member countries, although Turkey was never included in the report. For the first 16 years of the reports, only pipelines owned by oil industry companies were included, but from 1988 non-commercially-owned pipeline systems (essentially that owned and operated by NATO) were included in the annual survey. Following the reunification of Germany, pipelines in the former East Germany (DDR) were added to the database from 1991, followed by crude and product lines in the Czech Republic and Hungary in 2001, and similar pipelines in Slovakia in 2003.

The network covered by CONCAWE's membership includes around 150 pipeline systems, which, at the end of 2007 (the year covered by the current report) had a combined length of 34,721km, slightly less than the length of the network in 2006 (Fig.1). The difference is partly due to corrections to the reported data, as well as because a few companies did not report and were therefore not included in the statistics. The reported volume transported in 2007 was 762Mm^3 of crude oil and refined products, a figure that has been stable in recent years. The total 'traffic volume' in 2007 was estimated at 129 x 109m^{3}km.

The nine spillage incidents reported in 2007 correspond to 0.26 spillages per 1000km of pipeline, just under the five-year average and well below the long-term running average of 0.55 per 1000km, which has been steadily decreasing over the years from a high of 1.2 per 1000km in the mid 1970s. There were no reported fires, fatalities, or injuries connected with these spills, and the gross spillage volume was 988m^3, equivalent to 1.3 parts per million (ppm) of the total volume transported. This corresponds to 28m^3 per 1000km of pipeline compared to the long-term average of 56m^3. CONCAWE reports that 53% of the spilled volume was recovered or safely disposed of.

Most of the pipeline spillages were small, and just over 5% were responsible for half of the gross volume spilled. In the past, the pipelines carrying hot oils such as fuel oil have suffered very severely in Europe from external corrosion due to design and construction problems, and most have now either been shut down or switched to cold service; the great majority of pipelines now carry unheated petroleum products and crude oil, and only 270km of hot pipelines were still in service during 2007. There have been no reported spills from hot pipelines in the last five years of this survey.

* Performance of European cross-country oil pipelines: a statistical summary of reported spillages in 2007 and since 1971, prepared for the CONCAWE Oil Pipelines Management Group by its Special Task Force, OP/STF-1, November, 2009. See also www.concawe.org.

Of the 9 reported incidents in 2007 2 were related to corrosion and 7 were connected to third party activities, either accidental or malicious.

Over the long term, third-party activity has been regularly responsible for the majority of spillage incidents, although this cause has progressively reduced over the years. Mechanical failure is statistically the second greatest cause of spillages, although not relevant in 2007, and corrosion (both internal and external) has generally come third in the league table of spillage causes. Interestingly, after considerable progress in reducing the frequency of mechanical failures in the 1970s and 1980s, this frequency has been on an upward trend since the mid 1990s.

Most of the European network of pipeline systems operated by CONCAWE's members was constructed in the 1960s and 1970s and, in 1971 – at the time of the first report – around 70% of the network was 10 years old or less; by 2007, only 5% was 10 years old or less and 42% was over 40 years old. So far this does not appear to have led to any increase in spillages. The industry's concern to maintain this situation (or improve it) is testified to by the fact that, in 2007, 84 sections were inspected by at least one type of intelligent pig, representing total run length of around 9300km. However, most inspection programmes involved running more than one type of pig in the same section, so that the total actual length inspected was 5281km, 15% of the network. CONCAWE points out that, overall, there is no evidence to show that the ageing of the pipeline system poses any increase in the level of risk. The development and introduction of new inspection tools and techniques will allow these pipelines to continue reliable operation for the foreseeable future, although performance statistics such as these will be necessary to confirm the achievement.

Intelligent inspection

CONCAWE has been collecting data on intelligent pig inspection activities for the last 17 years, including a one-off exercise to collect back data from the time intelligent pigs were first used around 1977. Separate records have been kept for inspections by metal-loss pigs, crack-detection pigs, and geometry (or calliper) pigs. In 2007, as mentioned, the 84 sections that were inspected by at least one type of intelligent tool covered a 9300km, split as shown in Table 1.

As shown in Fig.2, the use of intelligent pigs for internal inspection grew steadily up to 1994, levelling off for a period during stabilisation of the industry, and resuming an upward trend in 2003, with an average annual pig run total of almost 8000km and an average actual length inspected of 4890km over the last five years.

Within the last ten years, a period considered as a reasonable cycle for this type of inspection, 443 out of a total of 699

metal loss pig	76 sections	4418km
crack-detection pig	18 sections	1195km
geometry pig	50 sections	3687km

Table 1. In 2007, 84 sections of pipeline were inspected by at least one type of intelligent tool, covering a total distance of 9300km.

active sections (63%) have been inspected at least once by at least one type of pig, representing 76% of the total length of the network. Of the balance of pipeline sections, there are certainly some – mainly the older ones – which were not designed to be pigged or, because of small sizes, small-radius bends, or lack of suitable pig launchers or receivers, cannot be intelligent pigged. The relatively-recent introduction of pigs to inspect 6-in diameter pipelines and smaller, and the increasing number if tools available to insect 'unpiggable' pipelines, means that these problems are diminishing in the network operated by CONCAWE's members. The length of un-inspected pipelines is therefore certainly less than the above figure, and will continue to decrease in future years.

As the association points out, intelligent pig inspections only find features (that may be flaws, corrosion, or other damage) in or on a pipe's internal or external walls. Over the past 37 years, 17 spills have been caused by mechanical damage of faulty welds that could, in principle, have also been detected by an intelligent pig; six of these occurred in the last decade.

There were also 100 spillages related to external corrosion, and 25 to internal corrosion, at least some of which could have been detected, the report says. Nearly two thirds of these spillages related to external corrosion in hot pipelines, most of which have now been retired. Over the last decade, these numbers have been reduced to 15 and 6 events related to external and internal corrosion, respectively.

It is also of interest to see how the spillages were reported, and the CONCAWE separates spillage reporting into seven categories (see Table 2) for three types of facility. The most common means of detection of pipeline spillages was by a third party (53%) who warned of spillages that, on average, were about 85% of the average size, while automatic leak-detection systems were involved in detecting only 10%. Although this may seem a rather small proportion, it has to be realized that third parties are often on the scene when a leak occurs, and leak-detection systems are relatively new additions. Within the last five years the proportion of spills discovered by leak-detection systems has increased to 28%.

When third parties have detected spillages, 18% of the total, the spills have tended on to be the smaller ones: presumably those that are below the warning capabilities of the instrumentation.

Continued on inside back cover

Don't drop the drop-weight tear test

by Dr Andrew Cosham[1*], David G Jones[2], Robert Eiber[3], and Dr Phil. Hopkins[4]

1 Atkins Boreas, Newcastle upon Tyne, UK
2 Newcastle upon Tyne, UK
3 Robert J Eiber Consultant, Inc., Columbus, OH, USA
4 Penspen Ltd, Newcastle upon Tyne, UK

FOR OVER 40 years, linepipe specifications have specified minimum requirements for the shear area in a drop-weight tear test (DWTT) to ensure the arrest of a long-running brittle fracture. The DWTT has been very successful in preventing long-running brittle fractures: however, most current pipeline engineers do not know the background to, nor the importance of, the test, or the shear area requirement. This can lead to problems, as this is an essential requirement, particularly for pipelines transporting gas or liquids with a high vapour pressure. The cognoscenti who developed the requirements are, of course, aware of all of the issues and the background. However, the cognoscenti are fewer in number than they were, and perhaps not as young as they used to be. Therefore, this paper summarizes the reasons for, and the background to, the DWTT requirements in the linepipe specifications, and considers some issues that have arisen in recent projects. It is concluded that we must not become complacent about the DWTT requirement and we must not allow this knowledge to be lost in time. Today, even 40 years after its introduction, the background to, the development of, the DWTT needs to be fully understood and recognized.

LINEPIPE STEEL MUST meet certain minimum mechanical property requirements, such as strength, ductility, and toughness. Linepipe specifications such as ANSI/API Spec 5L / ISO 3183 : 2007 (Modified), 44th Edition, 2009 [1] and ISO 3183 : 2007 [2] define these minimum requirements. Linepipe steel is defined in terms of its 'product specification level' (for example PSL 1 and PSL 2)1, its grade (for example X65), and its dimensions (such as diameter and wall thickness). The grade of the linepipe specifies the minimum yield and tensile strength in the transverse direction and the minimum elongation. The tensile test and concepts such as yield and tensile strength are well understood by the average pipeline engineer: less well understood are ductility and toughness.

Ductility is a measure of the amount of plastic deformation prior to failure. A ductile material will exhibit significant global plastic deformation prior to failure, while a brittle material will exhibit little or no global plastic deformation. Toughness is a measure of the resistance of a material to the presence of a flaw.

The toughness requirements for linepipe steel in the linepipe specifications are expressed in terms of the impact energy and shear area measured in a Charpy V-notch (CVN) test, and the shear area measured in a drop-weight tear test (DWTT).

Pipelines contain defects, and the defects in pipelines occasionally fail. The failure of a defect can result in either a leak or a rupture, and a rupture may result in a propagating fracture. Pipelines that transport gaseous fluids, two-phase fluids, dense-phase fluids, or liquid with a high vapour pressure[2], are susceptible to propagating fractures, which are described as either brittle or ductile (see Figs 5 and 6). The description relates to the appearance of the fracture surface.

Fracture propagation is a complex phenomenon and, to this day, it is not fully understood. This is the reason why, when new grades of linepipe steel are developed (such as X80 and X100), or when pipelines are to be used to transport new types of fluids (such as rich gas or carbon dioxide) or are

1 PSL 2 has additional mandatory requirements for chemical composition, notch toughness and strength properties, and additional non-destructive testing.
2 Liquid or dense phase carbon dioxide behaves as a liquid with a high vapour pressure.

This paper was presented at the Pipeline Technology Conference held in Ostend in October, 2009, and organized by the University of Gent.

*Author's contact details:
tel: +44 (0)191 230 6501
email: andrew.cosham@atkinsglobal.com

designed for higher pressures, full-scale fracture-propagation tests are usually undertaken. These tests are expensive, but necessary.

Nevertheless, the means of preventing propagating fractures is comparatively simple. Fracture propagation control is achieved by ensuring that the pipe will fracture in a ductile manner and that the toughness of the linepipe steel is sufficiently high to arrest a ductile fracture within an acceptable number of pipe lengths (say one to three).

The problem of brittle fracture propagation was highlighted by a number of in-service failures in the 1950s. It was understood in the 1960s and, to all intents and purposes, solved (economically) by the developments in steel making that occurred at the same time. Arguably, the need to solve the problem prompted these developments. The solution was the drop-weight tear test. Having solved one problem, the problem of ductile fracture propagation was then highlighted by in-service failures in the 1960s. The subject of this paper is the drop-weight tear test and its role in solving the problem of brittle fracture propagation. The paper explains what the DWTT is, where it came from, and why it was necessary then and is still necessary now. The Charpy V-notch test has a bit-part to play in this story.

Upper shelf and lower shelf, shear area

Notched-bar impact-testing methods were developed in the latter half of the Industrial Revolution to characterize the fracture behaviour of iron and steel. It was recognized that the fracture appearance of iron or steel changed from shear to cleavage (or fibrous to crystalline, in the terminology of the time) with reductions in temperature. Introducing a notch ('notch sensitivity') or loading at a high strain rate were shown also to cause a change in the appearance of a fracture. A simple laboratory test was required to characterize the fracture behaviour.

Notched-bar impact tests give a qualitative measure of toughness, expressed in terms of the energy absorbed (impact energy) and/or the percentage shear area. The tests are designed to increase the likelihood that the material will fail in a brittle manner. The specimens are notched and are loaded dynamically (an impact load). Notched-bar impact tests were, and are to this day, used as quality-control measures in the manufacture of iron and steel.

Fig. 1. A Drop Weight Tear Test specimen and a Charpy V-notch test specimen.

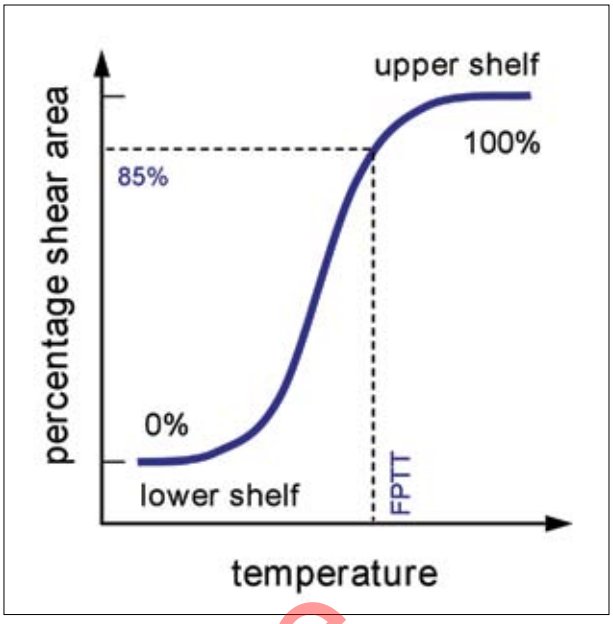

Fig. 2. A transition curve.

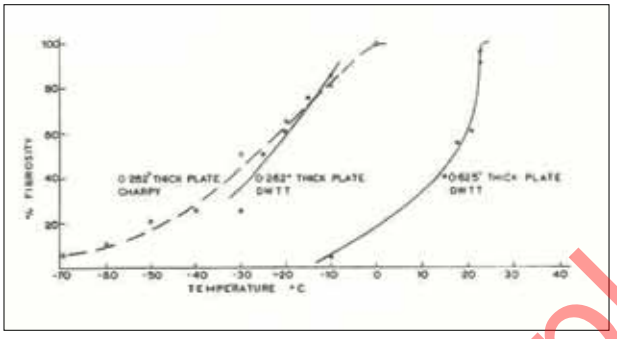

Fig. 3. The effect of thickness on the transition curve: a full-thickness Drop Weight Tear Test curve, a reduced thickness DWTT curve and a Charpy V-notch curve.

The Charpy V-notch test, the Izod test, and the pressed-notch drop-weight tear test, are examples of notched-bar impact tests. The Charpy V-notch (CVN) and pressed-notch drop-weight tear test (DWTT), Fig.1, are the two methods used in the pipeline industry.

A set of notched-bar impact tests conducted over a range of temperatures will define the transition curve for the material. A transition curve is a plot of the impact energy or the percentage shear area versus the test temperature, Fig.2. Transition curves determined from a series of DWTT and CVN tests of a linepipe steel are illustrated in Fig.3. At low temperatures, the fracture will be brittle; the impact energy will be low and the fracture surface will be 0% shear: this is the lower shelf. At high temperatures, the fracture will be ductile; the impact energy will be high and the fracture surface will be 100% shear, and this is the upper shelf. Between the lower and upper shelf is a transitional region through which the impact energy and the proportion of shear increases as the test temperature increases.

The ductile-to-brittle transition temperature (DBTT) is the temperature at which the appearance of the fracture changes from ductile (shear) to brittle (cleavage). The transition temperature will typically be defined with reference to a given percentage shear area; an example would the fracture-propagation transition temperature, which is defined with respect to an 85% shear area (as illustrated in Fig.2). The transition temperature (and the transition curve) increases with an increase in the loading rate, an increase in thickness (see Fig.3) or an increase in constraint, depending on the test specimen.

A qualitative measure of toughness is not necessarily representative of the behaviour of a structure. Impact tests may indicate that a material is ductile at a given temperature but, in the structure, the material may be brittle, if the loading rate is higher, or if the structure is thicker, or if the constraint is higher. The brittle-to-ductile transition temperature of the structure may be higher than that measured in the test specimen: nevertheless, in addition to their role as a quality-control measure, notched-bar impact tests can be calibrated to the behaviour of a structure, through full-scale and small-scale testing.

The Liberty ships (from World War 2) are the classic example of the use of the Charpy V-notch impact test to 'predict' the behaviour of a structure [3, 4]. The behaviour of the ship structure was correlated with the impact energy and the transition temperature of the steel.

Another example, still relevant in the 21st century, is propagating fractures in pipelines. This requires both the drop-weight tear test and the Charpy V-notch impact test.

The drop-weight tear test

The drop-weight tear test (DWTT), also referred to as the pressed-notch drop-weight tear test, was developed by the Battelle Memorial Institute in 1962 during the course of the (then) American Gas Association's NG-18 research programme. The DWTT is a modification of a drop-weight tear test developed by the US Naval Research Laboratory, the Pellini drop-weight test (developed by W.S. Pellini). The DWTT was subsequently standardized in API RP 5L3 [5].

The drop-weight tear test specimen is a rectangular bar with a length of 305mm (approx. 12 in), a width of 76mm (approxx. 3in) and a thickness equal to the thickness of the linepipe[3], see Fig.4. It is a full-thickness test specimen with a notch pressed into the centre of the longest side: the standards specify a 5-mm (approx. 0.200-in) deep notch and an indenter with a 45° included angle and a 0.025-mm (approx.0.001-in) radius of curvature. The root of the notch is severely cold worked during indentation, which is deliberate. A pressed notch is used to increase the likelihood of the initiation of a cleavage fracture at the root of the notch (and this is necessary for the test to be valid). A variant of the pressed-notch specimen, the chevron-notched drop-weight tear test, is used in high-toughness materials; it is difficult to initiate a brittle fracture at the base of a pressed notch in such materials. The chevron notch reduces the energy required to initiate a cleavage fracture.

The DWTT test specimen is a transverse test specimen, i.e. it has a T-L (or Y-X) orientation, and the notch is aligned with the axis of the pipe, as illustrated in Fig.1. In small-diameter linepipe a 'gull-wing' specimen is used in which the specimen is straightened either side of the notch in order to avoid the problems (due to work hardening) with the flattening of specimens extracted from linepipe with a small diameter.

The specimen is impacted in three-point bending in a drop tower (or a pendulum, but this is less common). The energy absorbed in fracturing the specimen cannot be determined in a drop tower unless the test is instrumented (and it is not normally instrumented). The percentage shear area is determined from the appearance of the fracture surface, neglecting a length equal to the thickness of the plate at each end. The material underneath the notch is cold worked when the notch is pressed and a fracture initiates at the root of the notch. The material at the back end of the specimen is cold worked by the impact of the hammer. Neither are representative of a fracture propagating through the linepipe steel.

[3] The specified distance between the two loading points on the side of the pressed-notch is 254 mm (10 in.).
[4] The West Jefferson tests were conducted at Battelle facilities located near West Jefferson, Ohio. The Athens tests were conducted in an abandoned strip mine located near Athens, Ohio.

Brittle and ductile propagation and arrest

In the 1950s, several long-running fractures occurred during the gas testing of a 24-in diameter pipeline in the USA [6]. These were the first recorded examples of extensive brittle fracture propagation in a pipeline.

In 1958, a 5.6-km (3.5-mile) long section of a 26-in diameter gas pipeline in Venezuela failed as a result of a brittle fracture during testing with gas, after having previously withstood the test pressure several times (this is also an example of a 'pressure reversal') [7]. A 180-m (600-ft) brittle fracture occurred in Europe [8, 9].

The most infamous example is the failure of a pipeline of the Transwestern Pipeline Co near Roswell, New Mexico, USA, in 1960. A brittle fracture in this 30-in diameter, X-56 pipeline propagated for approximately 8.1miles (13km) [6, 7]. The pipeline segment that failed was adjacent to a segment being pressure tested using gas. It failed at a pressure of 888psi (63% SMYS) as gas was being bled into this section from the section under test, and the fracture initiated from a 'rail-road' crack: it arrested at one end when it encountered a length of tougher pipe, and at the other when it encountered a heavier-wall-thickness tee.

Following the incidents of long-running brittle fractures, an extensive programme of experimental and theoretical work was sponsored by the then American Gas Association. The first experiment on fracture propagation in pipelines was conducted by the Battelle Memorial Institute in the 1960s [10-14] as part of the NG-18 research programme. Subsequently, a similar, smaller, programme was conducted by the-then British Gas Corporation [8, 15-17]. The experimental programmes consisted of three different types of test[4]:

1. complete gas-pressurized experiments on long test sections (150ft, excluding the anchored reservoirs at each end) – so-called Athens tests;

2. partial pneumatic-pressurized experiments on short test sections (15-20ft) – so-called West Jefferson tests;

3. laboratory-scale fracture tests (including Charpy V-notch and drop-weight tear tests).

The purpose of the test programme was to determine what small-scale laboratory test could be used to specify linepipe that was not susceptible to long-running brittle fractures.

The Athens and West Jefferson tests were used to investigate how the pipe fractured and the factors that influenced the characteristics of the fracture. The speed, fracture surface appearance, number of cracks, and fracture pattern were measured, and the tests were conducted over a range of temperatures to determine the full-scale fracture-propagation transition temperature.

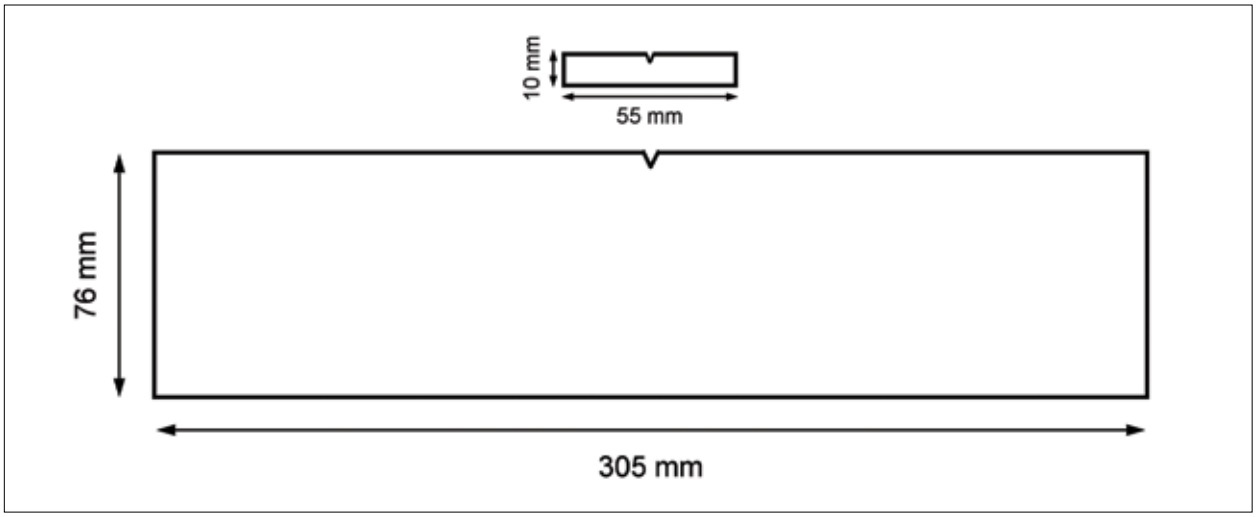

Fig.4. The geometry of a full wall thickness Drop Weight Tear Test specimen (and, to scale, a Charpy V-notch test specimen).

Table 1 – The range of the diameter, wall thickness and grade of the Athens and West Jefferson tests conducted at the Battelle Memorial Institute in the 1960s.

Diameter	168.3-1066.8 mm (6.625-42 in.)
Wall thickness	5.5-16.7 mm (0.218-0.656 in.)
Grade	API 5L X52, X60 & X65

The fracture speed and fracture appearance measured in the West Jefferson tests were found to be identical to those measured in the Athens tests [13]. However, the West Jefferson tests did not provide information on the extent of a fracture.

By 1969, Battelle had conducted 28 Athens tests and 137 West Jefferson tests, summarized in Table 1, giving a total of approximately 290 data points – a data point consisting of fracture speed and appearance data on a specific length of pipe at a given temperature [13]. Tests had been conducted at temperatures from -41 to 65°C (-41 to 149°F) and at nominal hoop stresses from 37 to 110% of the specified minimum yield strength.

Propagating fractures are described as either brittle or ductile. Propagating fractures observed in two Athens tests are shown in Figs 5 and 6: the former is a brittle fracture, and the latter a ductile fracture. Fractures between these two regimes are typically referred to as transitional fractures. The speed, appearance, and pattern of a propagating fracture, and the number of fractures, depends on the toughness of the linepipe steel. Figure 8 illustrates the relationship between the fracture appearance and the speed of the fracture.

Brittle fractures

A brittle fracture propagates at a very high speed, ranging from approximately 365m/sec (1,200ft/sec) to as high as 914m/sec (3,000ft/sec). Multiple fractures propagating simultaneous along the axis of the pipeline are common: the fractures typically propagate with a sinusoidal pattern (Fig.5) due to interaction between the fracture and the elastic stress waves. The fracture surfaces show cleavage fracture with any shear confined to narrow 'lips' on the internal and external surfaces of the pipe. There is no global plastic deformation associated with the propagating fracture.

Ductile fractures

A ductile fracture propagates at a lower speed, typically 400-800ft/sec, and a single fracture will propagate in a straight line along the axis of the pipeline. The fracture surfaces show shear fracture through the thickness, and local wall thinning. There is extensive global plastic deformation with the pipe ahead of the fracture ovalized and the pipe behind the fracture flattened (Fig.6).

IPC 2010

INTERNATIONAL PIPELINE CONFERENCE & EXPOSITION

September 27 – October 1, 2010 • Calgary, Alberta, Canada

Pipelines in a Changing World

Members of the international pipeline industry will gather at the International Pipeline Conference & Exposition 2010 to exchange leading edge information and experience the latest in products and services which will provide them with the tools to meet the challenges of pipelining in a changing world.

THE CONFERENCE

Sept. 27 – Oct. 1, 2010
The Hyatt Regency Hotel
Calgary, Alberta, Canada

- 14 Technical Tracks with over 300 quality papers
- Highly informative Tutorials
- International presenters and keynote speakers
- Panel Sessions
- Poster Sessions
- Student Paper Competition
- Networking opportunity luncheons & receptions

THE EXPOSITION

Sept. 28 – Sept. 30, 2010
Calgary TELUS Convention Centre
Calgary, Alberta, Canada

- Over 150 exhibiting companies
- Latest innovations in pipeline technology
- Over 3,000 visitors from 50 countries
- IPE Industry Reception
- Networking with the world's largest gathering of pipeline professionals
- Complimentary admission for Conference delegates

Visit our web sites for more detailed information
Conference: www.InternationalPipelineConference.com
Exposition: www.internationalpipelineexposition.com

Conference Patrons

ASME SETTING THE STANDARD · CEPA Canadian Energy Pipeline Association · CAPP Canadian Association of Petroleum Producers · Pipeline Systems · ERCB Energy Resources Conservation Board · National Energy Board / Office national de l'énergie · Alberta · Natural Resources Canada / Ressources naturelles Canada

Major Exposition Sponsor

BJ Pipeline Inspection Services

Media Sponsor

The Journal of Pipeline Engineering · PIPELINES INTERNATIONAL

Fig.5. A brittle fracture.

Fig.6. A ductile fracture.

The 85% shear area requirement

From the results of the full-scale tests conducted at Battelle, it was concluded that the factor that determined the speed and appearance of a fracture was the temperature of the steel relative to its fracture-propagation transition temperature (FPTT) [10]. The FPTT is the temperature at which the fracture-propagation mode changes from brittle to ductile (as illustrated in Fig.2).

Figure 7 shows that the transition curve for a full-scale test is abrupt. Fracture speeds undergo a transition from fast fracture (cleavage) to slow fracture (shear) over a temperature range of approximately 17°C (30°F). At temperatures below the transition temperature, multiple fractures travel as cleavage fractures at high speeds; at temperatures above it, a single fracture travels as a shear fracture at lower speeds. The fracture appearance in a full-scale test is related to the test temperature (Fig.7). The speed of a facture is related to the fracture appearance, as seen in Fig.8.

Two tests were found to correlate well with the results of the full-scale tests: the Charpy V-notch test and the pressed-notch drop-weight tear test. The fracture appearance in the CVN and DWTT tests could be related to the fracture appearance in the full-scale tests, as illustrated in Fig.7, indicating that these laboratory tests could be used to predict the behaviour in a full-scale test.

Figure 7 illustrates the general relationship observed between the percentage shear area measured in two-thirds' thickness Charpy V-notch, DWTT, and full-scale tests [11, 13]. The results are for a 30-in diameter, 0.375-in (9.52-mm) wall thickness, X52 semi-killed linepipe steel. The shape of the DWTT transition curve and the transition temperature are very similar to that of the full-scale test. The Charpy V-notch transition curve is more gradual and only agrees with that of full-scale test at shear areas above 80 to 85%.

The FPTT is typically taken as the temperature at which the shear area is 85%. The transition temperatures measured in DWTT and full-scale tests are then the same (see Fig.7) [13].

The 85% shear area measured in either a drop-weight tear test or a Charpy-V notch was found to correlate with the ductile-to-brittle fracture-propagation transition temperature in a full-scale test. The Charpy V-notch test specimen is a constant-thickness test specimen, and the specimen geometry is independent of the thickness of pipe; the DWTT is a full-thickness test specimen. It was found that the DWTT test provided an accurate transition temperature for the wall thickness that is tested, addressing the thickness problem associated with the Charpy V-notch test [11]. The Charpy V-notch test can be used to estimate the transition temperature, provided that it is corrected for the difference in thickness between the pipe and test specimen [13, 14]. The practical implication of this is that if the 85% shear area measured in a CVN test is used, then the test must be conducted at a lower temperature.

The experimental programme conducted at the Battelle Memorial Institute demonstrated that the fracture appearance observed in full-scale tests could be correlated with the fracture appearance observed in a DWTT. A fracture-propagation transition temperature could be determined from the change in the appearance of a fracture with temperature in a DWTT specimen; full-scale tests conducted above this transition temperature resulted in arrest. This behaviour was confirmed in investigations conducted by (the-then) British Gas Corporation – BGC – who historically required a 75% shear area at 0°C. The DWTT transition curve is relatively steep towards the upper end of the curve: the difference between 75%, as adopted

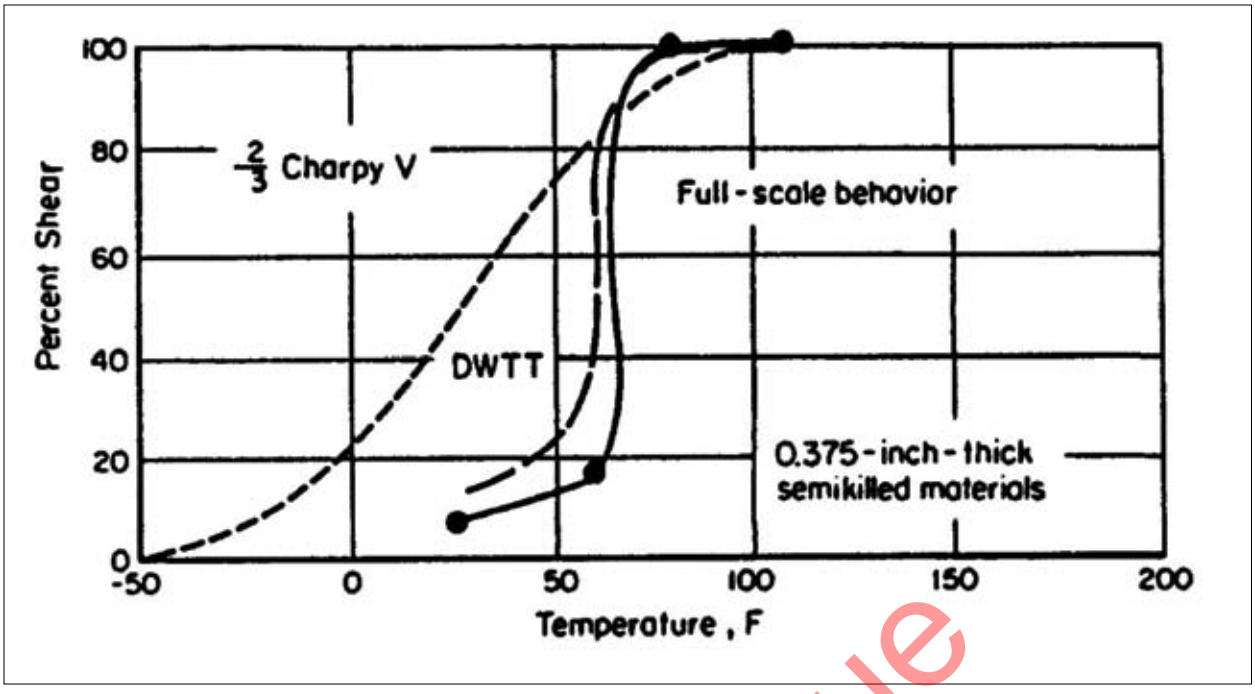

Fig.7. Fracture appearance measured in 2/3 Charpy V-notch, DWTT and full-scale tests on 30 in. x 0.375 in. (9.52 mm), X52 semi-killed line pipe steel [13].

by BGC, and 85%, as adopted by the Battelle Memorial Institute, is therefore insignificant.

The investigations conducted by BGC did identify that the hoop stress was also important (see Fig.9) [8, 15, 18]. Extensive brittle-fracture propagation did not occur in pipelines not meeting the 75% shear area requirement (i.e. with shear areas less than 75%) if the hoop stress was low. Extensive crack propagation appeared difficult at stress levels of 30% SMYS or below. The implications of this research were incorporated into IGE/TD/1 Edition 2 [18, 19].

The 85% shear area requirement in a DWTT to arrest a brittle fracture is now well established, and the need to meet this 85% shear area requirement at the minimum design/operating temperature of a pipeline in order to avoid brittle fractures appears in standard texts (such as Refs 20-22). Figure 10 shows the arrest of a brittle fracture in a ductile pipe [8]: the multiple-fronted brittle fracture arrested immediately (the girth weld is visible in the photograph) when it ran into a length of pipe that just met the (in this case) the 75% shear area requirement at the test temperature.

The applicability of the DWTT to larger-diameter, higher-grade, and thicker-wall linepipe has been demonstrated through further comparisons between the test specimens and full-scale tests [23]. The applicability to higher-toughness, controlled-rolled steels has also been demonstrated, although in this case it was necessary to develop the chevron-notched drop-weight tear test specimen as an alternative to the pressed-notch specimen [24].

The codification of the 85% shear area requirement

API Specification 5L

The American Petroleum Institute first published a specification for the manufacture of linepipe in January, 1928, the purpose of which was to provide standards for pipe suitable for use in conveying gas, water, and oil in both the oil and natural gas industries [25]. The first API 5LX specification was published in February, 1948 (as a tentative standard), entitled *Specification for high test linepipe* [25].

It was not until the 16th edition of API 5LX, published in April, 1969, that fracture-toughness testing was added through the addition of two supplementary requirements. The development of the toughness requirements in API 5L is summarized in Table 2. The DWTT requirements remained essentially unchanged from this edition of API 5LX until the 44th edition of ANSI/API Spec 5L / ISO 3183:2007 (Modified), published in October, 2007.

The research work conducted at the Battelle Memorial Institute in the 1960s demonstrated that the fracture-propagation transition temperature could be estimated directly from the DWTT 85% percent shear-area transition temperature. It could also be estimated from the Charpy V-notch 85% shear-area transition temperature provided that a thickness correction was applied [13, 14]. The

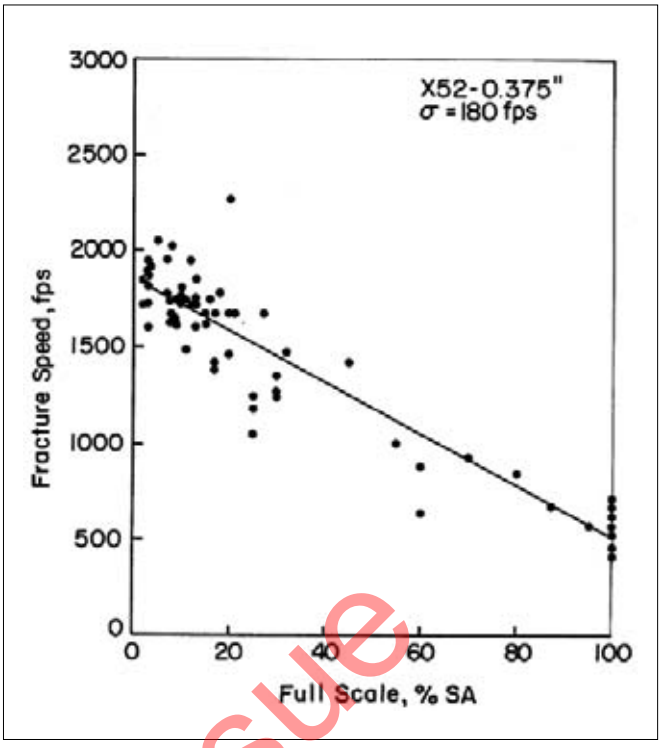

Fig.8. The relationship between fracture speed and the percentage shear area of a fracture in full-scale tests of X52 semi-killed line pipe steel [13].

problem of brittle-fracture propagation was solved by the DWTT.

Accordingly, a shear area requirement, expressed in terms of the DWTT was incorporated into API 5LX in 1969. API RP 5L3 was drafted to standardize the test method.

In the drafting of the revised specification, the users of the linepipe specification were of the view that the specification should include a toughness requirement that would prevent long-running fractures[5] [12]. This was in recognition of the fact that a pipeline will inevitably contain flaws, either defects arising from manufacture and construction, or damage introduced during operation. It was decided that the toughness requirements would be a supplementary requirement so that the user could choose when such requirements should be applied [12].

The DWTT and the Charpy V-notch requirements were limited to welded pipe, of 20-in diameter and above, and of grade X52 and higher, for what were – at the time – practical reasons. Similarly, the requirements only applied to wall thicknesses less than or equal to 12.7mm (0.5in), but this limit was subsequently removed in later editions as the capabilities of the plate and pipe mills improved.

The requirement for the DWTT shear area was that at least 80% of the heats exhibit a fracture-appearance shear area of 40% or more at the specified test temperature (with two tests per heat). This was a compromise based on a statistical analysis of data from more than 2,000 heats of pipe collected by the American Petroleum Institute and others [11-13]. It ensured an all-heat average of approximately 75-80% shear area, i.e. about half of the pipe lengths would arrest a brittle fracture[6] [13].

The requirement for Charpy V-notch testing was extended in later editions of API 5L.

The requirement for drop-weight tear testing remained limited to welded pipe, diameters of 20 in and above, and grade X52 and higher, up until the 44th edition. Similar limits on the requirement for the drop-weight tear testing can be found in other codes and standards, such as ISO 3183-3:1999 [26] and DNV-OS-F101 [27]. These limits have their origins in the requirements in API 5L.

ANSI/API Specification 5L / ISO 3183:2007 (Modified)

The 44th edition, ANSI/API Specification 5L / ISO 3183:2007 (Modified), published in 2007, is a result of the harmonization of the 43rd edition of API Specification 5L [28] and ISO 3183-1, -2:1996, and -3:1999 [26, 29, 30]. The notch-toughness requirements for PSL 2 linepipe are summarized in Table 3. It incorporates elements of API 5L and ISO 3183-3:1999.

[5] It is of historical curiosity to note that the manufacturers were of the view that the prevention of fracture initiation was the primary concern [12].

[6] British Gas adopted a similarly pragmatic approach to brittle fracture propagation that accepted that complete knowledge of the toughness of a pipeline could only be obtained by testing every pipe that was in the pipeline, and this was impractical. A pipe mill sampling procedure was developed, where one or two samples are taken for each heat. The procedure was developed to ensure that when the supplied lengths of pipe were constructed into a pipeline there was a 95% confidence level of arrest of a brittle fracture within two pipe lengths [16]. Each sample consisted of three test specimens, and the requirement was a minimum shear area of 75% at 0°C.

Kuala Lumpur

PPIM

Pipeline Pigging and Integrity Management

ASIA PACIFIC

8-11 NOVEMBER 2010

CROWNE PLAZA HOTEL• KUALA LUMPUR, MALAYSIA

The world renowned Pipeline Pigging and Integrity Management Conference will come to Asia in 2010.

The Asia Pacific Pipeline Pigging and Integrity Management Conference will allow pipeline professionals in the region access to an exciting programme of papers, great networking events and the latest technology on display at the exhibition.

If you are responsible for the management of oil and gas pipelines, make sure you don't miss this event.

Plan to be there: www.clarion.org or call us at +61 3 9248 5100

CONFERENCE • TRAINING COURSES • EXHIBITION

ORGANIZED BY

CLARION TECHNICAL CONFERENCES

TIRATSOO TECHNICAL

SUPPORTED BY

PIPELINES INTERNATIONAL

The Journal of Pipeline Engineering

PIPE

ASME SETTING THE STANDARD 1880 2006

PRCI Pipeline Research Council International

ILI Inline Inspection Association

January 1928	A.P.I. Standard No. 5-L, First Edition, A.P.I. Line Pipe Specifications
February 1948	API Tentative Standard 5LX, Specification for High test Line Pipe The first and second editions only included one grade, X42.
April 1969	The twenty-fourth edition of API 5L includes an indirect mention of the drop weight tear test, through a reference to API RP 5L3 Recommended Practice for Conducting Drop-Weight Tear Test on Line Pipe.
April 1969	The sixteenth edition of API 5LX adds two supplementary requirements in a new Appendix E: SR-5 Charpy Impact Testing on Welded Pipe 20-inch Diameter or larger, Grade X52 or Higher; and SR-6 Drop Weight Tear Testing on Welded Pipe 20-inch Diameter or larger, Grade X52 or Higher. SR-6 specified that at least 80% of the heats exhibit a fracture appearance shear area of 40% or more at the specified test temperature. SR-5 specified a minimum all-heat average shear area of 50%. The introduction of supplementary notch toughness requirements in terms of DWTT and CVN shear area followed from the research on brittle fracture propagation.
March 1978	The twenty-second edition of API 5LX adds the supplementary requirement SR-8 Fracture Toughness Testing of Line Pipe (requirements for the Charpy V-notch absorbed energy). The introduction of a supplement requirement in terms of CVN impact energy followed from the research on ductile fracture propagation.
March 1983	The 5LX and 5LS specifications are merged with the thirty-third edition of API Specification 5L
May 1988	The thirty-third edition reorganises the supplementary requirements. SR5 Fracture Toughness Testing (Charpy V-Notch) for Pipe of Size 4½ or Larger is divided into SR5A, which gave the requirements for shear area, and SR5B, which gave the requirements for absorbed energy. SR8 is deleted. SR6 is unchanged. SR5A specified a minimum all-heat average shear area of 80% (an increase from the previously specified 50%).
January 2000	The forty-second edition of API 5L introduces the 'product specification level' (PSL). The two designations, PSL 1 and PSL 2 defined different levels of standard technical requirements. PSL 2 had mandatory requirements for carbon equivalent, notch toughness, maximum yield strength, and maximum tensile strength. It adds the supplementary requirement SR19 Additional Fracture Toughness Requirements (Transverse Charpy V-Notch) for PSL 2 Pipe. The introduction of product specification levels was a response to industry concerns (i.e. the users of line pipe) that the specification did not sufficiently address line pipe with higher quality and toughness levels needed for many potential service environments, and to reduced the need for company supplementary specifications that were often written to 'plug the holes' that were considered to exist in API 5L.
October 2007	ANSI/API Specification 5L, Forty-Fourth Edition / ISO 3183:2007 (Modified), Petroleum and natural gas industries—Steel pipe for pipeline transportation systems

Table 2. Chronology of the DWTT and CVN requirements in API Specification 5L (based on Kiefner and Clark (1996) [25]).

UPCOMING CONFERENCES

International Forum on the Transportation of CO_2 for CCS

1 – 2 July 2010 • Hilton Hotel, Newcastle, UK

The First International Forum on the Transportation of CO_2 for CCS (carbon capture and storage) is organised by Newcastle University in partnership with Tiratsoo Technical and Clarion Technical Conferences. The event is supported by the Carbon Capture and Storage Association.

As the world looks for solutions to carbon emissions, this forum will discuss the most critical element in CCS – the transportation of CO_2 from its source to its storage location. While there is significant experience with CO_2 transportation, CO_2 from anthropogenic sources, such as power stations, has a wide array of issues that must be solved. These issues will be discussed. If you are interested in the rapidly expanding area of CO_2 pipelines, you cannot afford to miss this forum.

››››››For more information visit **www.clarion.org**‹‹

Evaluation, Rehabilitation & Repair of Pipelines Conference and Exhibition

18 – 21 October 2010 • Berlin Marriot Hotel, Berlin

If you are interested in extending the life of pipelines via rehabilitation, make sure you don't miss the premier conference dedicated to the field.

The event will cover pipeline rehabilitation, ranging from the initial stages of evaluation of a pipeline's condition to the steps required to undertake rehabilitation to ensure its continued fitness-for-purpose and prolong its economic lifetime.

With over 60 per cent of the world's major oil and gas transmission pipelines now more than 50 years old rehabilitation is an increasingly important aspect to pipeline engineering, operations and construction.

Hear the latest advances, network with experts and see the latest evaluation and rehabilitation technology up close.

››››››Visit **www.piperehabconf.com** for more information ‹‹

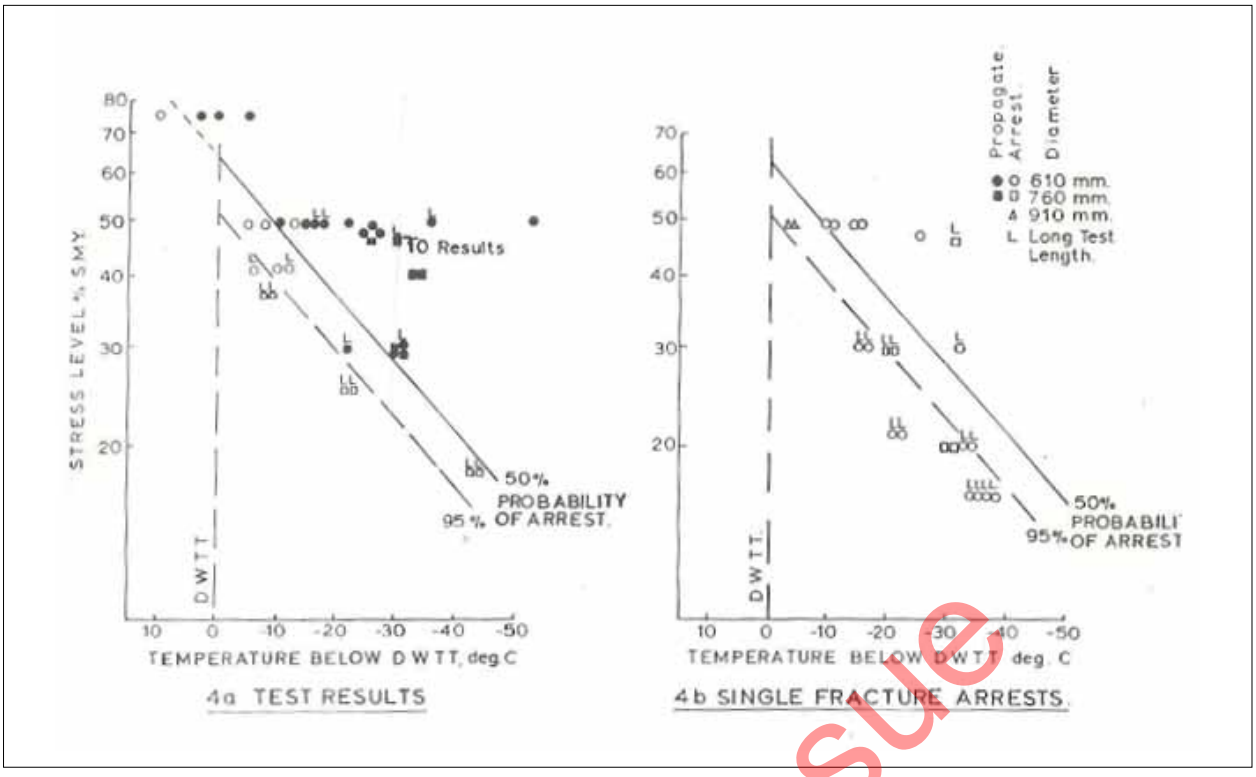

Fig.9. The effect of hoop stress on the arrest of a brittle fracture [8].

ISO 3183-3:1999 specified drop-weight tear testing for linepipe with a diameter of 508mm or larger, a wall thickness of greater than 8mm, and grades X60 (L415) and above, that is intended for gas pipelines. The shear area requirement was 85%, based on two tests per heat.

ANSI/API Specification 5L / ISO 3183:2007 (Modified) indicates that drop-weight tear testing is a mandatory requirement for PSL 2 linepipe (it was previously a supplementary requirement), but it is only required for welded pipe with a diameter of 508mm (20in) or above (it was previously also limited by grade)[7]. The average shear area (two test specimens) must be greater than or equal to 85% (the previous requirement was that at least 80% of the heats exhibit a shear area of 40% or more).

It is interesting to note that ANSI/API Spec 5L maintains the tradition of not requiring drop-weight tear testing in linepipe with diameters less than 508mm (20in), introduced for practical reasons in 1969. In small-diameter and thin-walled linepipe it is difficult (but not impossible) to extract and gull wing a satisfactory DWTT specimen.

The long-running brittle fractures in in-service pipelines have all occurred in larger-diameter pipe (although one of the longest ductile fractures occurred in a 16-in diameter pipe). Long failures have not been observed in small-diameter lines. The failures that have occurred in North America have been limited to lengths of the order of 20-40ft. The likely explanation for this is the fact that the small-diameter pipelines were operating at less than 50-72% SMYS, i.e. consistent with the effect of stress level on the extent of brittle fracture propagation. An Athens test in December, 1965, on 6.625-in diameter, 0.250-in wall thickness, semi-killed X52 linepipe, at a nominal hoop stress of 71% SMYS, clearly demonstrates that brittle fracture propagation is not limited to larger-diameter pipe. Cleavage fractures ran through all five test joints. The number of individual fractures varied from one to seven. The shear area measured in the DWTTs ranged from 7 to 22%.

IGEM/TD/1 and GBE/LX1, LX4 and LX5

IGEM/TD/1 Edition 5 is the latest edition of the TD/1 recommendations for the design, construction, and operation of high-pressure onshore gas transmission pipelines. The onshore gas transmission system in the UK was designed to the various editions of TD/1. IGEM/TD/1 Edition 5 requires drop-weight tear testing for all linepipe with a diameter exceeding 323.9mm (12.75in) [31]. Similarly, AS 2885.1, an Australian pipeline design code, requires it on diameters of 323.9mm or above [32].

The internal specifications of the-then British Gas (BGC), GBE/LX1, LX4, and LX5 [33-35] for submerged-arc-welded, seamless, and electric-welded pipe, respectively, similarly require a minimum shear area in a DWTT for all linepipe with a diameter exceeding 323.9mm (12.75in), i.e. a nominal size exceeding 300mm. The shear area requirement is a

[7] ANSI/API Spec 5L does not require drop weight tear testing for seamless line pipe. ISO 3183-3:1999 did require it. However, the practical implications of the difference are small because seamless line pipe is not widely available in diameters of 508 mm (20 in.) or larger.

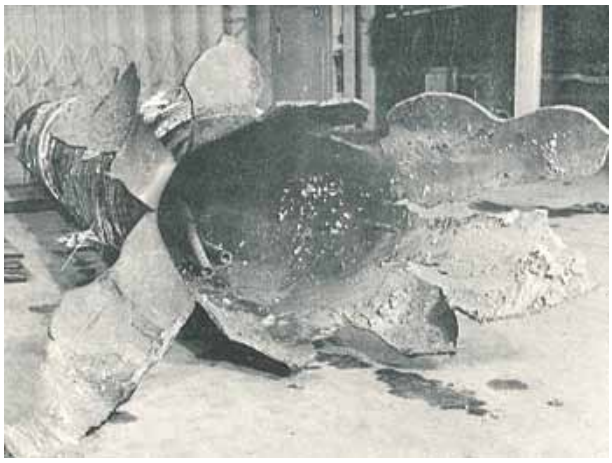

Fig. 10. Arrest of a brittle fracture by ductile pipe [8].

minimum of 75% at 0°C. A minimum shear area in a Charpy V-notch test is required for smaller-diameter seamless and electric-welded line pipe, but at a lower test temperature.

The requirements in LX4 and LX5 are based on an extensive (unpublished) study of small-diameter seamless linepipe conducted by BGC in the early 1970s, in order to define the impact testing requirements. Charpy V-notch and DWTTs were conducted to determine an equivalence between the tests. It was demonstrated that a 50% shear area at -15°C in a longitudinal Charpy V-notch test was equivalent to a 75% shear area at 0°C in a DWTT in diameters less than 323.9mm (12.75in). In diameters 323.9mm or smaller, the specifications only cover wall thicknesses up to and not exceeding 12.7mm (0.5in); the cut-off at 323.9mm was based on engineering judgement.

Four recent examples

Brittle fractures in pipelines constructed after the incorporation of the toughness requirements into API 5LX in 1969 are rare and, indeed, have been considered highly improbable for several decades. This is based on the expectation that modern linepipe should easily meet the DWTT shear-area requirement. However, in more recent times, there have several instances of 12.75 to 24-in diameter pipe having been produced with high fracture-propagation transition temperatures, i.e. low shear area, and this is a cause of concern.

The following four examples illustrate the difference between impact energy and shear area, and the importance of the DWTT in both large and small diameters. All of the examples relate to welded linepipe, but the lessons are equally applicable to seamless linepipe.

- 1. 18-in and 24-in diameter, X52

The first example concerns two orders of X52 linepipe of mid-1990s vintage purchased to API 5L without specifying any additional requirements. One was 24-in diameter, DSAW linepipe, and the other 18-in diameter, ERW linepipe. DWTTs were conducted at -10°C. The average shear areas (from three tests) were 25% and 29%, respectively. Charpy V-notch tests were conducted at 0 and -10°C, and the average impact energies (from three tests) at -10°C were 116J and 143J, respectively, and 160J and 174J at 0°C. The average shear area at 0°C was 80% and 90%, respectively.

- 2. 18-in diameter, X60

A more recent example relates to an order of 457.2-mm (18-in) diameter, 15.9-mm wall thickness, X60, HFI linepipe of mid-2000s vintage. DWTTs were conducted at a test temperature of +15°C (the legacy of a concession in the early 2000s), although the design temperature was 0°C. The average shear areas (from two tests) at +15°C in five sets of tests from three heats varied from 43 to 80%, i.e. below the specified value of 85%. Additional tests conducted between -10 and +20°C indicated that the linepipe steel was in the transitional region at +15°C; the fracture-propagation transition temperature was around +15°C.

Charpy V-notch tests were conducted at 0°C. The impact energy in the five lengths of pipe varied from 84 to 141J, and the shear area varied from 73 to 100%. The average shear area was higher than 85% in all but two of the CVN tests.

A further problem, though secondary to the inappropriate test temperature in this second example, was a reduction in the testing frequency. The testing frequency is integral to ensuring that the requisite proportion of the linepipe in an order has the required toughness.

- 3. 14-in diameter, grade B

The third example concerns a recent order of 355.6-mm (14-in) diameter, 11.6-mm wall thickness, grade B, ERW linepipe of late-2000s vintage. The linepipe was specified to PSL 2. Charpy V-notch tests of two heats were conducted at a test temperature of 0°C. The average impact energies of the two heats were 39J and 55J, respectively, and the average shear area was 95% for both heats. DWTTs were subsequently conducted at 5°C, to comply with the requirements of the particular design code. Two tests were conducted for each heat: the shear areas were 10 and 15%, and 20 and 70%, respectively (and the DWTTs were conducted at a higher temperature than the CVN tests).

- 4. 14-in diameter, X42

The fourth example concerns a recent order of 355.6-mm (14-in) diameter, 12.7-mm wall thickness, X42, ERW linepipe also of late-2000s vintage. The

linepipe was specified to PSL 2. Charpy V-notch tests were conducted at a test temperature 0°C. The average impact energy was 111J, and the shear area was 64%. DWTTs were conducted at -10 and 0°C, and the shear areas were 8 and 50%, respectively.

Low shear area in the DWTT

In all four examples, the linepipe steel had an insufficient toughness to arrest a running brittle fracture in a typical onshore pipeline; the fracture-propagation transition temperature is higher than the operating temperature. Fortunately, in the first two of the examples discussed above the linepipe was intended for pipelines designed to operate at a hoop stress less than or equal to 30% SMYS. The linepipe does have sufficient toughness to arrest brittle fractures under these particular conditions.

The Charpy V-notch impact energy in all four examples is relatively high and, in all of the examples, the impact energy is higher than that specified for PSL 2 linepipe in ANSI/API Spec 5L. The linepipe steel in the first example is close to the lower shelf at -10°C (from the DWTT results), but the impact energy is greater than 100J. In the first example it is also questionable whether a shear-area criterion based on the Charpy V-notch test would have been sufficient. This is more clearly illustrated in the third example, in which ANSI/API Spec 5L would not require DWTT testing because of the small diameter. The shear area measured in the CVN tests is greater than that required for PSL 2 pipe with resistance to ductile fracture propagation (as specified in Annex G of ANSI/API 5L), but the linepipe does not in fact have sufficient toughness to arrest a running brittle fracture. The linepipe in the fourth example would not satisfy the requirements of Annex G, but is notionally PSL 2 linepipe. If the 'if agreed' CVN shear area criterion for small-diameter PSL 2 linepipe in clause 9.8.2.2 of ANSI/API 5L was invoked, then the linepipe would not satisfy the requirements of PSL 2.

All four examples illustrate that the Charpy V-notch impact energy is not a sufficient criterion. Shear area is important, either measured in a DWTT or CVN test. The fourth example illustrates the importance of specifying the 'if agreed' Charpy V-notch shear area criterion, in the absence of a DWTT criterion. However, the third example illustrates that the Charpy V-notch shear-area criterion is not sufficient unless it is conducted at an appropriate test temperature, which needs to be lower than that at which the DWTT would be conducted.

In all four examples, conducting the DWTTs at the correct test temperature identified the sub-standard linepipe.

Conclusions

Pipelines that transport gaseous fluids, two-phase fluids, dense-phase fluids, or liquids with high vapour pressure, are susceptible to propagating fractures. A fracture, once initiated, can propagate for long distances in either the brittle or the ductile mode, and consequently it has been necessary to develop toughness specifications for linepipe to ensure that any propagating fracture is arrested within an acceptable length.

The drop-weight tear test shear area requirement was developed to ensure that long-running brittle fractures will not occur. A brittle fracture will not propagate if the shear area measured in a DWTT is greater than or equal to 85% at the minimum design temperature.

The research leading to the development of the DWTT requirement was conducted in the 1960s. The suitability of the test has been demonstrated in full-scale tests of small- and large-diameter, thin- and thick-walled, pipe of both and low and high grades. The DWTT requirement was incorporated into API 5L in 1968, and has proved to be very successful in preventing in-service long-running brittle fractures. The introduction of the DWTT also led to significant improvements in the manufacturing of linepipe steel. Consequently, and for many years, linepipe has met the shear-area requirement with no difficulty.

The background to the development of the DWTT is in danger of being lost in time, and there is now a risk of complacency. Indeed, in a number of recent projects, linepipe has been supplied that does not meet the DWTT shear-area requirement. Additionally, there are inconsistent and arbitrary limits on drop-weight tear testing (for example, only being required for welded pipe of 508-mm (20-in) diameter or above) in the current linepipe specifications which have their origins in practical limitations relevant at the time, but which now need to be reviewed and revised.

It is concluded that, even 40 years after its introduction, the background to the development of the drop-weight tear test needs to be fully understood and recognized. The test shear-area requirement is still relevant today:

"Don't drop the drop-weight tear test."

Acknowledgements

The authors gratefully acknowledge the assistance provided by Ted Clark and Leigh Fletcher.

References

1. American Petroleum Institute, 2007. Specification for Line Pipe, ANSI/API Specification 5L, 44th Edn, October. Also ISO 3183:2007 (Modified), Petroleum and natural gas industries—Steel pipe for pipeline transportation systems.

2. International Organisation for Standardization, 2007 Petroleum and natural gas industries – Steel pipe for pipeline transportation systems, ISO 3183:2007, Geneva, Switzerland.
3. H.P.Rossmanith, 1999. The Struggle for recognition of engineering fracture mechanics. Fracture research in retrospect, A.A.Balkema Publishers.
4. T.L.Anderson, 1995. Fracture mechanics fundamental and applications. 2nd Edn, CRC Press.
5. American Petroleum Institute, 1996. Recommended practice for conducting drop-weight tear tests on line pipe. API RP 5L3, 3rd Edn, February.
6. R.J.Eiber and W.A.Maxey, 1979. Fracture propagation control methods. Paper L, 6th Symposium on Linepipe Research, American Gas Association, Catalog No L30175, October.
7. Anon., 1960. Rupture will not delay Transwestern's line. Oil & Gas Journal, 58, 17, April 25, p105.
8. G.D.Fearnehough, 1974. Fracture propagation control in gas pipelines: a survey of relevant studies. Int. J. Pressure Vessels and Piping, 2, 4, October, pp257-282. Also JIG Symposium on crack propagation in pipelines, Newcastle, UK, March.
9. J.Stransky, 1968. Brittle fractures in piping. International Institute of Welding, Doc. XI-202-68.
10. A.R.Duffy, 1965. Full-scale studies. 3rd Symposium on Linepipe Research, American Gas Association, Catalog No. L30000, November, pp43-82.
11. R.J.Eiber, 1965. Correlation of full scale tests with laboratory tests. Ibid, Catalogue No 30000, pp83-118.
12. L.L. Elder, 1965. Activities towards specifications for fracture toughness. Ibid, Catalog No. L30000, pp119 126.
13. R.J. Eiber, 1969. Fracture propagation. Paper I, 4th Symposium on Linepipe Research, American Gas Association, Catalog No. L30075, November.
14. R.J.Eiber, A.R.Duffy, and G.M.McClure, 1970. Significance of the drop-weight tear test and Charpy V-notch impact test results. Impact Testing of Metals, ASTM STP466, American Society for Testing and Materials.
15. G.D.Fearnehough, D.W.Jude, and R.T.Weiner, 1971. The arrest of brittle fracture in pipelines. IMechE Conference on Practical Application of Fracture Mechanics to Pressure Vessel Technology.
16. D.G.Jones, 1981. The British Gas approach to fracture arrest in pipelines. AGA-EPRG Linepipe Research Seminar IV, Duisburg, Germany, 22-24 September.
17. A.Rothwell and G.D.Fearnehough, 1984. Application of fracture technology and design philosophies for major gas pipelines. International Seminar on Fracture in Gas Pipelines, Moscow, Russia, March.
18. A.E.Knowles, J.L.Van der Post, and F.Tweedley, 1977. The background and implications of IGE/TD/1 2nd Edn. Institute of Gas Engineers, Communication 1044, IGE 43rd Autumn Meeting, London, UK, November.
19. Institute of Gas Engineers, 1984. Steel pipelines for high pressure gas transmission: recommendations on transmission and distribution practice. IGE/TD/1 Complete Edition 2: 1984, Communication 1234.
20. D.T.Llewellyn and R.C.Hudd, 1998. Steels: metallurgy and applications, 3rd Edn. Butterworth Heinemann, Oxford, UK.
21. M.Mohitpour, H.Golshan, and A.Murray, 2007. Pipeline design and construction, a practical approach, 3rd Edn. ASME Press, New York.
22. A.C.Palmer and R.A.King, 2008. Subsea pipeline engineering, 2nd Edn. PennWell Books, Tulsa, OK.
23. V.Pistone, G.Demofonti, and G.Junker, 2000. Transition temperature determination for thick wall line pipes. 3R International, 39, March, pp199-204.
24. W.A.Maxey and C.R.Barnes, 1991. Use of the chevron notch DWTT as a means of avoiding high initiation energies. Paper 37, II, Proc. EPRG/NG-18 8th Biennial Joint Technical Meeting on Linepipe Research, Paris.
25. J.F.Kiefner and E.B.Clark, 1996. History of linepipe manufacturing in North America. ASME Research Report, CTRD-Vol. 43, The American Society of Mechanical Engineers, New York.
26. British Standards Institute, 1999. Petroleum and natural gas industries – Steel pipe for pipelines – Technical delivery conditions – Part 3: Pipes of requirement class C. BS ISO 3183-3:1999, London.
27. Det Norske Veritas, 2007. Submarine pipeline systems. Offshore Standard DNV-OS-F101, October.
28. American Petroleum Institute, 2004. Specification for line pipe, exploration and production department. API Specification 5L, 43rd Edn.
29. British Standards Institute, 1996. Petroleum and natural gas industries – Steel pipe for pipelines – Technical delivery conditions – Part 3: Pipes of requirement class A. BS ISO 3183-1:1996, London.
30. Ibid.
31. Institute of Gas Engineers & Managers, 2008. Steel pipelines and associated installations for high pressure gas transmission. IGEM/TD/1, 5th Edn, Communication 1735, UK.
32. Standards Australia, 2007. Pipelines - gas and liquid petroleum - design and construction. AS 2885.1-2007 Amdt 1-2009, Sydney, January.
33. Anon., 1993. Technical specification for seamless pipe 150mm to 450mm inclusive nominal size for operating pressures greater than 7 bar. GBE/LX4, J072 (Rev08/98), Transco, April.
34. Anon., 1993. Technical specification for electric-welded pipe 150mm to 450mm inclusive nominal size for operating pressures greater than 7 bar. GBE/LX5, J073 (Rev 08/98), Transco, September.
35. Anon., 1993. Technical specification for submerged-arc welded pipe 400mm to 1400mm inclusive nominal size for operating pressures greater than 7 bar. GBE/LX1, J071 (Rev 08/98), Transco, September.

A parametric study on the effect of weld misalignment on the local buckling response of pipelines

by Aiman Al-Showaiter[1], Professor Farid Taher[2], and Dr Shawn Kenny[3*]

1 MCS Kenny, Houston, TX, USA, *and formerly of* Department of Civil and Resource Engineering, Dalhousie University, Halifax, NS, Canada
2 Department of Civil and Resource Engineering, Dalhousie University, Halifax, NS, Canada
3 Faculty of Engineering and Applied Science, Memorial University of Newfoundland, St John's, NL, Canada

PIPELINES ARE VITAL elements used for the transportation of oil and gas from field to consumption regions or exporting ports. Pipelines traverse various terrains and may be subject to ground movements such as subsidence, slope movement, frost heave, thaw settlement, or offshore ice gouging. Therefore, it is essential to understand the reliability and the integrity of these pipelines. Moreover, the mechanical behaviour of shell structures, such as pipelines, is 'imperfection sensitive', and the presence of initial geometric or material imperfections can significantly affect the pipeline load and deformation capacity.

This paper deals with the examination of the influence of initial geometric imperfections associated with joint to joint offset misalignment that may be present due to the girth welding process when connecting pipeline segments. This investigation was conducted using finite-element methods to assess the effects of internal pressure, axial force, misalignment amplitude, and misalignment orientation on the local buckling response of pipelines. Through this parametric analysis, the moment-curvature response and variation in section geometry with increasing global curvature was examined.

PIPELINE SEGMENTS ARE joined in the field by circumferential girth welding. The girth welds introduce residual stresses and misalignment imperfections into the pipeline; therefore, their effects on the structural behaviour of the pipeline need to be studied. This paper presents a parametric study of the effect of misalignment imperfection on the local buckling response of a pipeline, and a subsequent paper will discuss the effect of the presence of residual stresses. Many experimental and numerical research studies have been conducted in the past 70 years on the behaviour of pipelines, and a list of some of those studies is presented by Fatemi *et al.* [1]. The following literature review focuses on some of the more relevant studies on the effect of girth-weld misalignment on the local buckling response.

Yoosef-Ghodsi *et al.* [2] carried out a series of tests at the University of Alberta on seven pipeline segments, all of which had a girth welds at the mid-span. The pipeline moment-curvature response was obtained for each test specimen, subjected to combined loading. The results from this experimental study were compared to the experimental results for plain pipe: the results indicated that the presence of the girth weld reduces both the capacity of the pipe, by approximately 10% on the limit moment, and the curvature at initiation of buckling.

Dorey *et al.* [3] developed a finite-element model that included a misalignment imperfection at the girth weld; the

* Author's contact details:
tel: +1 709 737 2656
email: spkenny@engr.mun.ca

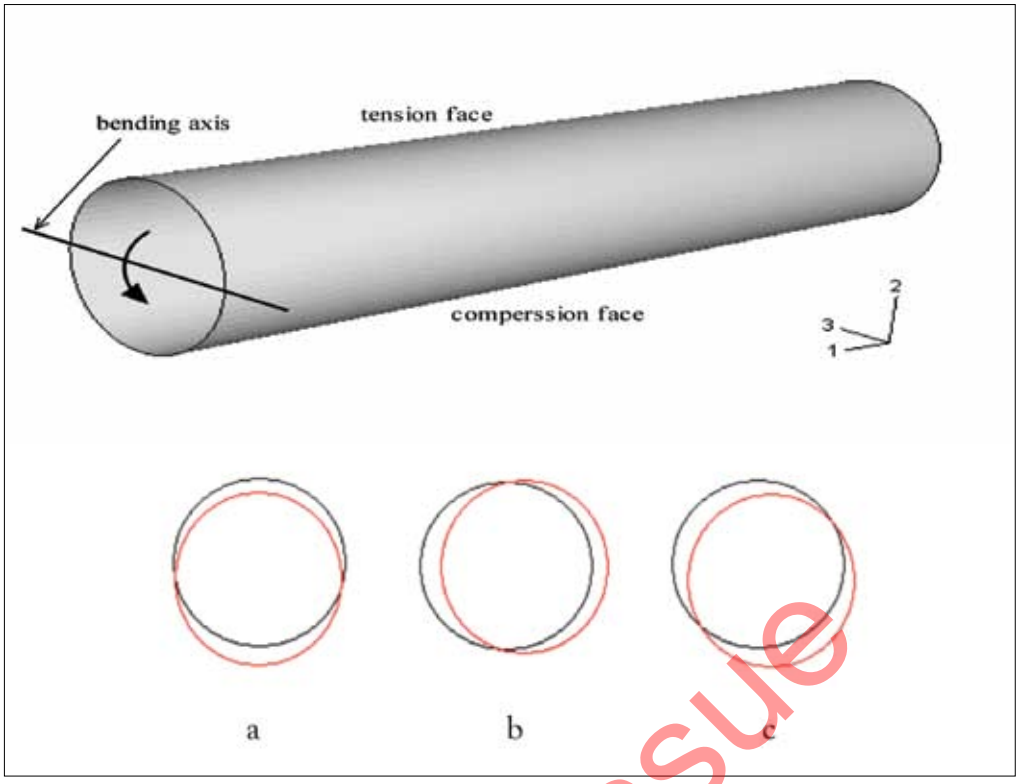

Fig. 1. Misalignment orientations (a) 0°, (b) 90°, (c) 45°.

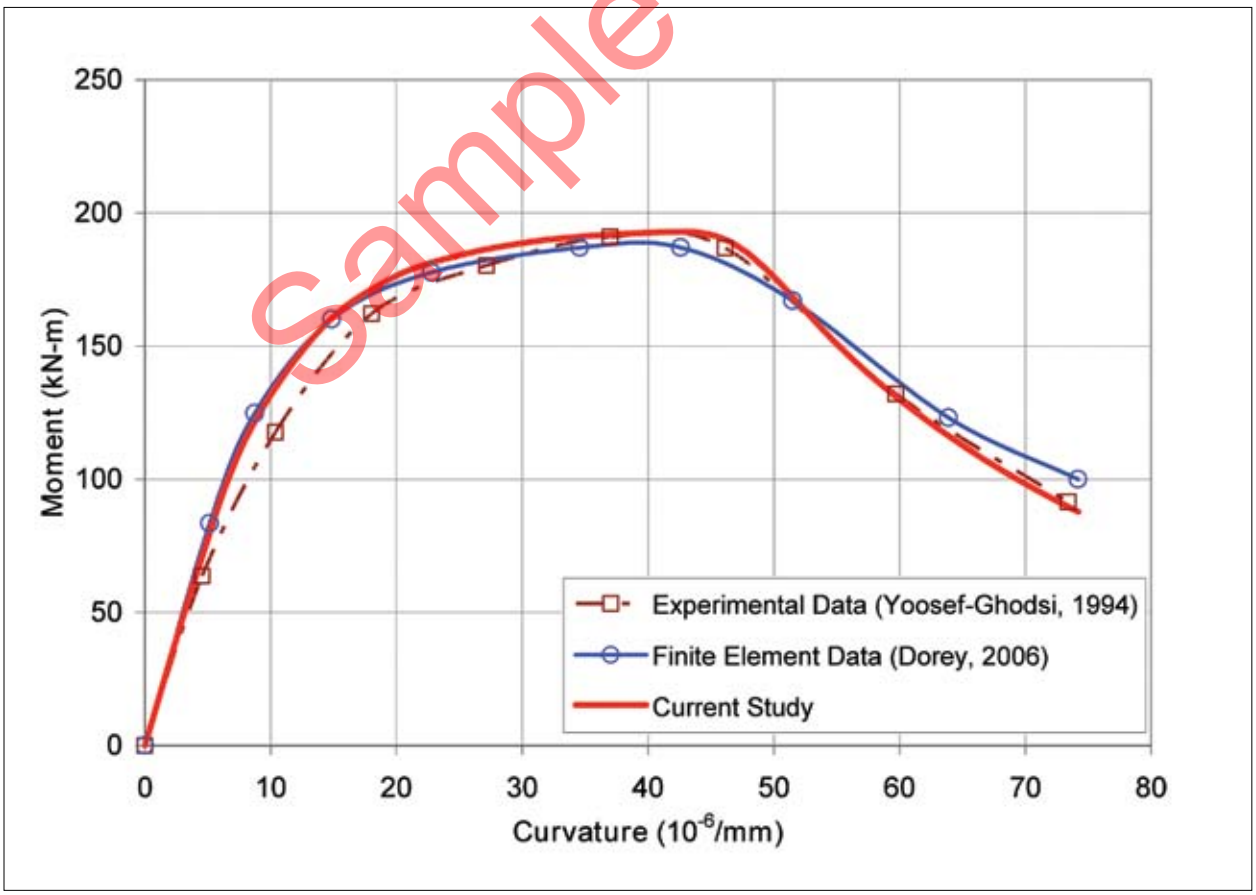

Fig. 2. Comparison of the computational results developed in this study with the experimental and numerical results presented by Dorey [3] for the pipeline specimen HGA12W.

model implemented an idealized misalignment imperfection, where all other laboratory-measured imperfections existed in the pipeline were neglected. These researchers used this approach to model some of the pipelines tested by Yoosef-Ghodsi *et al.* [2] with assumed initial misalignment imperfections, and the results showed good agreement with the experimental results. Dorey *et al.* [4] also conducted a parametric study to investigate the influence of initial geometric imperfections on the behaviour of pipelines as a function of internal pressure: the study only considered misalignment imperfections in the direction corresponding to a geometric offset normal to the bending neutral axis. The misalignment imperfection was always combined with blister imperfection (2% of wall thickness) in the models that were studied. Based on these investigations, Dorey *et al.* [3] developed equations to predict the critical buckling strain for girth-welded pipes.

Torselletti *et al.* [5] performed a parametric study on the effect of the presence of a girth weld on both the moment capacity and corresponding buckling strain. They looked at both misalignment offset and misalignment due to ovality for pipelines with diameter-to-thickness ratios of between 35 and 60. The study concluded that misalignment imperfection is more important for pipelines with diameter-to-thickness ratios of 45 and higher. The results showed that the DNV OS-F101 design formulae are only valid for D/t ratios of 55 or lower. The study also found that a reduction of 10% of the limit moment for 3mm offset with respect to the DNV OS-F101.

This study extends previous limited work available in the literature to examine offset misalignment amplitude and orientation, internal pressure, and axial force, and evaluates the influence of these parameters on the moment-curvature response of girth-welded pipelines.

Finite-element modelling procedure

In this paper, ABAQUS (ver. 6.6) commercial finite-element software package [6] was used to predict the pipelines' behaviour. A reduced four-noded shell element (S4R) with large displacement-large rotation formulation was used in the analysis. This element was identified as the most suitable element for buckling and post-buckling analyses by Fatemi *et al.* [1]. The pipeline geometry selected for this study was an outside diameter of 508mm and length of 2.6m: these parameters were consistent with the study conducted by Fatemi *et al.* [7] where the effect of blister-type geometric imperfections on the pipeline buckling response was examined. This paper extends the previous research to examination of the influence of misalignment, due to the girth welding and joining process, on the pipeline buckling response to combined loads.

As shown in Fig.1, the misalignment was modelled by offsetting half of the pipeline segment with a constant amplitude in the vertical (6 o'clock position: 0°), horizontal (3 o'clock position: 90°) and oblique (4.30 o'clock position: 45°). The misalignment directions correspond to geometric offsets normal to the bending neutral axis, parallel to the bending neutral axis, and oblique to the bending neutral axis. The misalignment transition occurs though one element length at the mid-section of the pipeline. In this study, the effect of residual stress state and weldment/base-metal

Parameters	Case 1		Case 2
	Stage 1	Stage 2	
Nominal outside diameter	508mm		
Length	2.6m (~5 × Diameter)		
Material grade	X65 (API 5l, 2000; Walker and Williams, 1995)		
Nominal wall thickness	7.1 mm		
D/t ratio	50, 70, 90		
Pressure stress ratio (%)	0, 40, 60, 80		80
Axial load (kN)	Not applicable		-1000 to 1500 with 500 increment
Misalignment Amplitude (mm)	0.2 to 1.6 with 0.35 increments	1.6	0.2, 0.9, 1.6
Misalignment Orientation	0°	0°, 45°, 90°	0°
Total analysis cases	60	36	54

Table 1. Parameters used in the computational study.

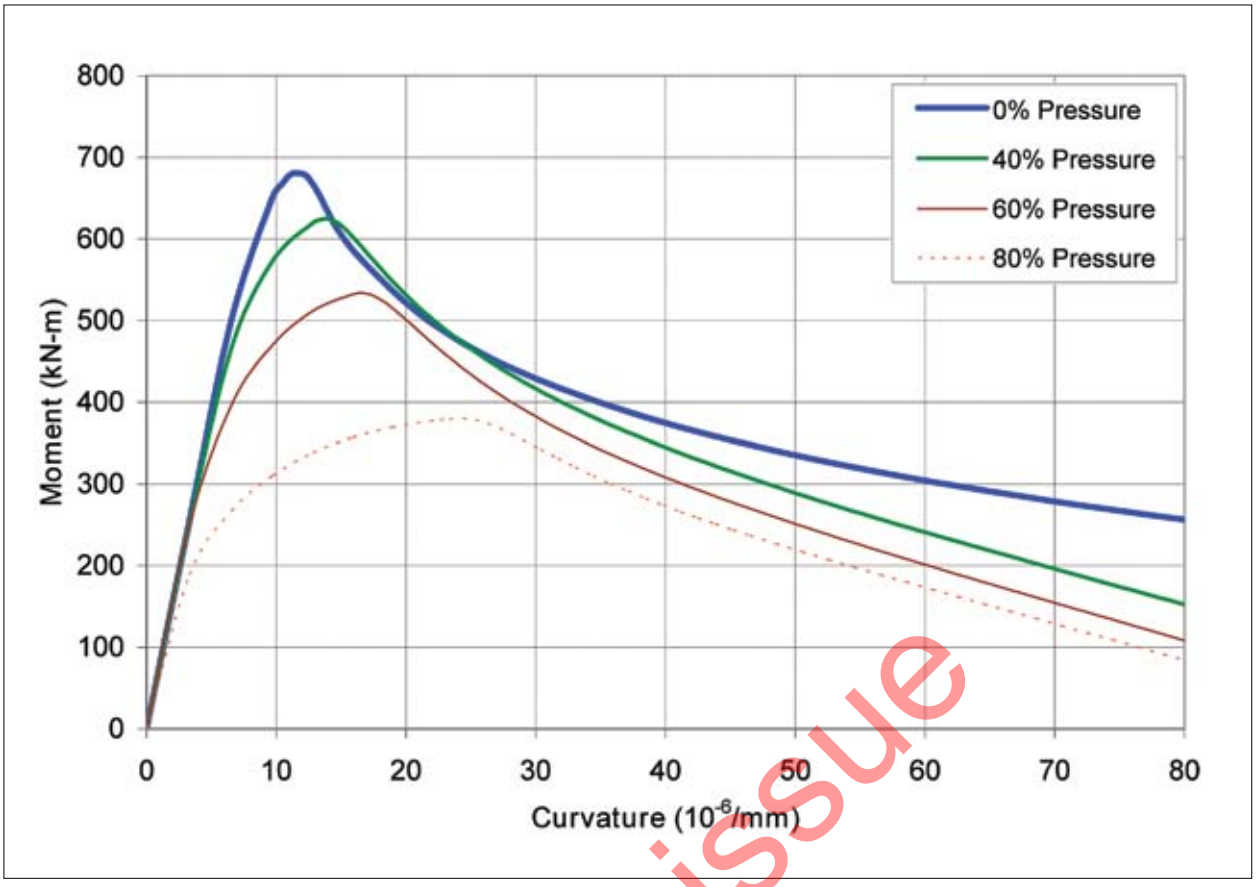

Fig.3. Moment-curvature response for a pipeline (D/t = 70, misalignment = 1.6 mm, and offset orientation = 0°) with different internal pressure stress ratios.

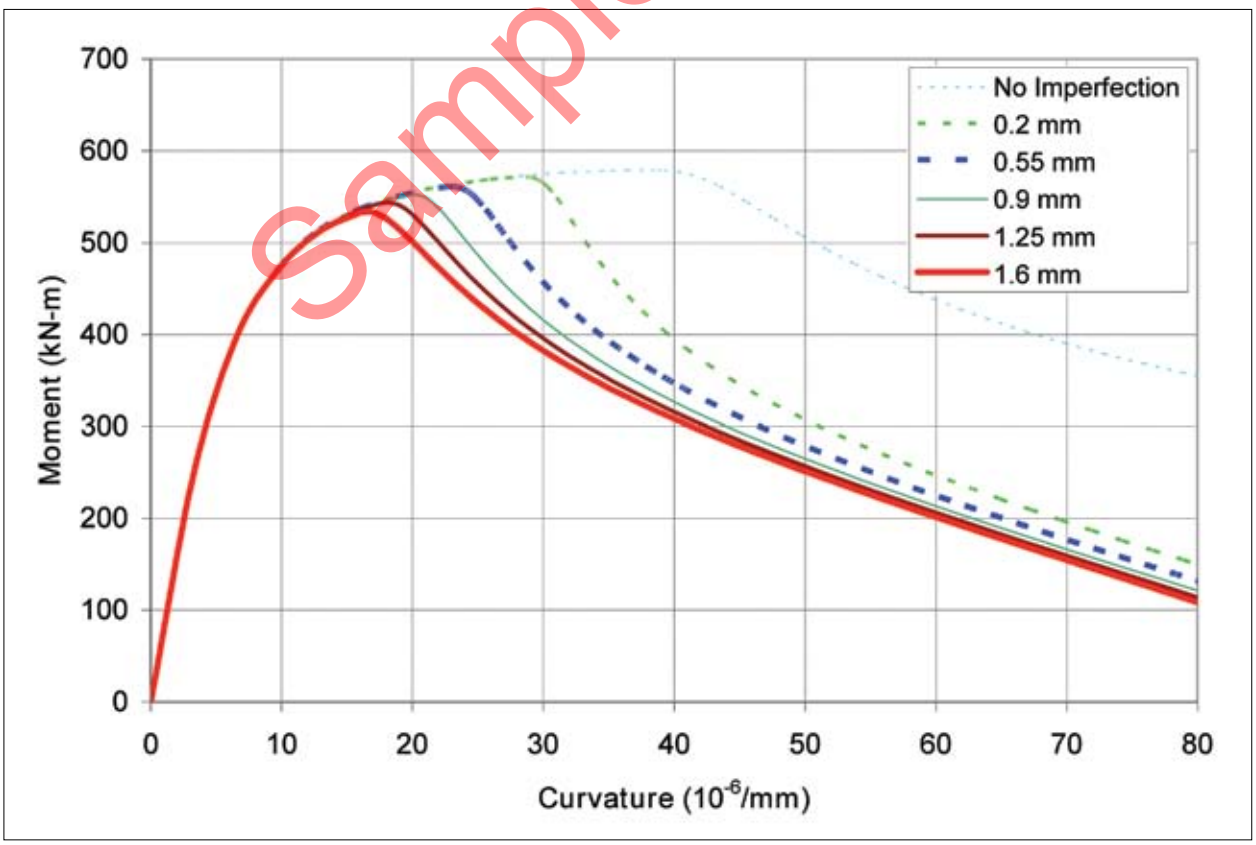

Fig.4. Moment-curvature response for a pipeline (D/t = 70 and internal pressure = 60%) with different misalignment amplitudes.

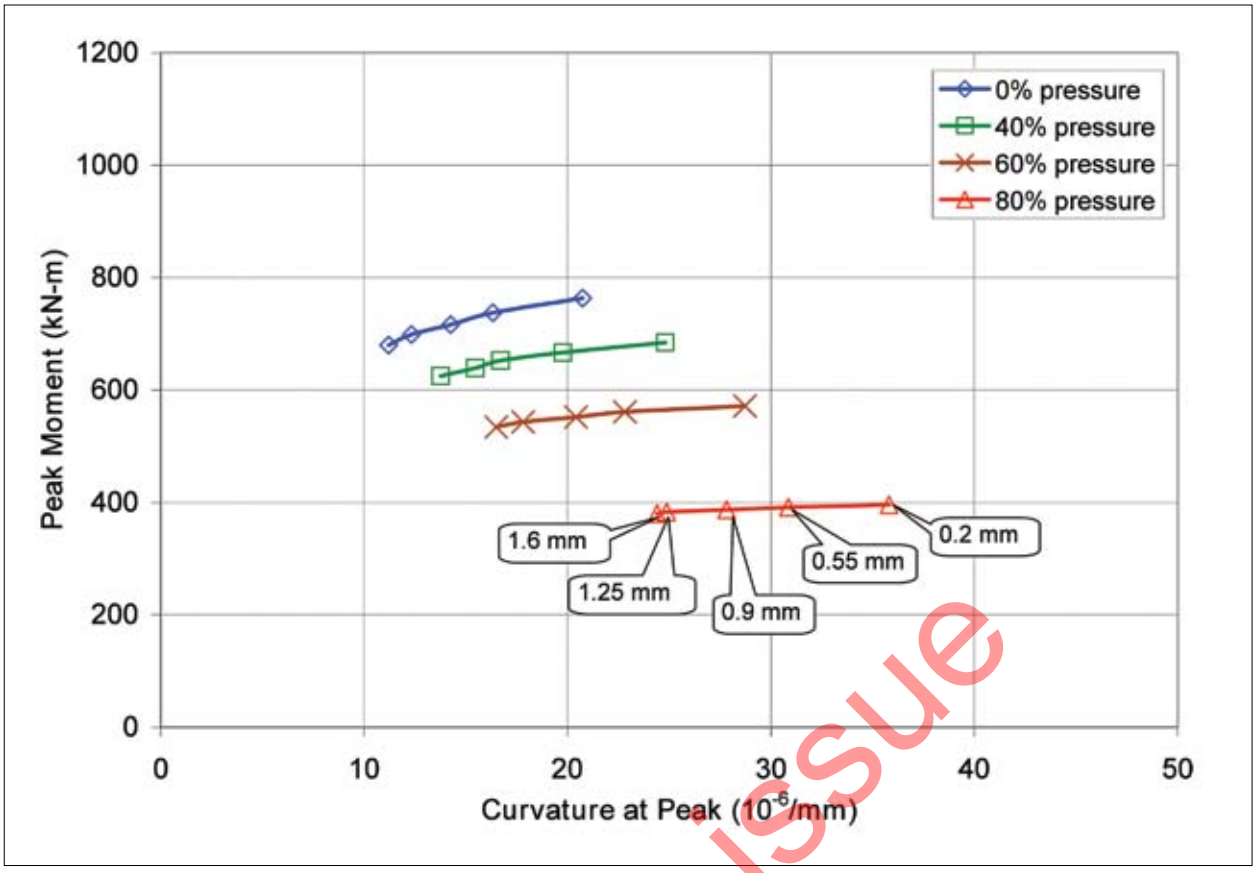

Fig. 5. Combined effects of misalignment amplitudes (misalignment orientation = 0°) and internal pressure for pipeline with D/t of 70.

strength parameters associated with the circumferential girth weld were not considered. The combined effect of residual stresses, weld mismatch, and misalignment imperfection has been assessed by the authors, and will be presented in a future paper.

A mesh-convergence study indicated 60 elements in the circumferential direction and 261 elements in the longitudinal direction were appropriate for this analysis. A uniform mesh topology with a large number of elements in the longitudinal direction was dictated by the width of the girth weld zone where the misalignment occurs. Preliminary studies indicated that a graded or biased mesh would trigger buckling at the mesh transition region even in the absence of any geometric imperfection.

The misalignment amplitude imposed in the analysis had a maximum value of 1.6mm, as recommended by CZ662 [8], and a minimum value of 0.2mm [3], with increments of 0.35mm.

The boundary conditions were defined by reference nodes at each end of the pipe located on the longitudinal centreline axis and were rigidly connected to each end of the pipeline. The axial force and end moment were applied to the reference nodes.

The material used in all models was X65 as defined by the API 5L [9]. The elasto-plasticity formulations employed in this study were adapted from Walker and Williams, 1995, and in this study, the von Mises' yield criterion was been used.

Model calibration

The finite-element model explained above was calibrated to the experimental data available through University of Alberta test series [10]. Figure 1 shows the global moment-curvature response for the test pipe HGA324W for experimental and numerical results: the excellent agreement obtained between the numerical analysis, presented here, and the experimental data gives confidence that the current study model can predict the physical test behaviour in an accurate way. An offset misalignment amplitude of 0.2mm for the initial imperfection was assumed as suggested by Dorey *et al.* [3].

Parametric investigations

Overview

In this paper, two different case studies were conducted to examine the effect of misalignment imperfection on pipeline moment and strain capacity. The parameters investigated

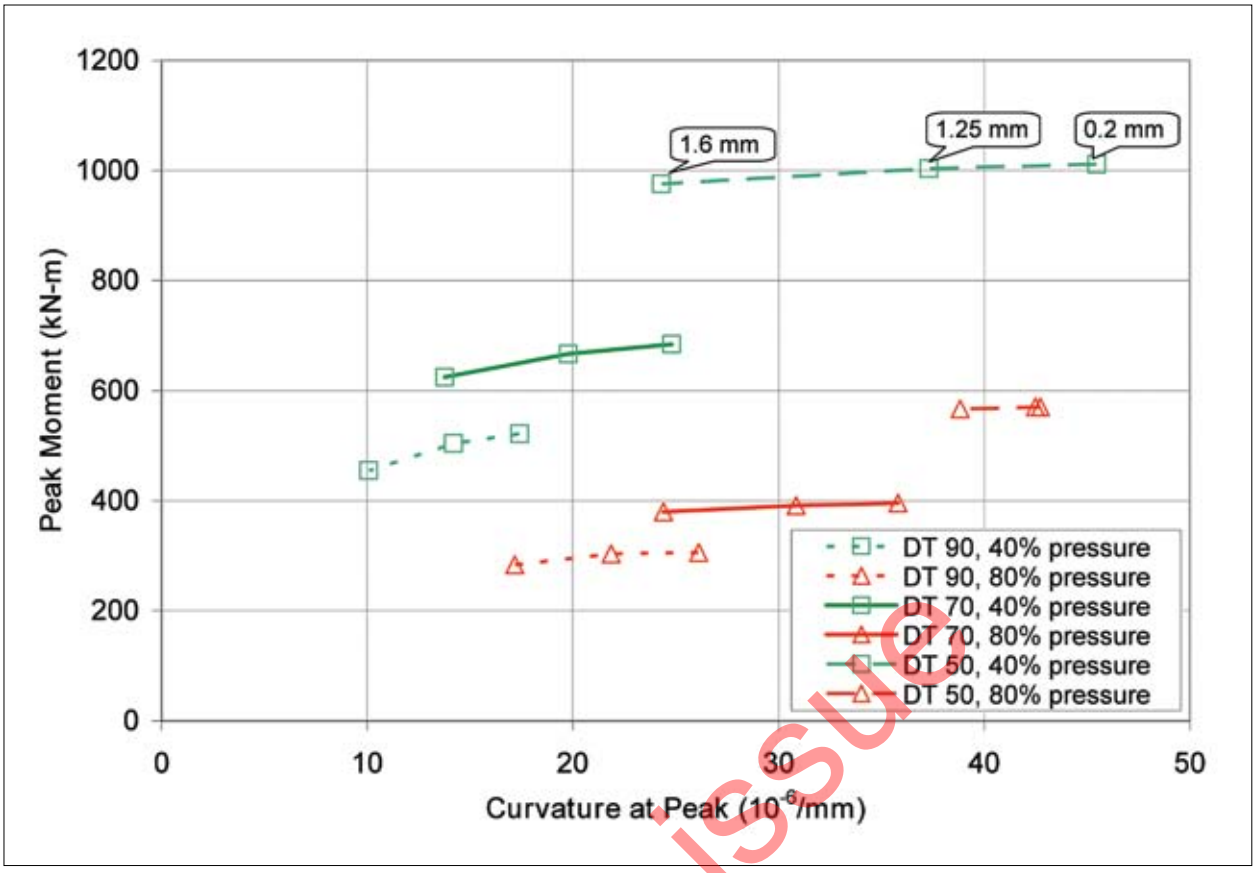

Fig.6. Combined effect of misalignment amplitudes (misalignment orientation = 0°) and internal pressure for pipeline with varying D/t ratio.

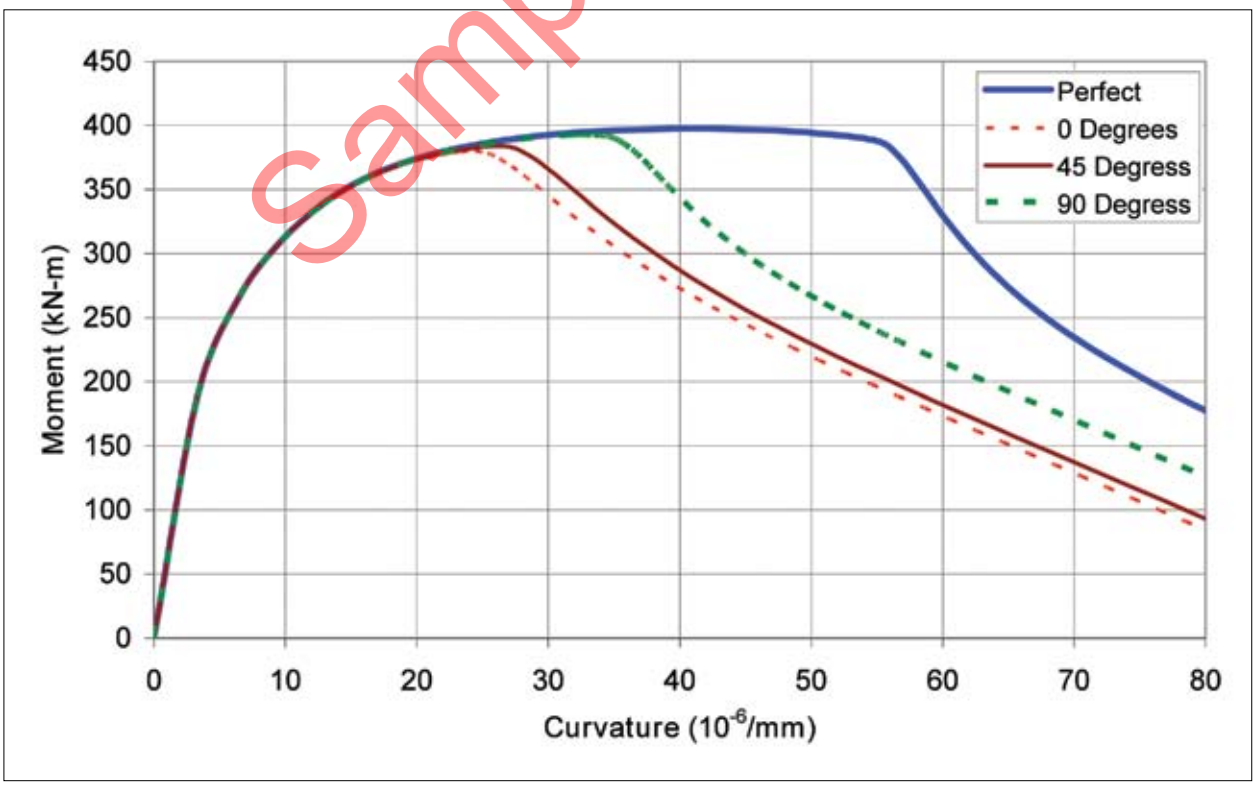

Fig.7. Moment-curvature response for a pipeline (D/t = 70, pressure = 80%, and misalignment = 1.6 mm) with different misalignment orientations.

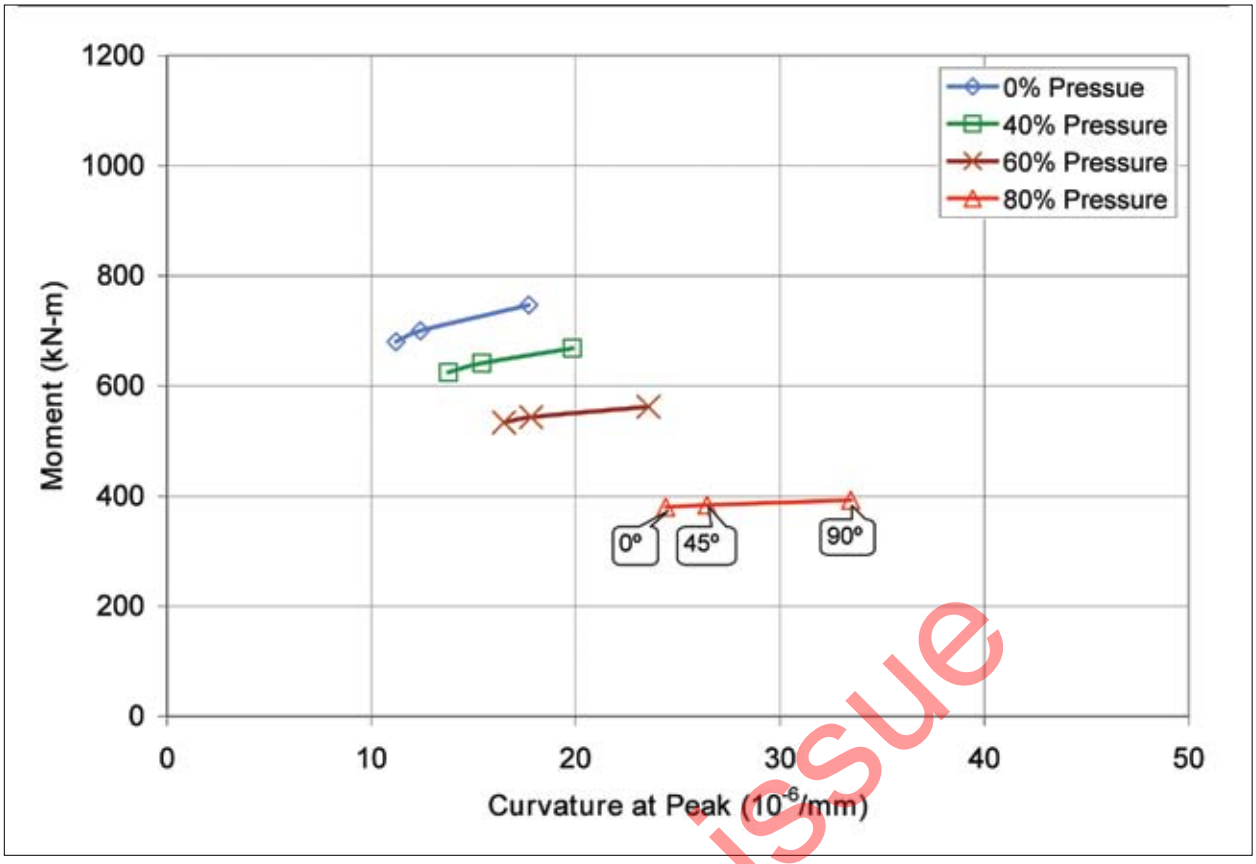

Fig.8. Combined effect of misalignment orientations (misalignment amplitude = 1.6 mm) and internal pressure for pipeline with D/t of 70.

were misalignment amplitude, misalignment orientation, internal pressure, axial force, and diameter-to-wall thickness ratio. For Case 1, the effect of internal pressure for varying misalignment amplitudes and orientations was studied. Case 1 was divided into two study groups: Group 1 examined the effect of internal pressure for varying misalignment amplitudes with the misalignment orientation in the vertical orientation (0°); Group 2 investigated the effect of internal pressure for various misalignment orientations with the misalignment amplitude kept constant at 1.6mm. Case 2 examined the effect of compressive and tensile axial force on the pipeline response with constant internal pressure and varying misalignment amplitude in the vertical orientation (0°). A pressure stress ratio (σ_h/σ_y) used in this study represents the fraction of hoop stress (σ_h) with respect to the specified minimum yield stress (σ_y). Over 80 analyses were conducted for all four cases: Table 1 summarizes the parametric study conducted here.

Effect of internal pressure

The pressure is first applied in an initial step before imposing the curvature. Since the pressure here is applied as a fraction of the yield hoop stress, the pipeline remains elastic after applying the internal pressure field. The pipeline deforms plastically during the imposition of end rotation.

Figure 3 presents the moment-curvature relationships for a pipe with a D/t ratio of 70 and a misalignment of 1.6mm in the 0° orientation as a function of internal pressure. For these parameters, increasing internal pressure decreases the pipeline moment capacity, but stabilizes the moment curvature response, and shifts the onset of strain softening to initiate at higher curvature. Figure 4 illustrates the moment-curvature response for a pipeline with a D/t ratio of 70 and 60% internal pressure as a function of misalignment amplitudes. The introduction of a small misalignment amplitude (of 0.2mm) had limited influence on the ultimate moment capacity but decreased the pipeline curvature (strain) limit at the descending branch (strain localization) of the moment-curvature diagram by 75%. In comparison with the perfect pipeline geometry (no imperfection) analysis case, the maximum 1.6mm misalignment amplitude decreased the limit moment by a factor of 0.9 and the pipeline curvature (strain) limit by a factor of 0.40.

The effect of misalignment amplitude and internal pressure on the peak moment and its corresponding global curvature is shown in Fig.5 for a pipe with a D/t of 70; for these parameters, at high internal pressure, the misalignment amplitude does not have a major influence on the ultimate peak moment. For low internal pressure (≥ 40%), the increase in misalignment amplitude decreases the-peak moment capacity, but not significantly. For instance, a drop of about 11% in the moment capacity was observed in the non-pressurized pipe between 0.2mm and 1.6mm misalignment offsets, compared to a drop of only 4% in moment capacity for 80% ratio pressurized pipes. The increase in misalignment amplitude, however; does reduce

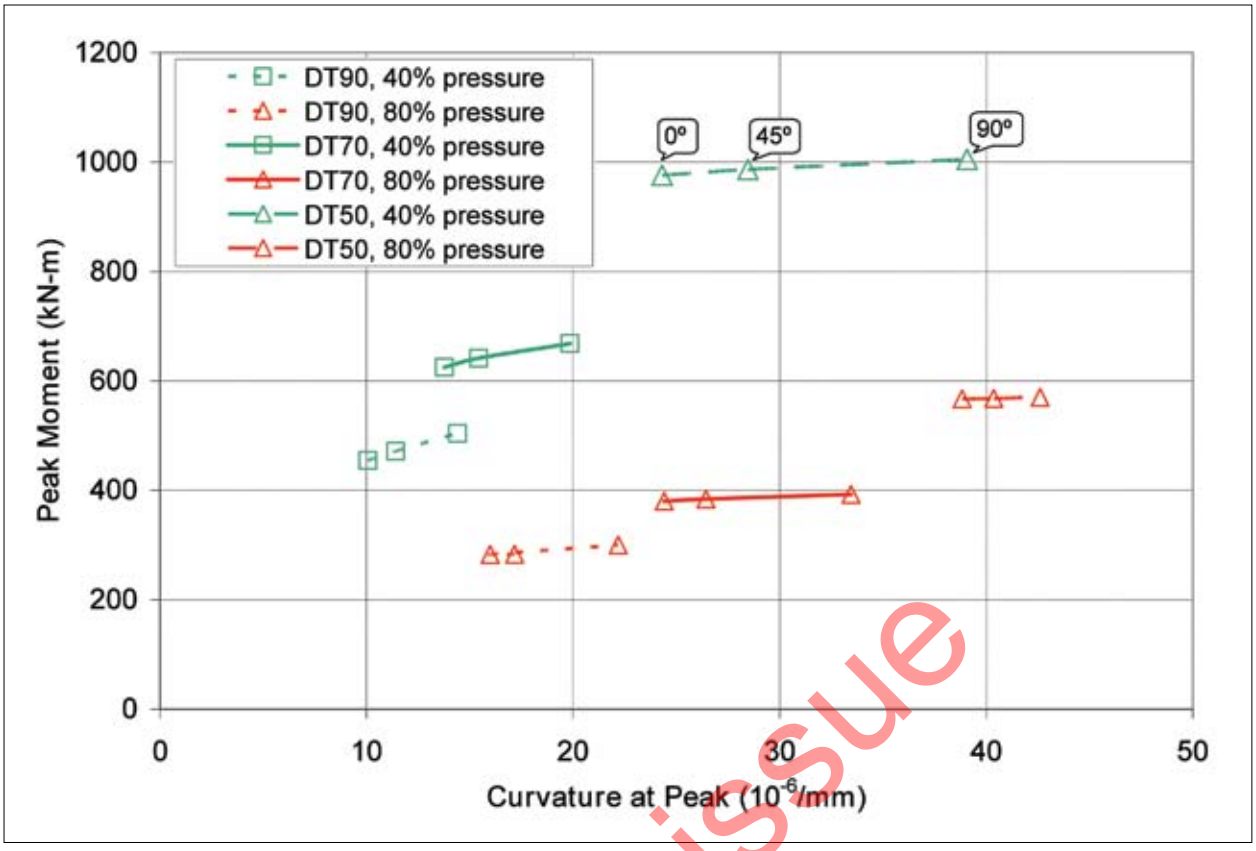

Fig.9. Combined effect of misalignment orientations (misalignment amplitude = 1.6 mm) and internal pressure for pipeline with varying D/t ratio.

the yielding prior to strain localization of the pipeline and changes the point of softening initiation for all ranges of internal pressure considered. For instance, a drop of about 46% and 32% in the strain at limit point between 0.2mm and 1.6mm misalignment was observed for the non-pressurized pipe and 80% pressurized pipe, respectively.

The study was extended to investigate the effect of the diameter-to-wall-thickness ratio (D/t). It was seen that the same behaviour continues to be valid for higher and lower D/t ratios. There was a slight change in the rate of moment capacity reduction for the low pressurized pipes; that is, as the D/t ratio increased, the drop in the ultimate moment capacity increased. For the 40% internal pressurized pipes, a drop of 3.7%, 9.6%, and 14.7% in the moment capacity was observed for D/t ratios of 50, 70, and 90, respectively. These values were calculated for misalignment amplitudes in the range of 0.2mm to 1.6mm, as shown in Fig.6. The figure also shows an upward shift in the curves as the D/t ratio increases due to the increase in the moment capacity for thicker pipes, and forward shift in the curves as the internal pressure ratio increases due to the more stable response of the pipeline, as discussed earlier. It is noted that the response of pipelines with a D/t ratio of 50 and 80% internal pressure changes, the peak moment does not occur at the point of strain localization. However, the moment-curvature response shows a yield plateau and the softening point occurs at higher values.

The moment-curvature response for pipelines with a D/t of 70, internal pressure of 80%, and misalignment offset of 1.6mm as a function of misalignment orientations is illustrated in Fig.7. The figure shows that the 0o misalignment orientation is the most critical case. It is also noted that there is a negligible effect between the 0° and 45° misalignment orientation. For the 90° offset orientation, the pipeline response shows higher ultimate moment capacity and also higher ductility.

The combined effect of misalignment orientation and internal pressure for pipelines with a D/t ratio of 70 is shown in Fig.8. The figure shows a similar pattern to the one observed between misalignment amplitude and internal pressure. For high internal pressure ratios, the misalignment orientation only affected the deformation capacity of the pipeline and the moment capacity was almost unaffected. For the low internal pressure ratios, however, some moment reduction in the pipeline capacity was noted along with the drop in the deformation capacity.

The D/t ratio effect was also extended for the misalignment orientation effect. Figure 9 shows the peak moment to the curvature at peak relationship for D/t ratios of 50, 70, and 90. It is noted that the pipes with higher and lower D/t ratios still behave in the same manner as discussed earlier in Fig.6. The rate at which the peak moment decreases with increasing misalignment amplitudes varies as the D/t changes, as it tends to change at a higher rate for larger D/t ratios.

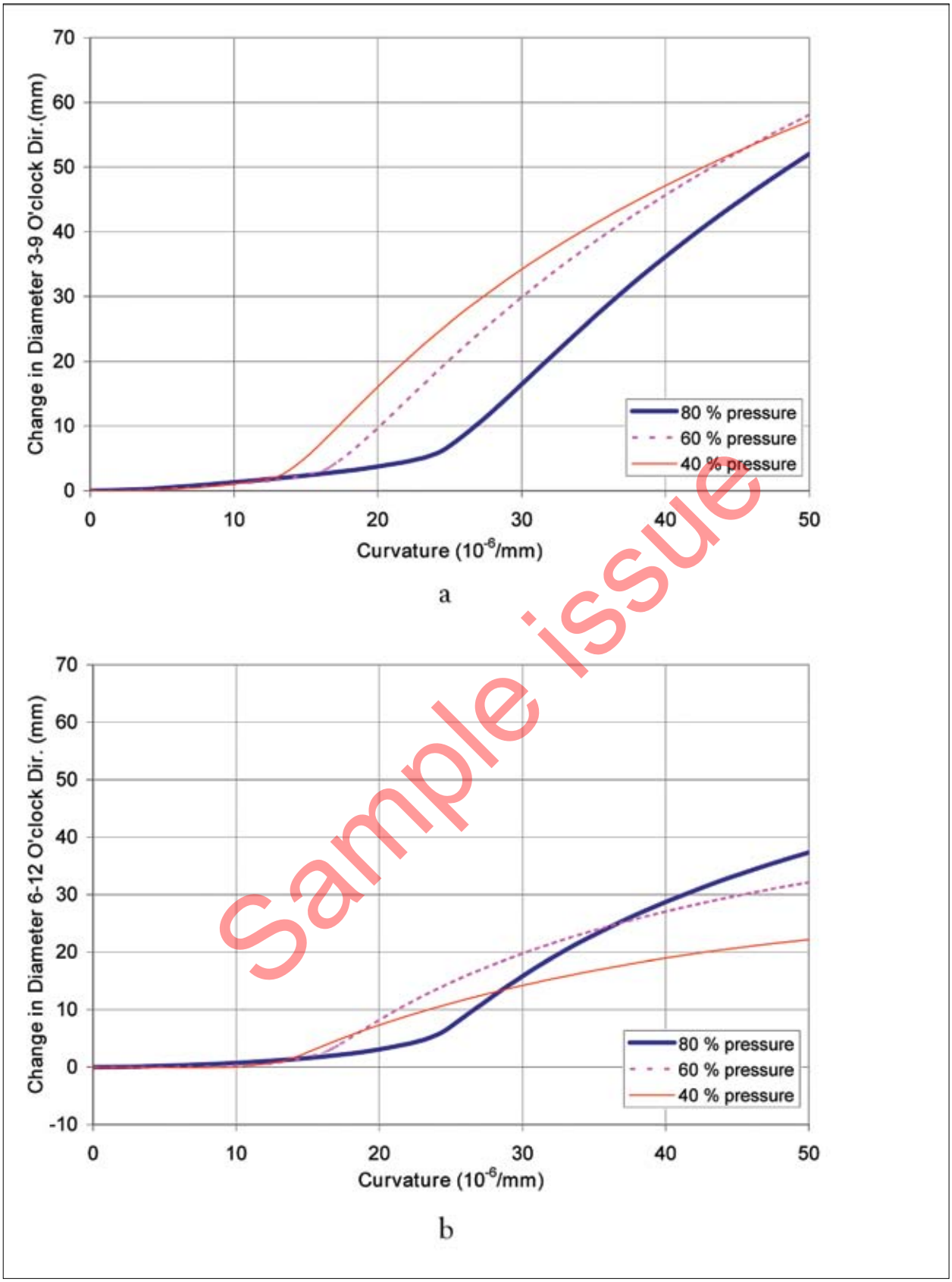

Fig.10. Influence of internal pressure and misalignment (misalignment amplitude = 1.6 mm and misalignment orientation = 0°) on change in diameter; (a - top) 3-9 o'clock direction, (b - bottom) 6-12 o'clock direction.

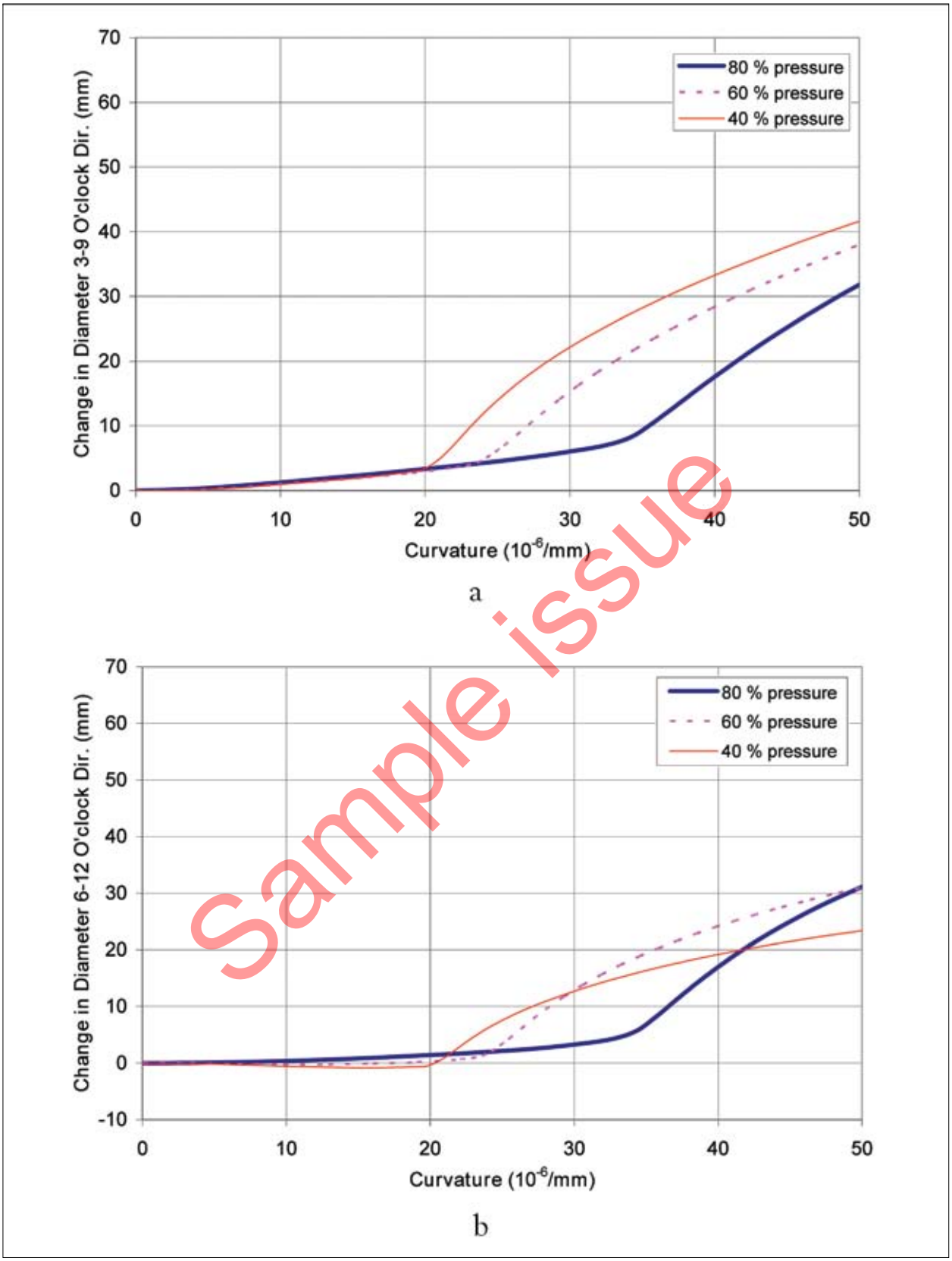

Fig. 11. Influence of internal pressure and misalignment (misalignment amplitude = 1.6 mm and misalignment orientation = 90°) on change in diameter; (a - top) 3-9 o'clock direction, (b - bottom) 6-12 o'clock direction.

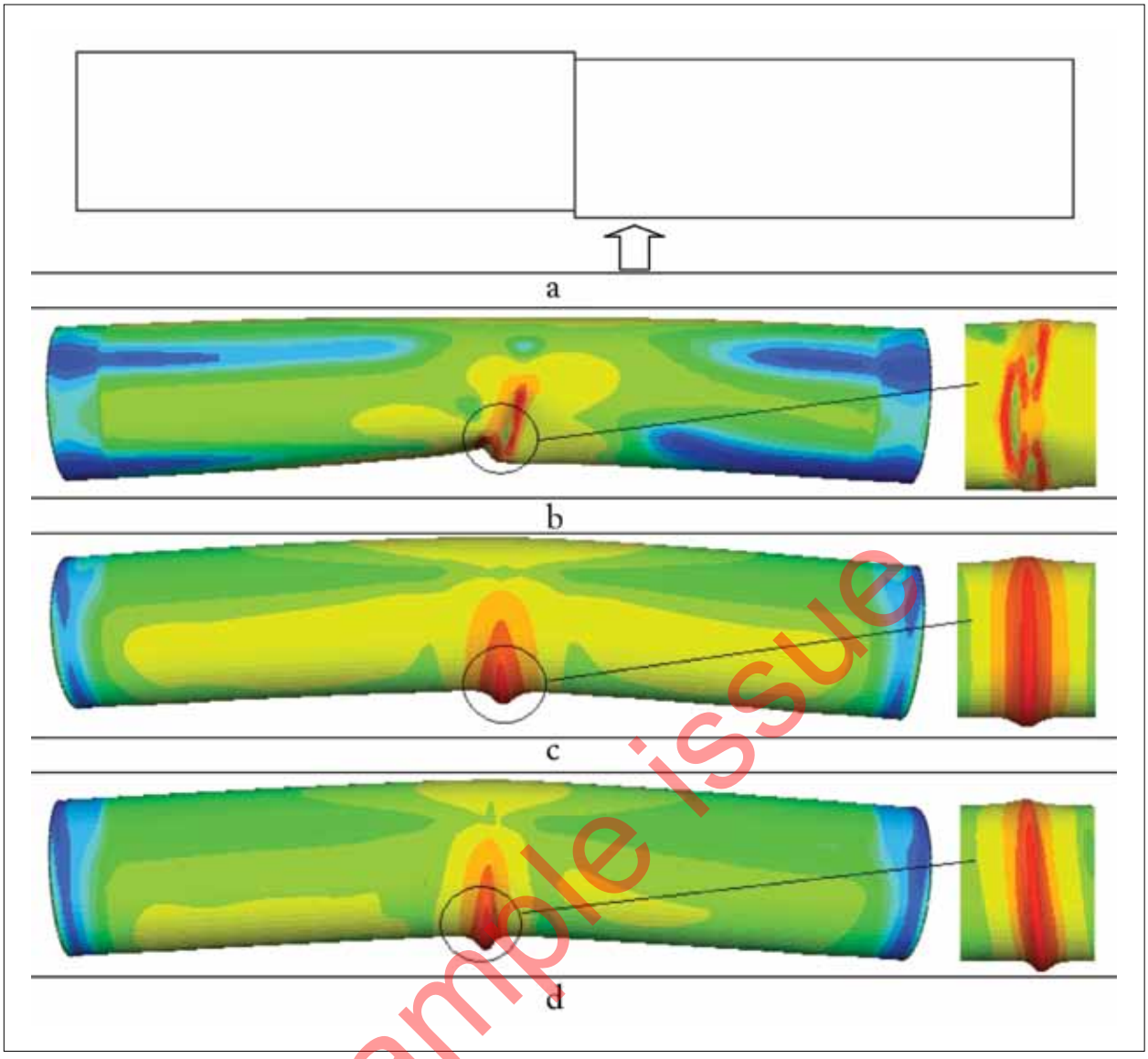

Fig. l 2. Deformed shapes of pipelines and shape of the buckle bulge (top-bottom)
a: location of the buckle relative to pipe misalignment
b: non-pressurized pipe
c: pressurized pipe with 0° misalignment
d: pressurized pipe with 90° misalignment

The change in the pipeline section was also studied at the buckle for the pressurized pipes. The non-pressurized pipe section's behaviour was not considered, as it had a non-uniform inward buckle. In fact, due to the complex shape of the local buckling, the assessment of change in diameter is very difficult (see Fig.13). Figures 14 and 15 show the change in diameter in the 3-9 o'clock and the 6-12 o'clock directions for 1.6-mm misalignment offset and 0° and 90°orientations, respectively. It is observed that the change in 3-9 o'clock direction appears as two linear regions: a region before buckling initiation which has the same slope for all pressures, and a region after buckling initiation which has an increasing slope as the pressure increases.

As for the section change in the 6-12 o'clock direction (Fig.15), the change in diameter also appears to have two linear regions. The initial region has a slope that slightly increases as the pressure increases. The figure also shows that the change in diameter in the 6-12 o'clock direction is small before buckling initiation for the lower pressurized pipes. It is also observed that, for the 90° misalignment orientation, the slope is negative, which indicates that the pipe tends to bulge inward before strain localization for the lower-pressurized pipes. The second region, after buckling initiation, is somewhat linear and the slope increase as the pressure increases.

It was also noted that the buckle always occurs for the 0° and 45° oriented misalignment, and is symmetrical on the girth weld for the 90° oriented misalignment. Figure 12 shows the buckle shapes for non-pressurized pipe and pressurized 0° and 90° oriented misalignment pipes.

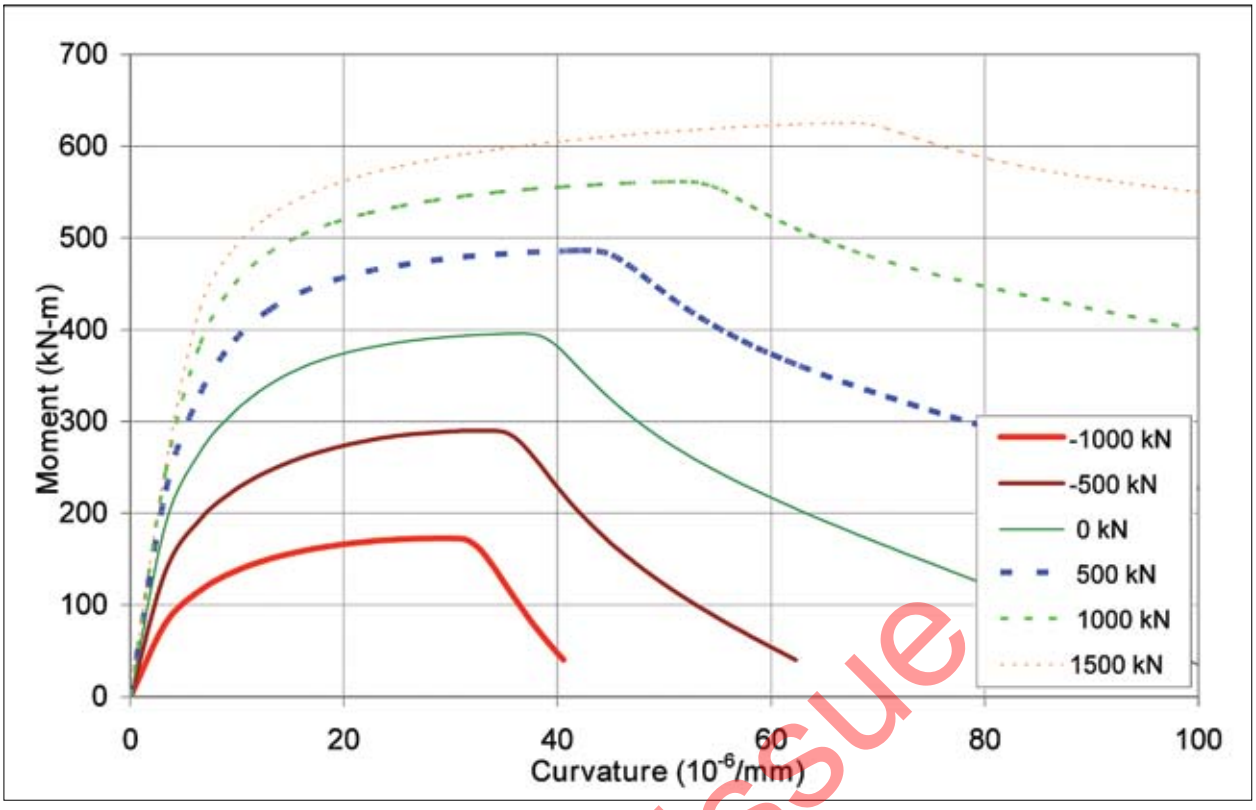

Fig. 13. Moment-curvature response for a pipeline (D/t = 70, pressure = 80%, misalignment = 1.6 mm, and offset orientation = 0°) with varying tensile and compressive axial loads.

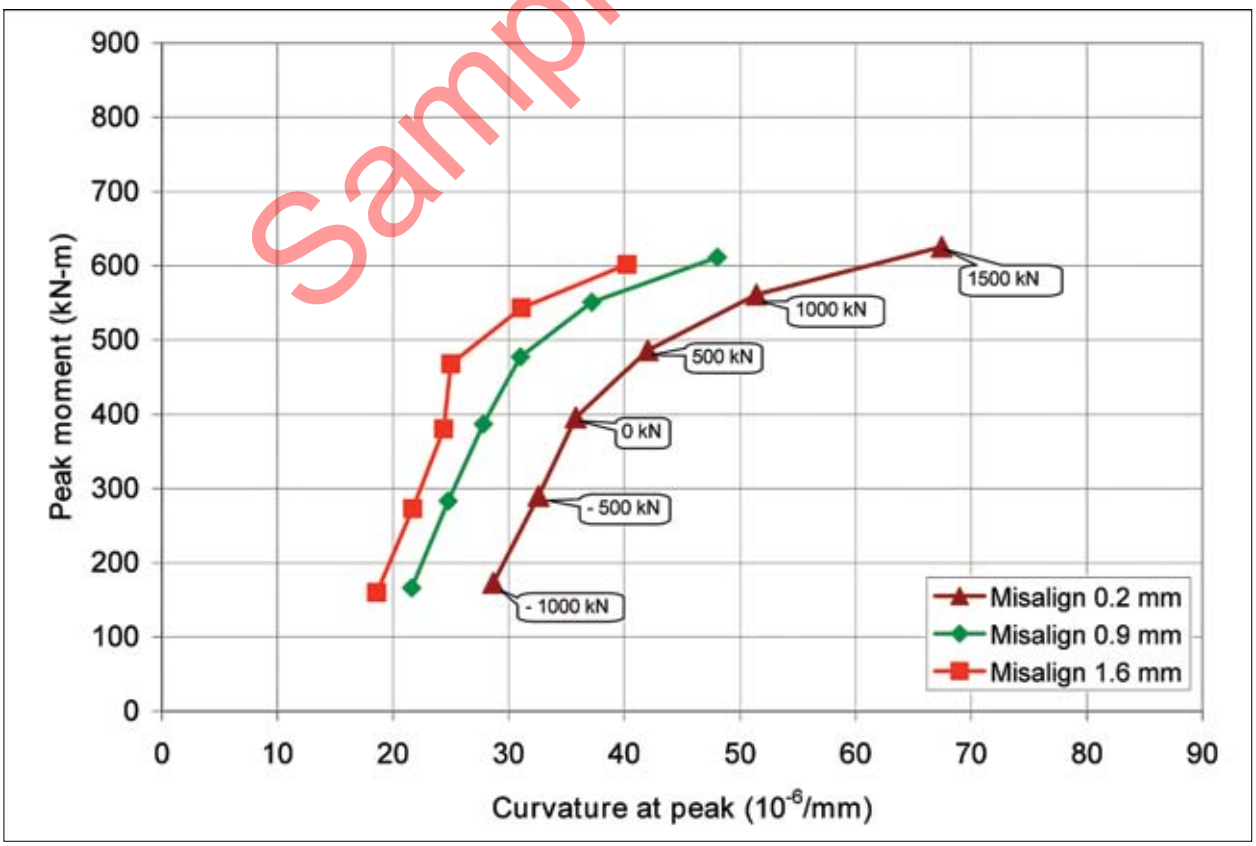

Fig. 14. Combined effect of misalignment amplitude (misalignment orientation = 0°) and axial force for pipeline with D/t of 70.

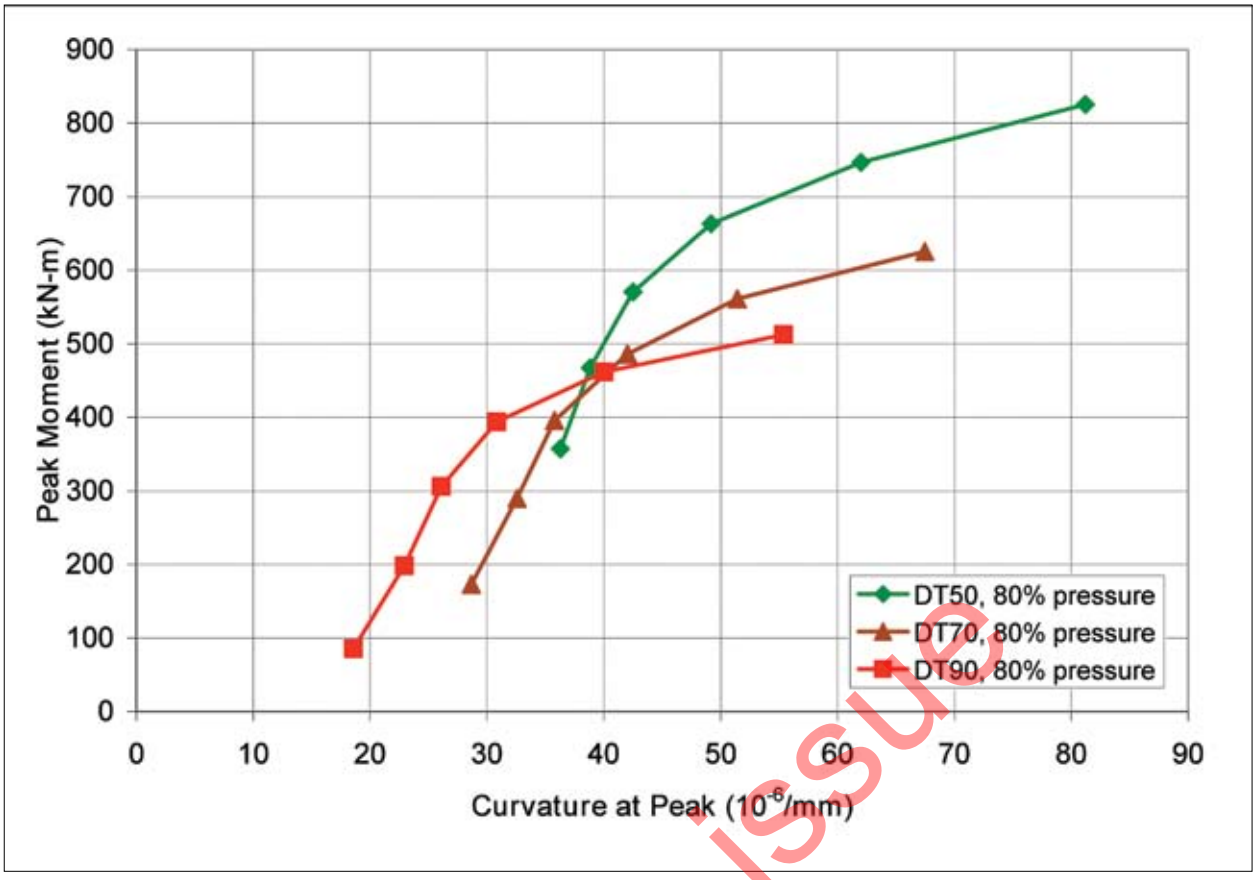

Fig.15. Combined effect of misalignment (misalignment amplitude = 0.2mm) misalignment orientation = 0°) and axial force for pipeline with varying D/t ratios.

Effect of axial load

The effect of axial force on the moment-curvature response was investigated with the internal pressure held constant at 80% of the hoop stress capacity of the section. This was done to keep in line with the previous study performed by Fatemi *et al.* [5] for ideal pipelines, to be able to draw conclusions.

The axial loads applied in this investigation were from 500 to 1500kN in tension with 500-kN increments, and 500kN and 1000kN in compression, where 500kN, 1000kN, and 1500kN represent 10%, 20%, and 30% of the elastic axial capacity of the pipeline section, respectively. Considering the von Mises' criterion for the biaxial state of stress adopted here, the section still remains in the elastic regime after the application of both pressure and any of the axial loads mentioned above.

As shown in Fig.10, the increase in the tensile axial load increased the ultimate moment capacity of the pipe, and the increase in the compressive axial load decreased the ultimate moment capacity. The tensile axial load also increased the curvature at the softening point initiation, whereas the compressive axial load decreased the curvature for the softening point initiation. This is consistent with the study conducted by Fatemi *et al.* [5].

The effect of misalignment amplitude on the axially-loaded pipes with end rotation is shown in Fig.11, in which it is observed that the increase in the misalignment amplitude has no effect on the ultimate moment capacity of the pipe. The misalignment amplitude only affected the value of the curvature at which the peak moment occurred. Figure 11 also shows that the relationship between peak moment and curvature at peak for increasing compressive loads is linear.

The effect of D/t ratio was also studied for the axially-load pipelines, and Fig.12 illustrates the relationship between peak moment and curvature at peak for pipes with D/t ratios of 50, 70, and 90. The same general behaviour is observed for the higher and lower D/t ratios pipelines.

Conclusion

This paper presented the details and the results for a parametric study on the effect of weld misalignment on the local buckling response of pipelines. The paper investigated the effect on misalignment amplitude and orientation, internal pressure, and axial force on the local buckling response of girth-welded pipeline. The study concluded:

- Misalignment imperfection has a detrimental effect on both the load capacity and the deformation capacity of the pipeline.

- Depending on the internal pressure ratio and the misalignment amplitude, a reduction of up to 10% in the moment capacity is observed.
- Depending on the internal pressure ratio and the misalignment amplitude, a reduction of up to approx. 50% in the deformation capacity (curvature at peak moment) is also observed.
- Misalignment orientation of 0° is the most critical misalignment orientation. Misalignment orientations 0° and 45° show a very similar effect on the pipeline behaviour.
- Increasing the internal pressure results in reduction in load capacity and increases in the curvature at limit load, and therefore a more stable pipeline response.
- Increasing the compressive axial force results in reductions in both the load capacity and the curvature at the limit point. Increasing the tensile axial force results in increases in both the load capacity and the curvature at the limit point.

Acknowledgement

The financial support from C-CORE and Canadian Research Network for Mathematics of Information Technology and Complex Systems (MITACS) is gratefully appreciated.

References

1. A.Fatemi, S.Kenny, and F.Taheri, 2007. Continuum finite element methods to establish compressive strain limits for offshore pipelines in ice gouge environments. Proc. Offshore Mechanics and Arctic Engineering Conf., paper 29152, San Diego, California.
2. N.Yoosef-Ghodsi, G.L.Kulak, and D.W.Murray, 1995. Some test results for wrinkling of girth welded line pipe. Proc. OMAE, **V**, pp379-387.
3. A.B.Dorey, D.W.Murray, and J.J.R.Cheng, 2006. Initial imperfection models for segments of line pipe. *Journal* OMAE, **128**, pp322 329.
4. A.B.Dorey, D.W.Murray, and J.J.R.Cheng, 2006. Critical buckling strain equations for energy pipelines – a parametric study. Ibid.,**128**, pp248 255.
5. E.Torselletti, L.Vitali, and R.Bruschi, 2005. Bending capacity of girth-welded pipes. Proc. Offshore Mechanics and Arctic Engineering Conf., Halkidiki, Greece, **3**, pp 619-627.
6. Hibbit, Karlson & Sorensen, Inc., 2006. ABAQUS/Standard Version 6.6-4 software package, Hibbit, Karlson & Sorensen, Inc., Pawtucket, RI, USA.
7. A.Fatemi, S.Kenny, N.Cheraghi, and F.Taheri, 2006. Parametric study on the local buckling response of pipelines under combined loading conditions. *J. of Pipeline Integrity*, **5**, **4**, pp 197-212.
8. CSA Z662, 2003. Oil and gas pipeline systems. Canadian Standards Association.
9. API 5L, 2000. Specification for line pipe, 42nd. Edn, American Petroleum Institute.
10. N.Yoosef-Ghodsi, G.L.Kulak, and D.W.Murray, 1994. Behavior of girth-welded line pipe. Structural Report No. 203, Department of Civil Engineering, Univ. of Alberta, Edmonton, Canada.

Thickness limits for welded joints between pipes of different yield strengths

by Dr Michael Law[1*], Peter Tuft[2], and Phillip Venton[3]

1 Australian Nuclear Science & Technology Organization, Materials Division, Menai, NSW, Australia
2 Peter Tuft & Associates, West Pymble, NSW, Australia
3 Venton & Associates Pty Ltd, Bundanoon, NSW, Australia

WHERE TWO PIPES of unequal strength are joined, any thickness variation may be accommodated by a taper on the thicker weak pipe. Codes currently limit the grade variation to a yield strength ratio of 1.5. All possible combinations of grades were examined by finite-element modelling and all transitions withstood pressures > 114% SMYS of the stronger thin pipe material. The same joints under tensile axial load fail at a stresses below the SMYS of the thin pipe. Compressive axial load significantly reduces the pressure capacity. The use of the 1:4 taper is satisfactory. The current grade ratio limits should not be relaxed without validation testing.

WHEN TWO PIPES of different thicknesses are joined, the wall of the thicker pipe is machined so that there is a tapered transition in wall thickness to minimize stress concentrations at the joint with the thinner pipe. When the thickness difference is a consequence of different material strengths, the thickness in the tapered transition region of the thicker (lower-strength) pipe is less than the pressure-design thickness of the thick, lower-strength pipe. This apparent lack of strength is acceptable because of the support from the full-thickness sections on either side of the transition, known as the 'bridging effect'.

This paper was presented at the Pipeline Technology Conference held in Ostend in October, 2009, and organized by the University of Gent.

*Author's contact details:
tel: +61 2971 79102
email: mlx@ansto.gov.au

The Australian pipeline design standard (AS 2885) requires that the pipe pressure-design thickness is calculated using a maximum design factor of 0.80. However at any location, the pipe thickness must be designed to accommodate all identified loads at that location. In high-consequence locations the pipe must be 'no rupture', and in the event of puncture the maximum energy release rate from a credible puncture event must be less than 10GJ/s (in residential) and 1GJ/s (in high-density) areas.

This has resulted in a need to provide relatively-short lengths of 'thick', low-strength pipe adjacent to long lengths of 'thin', high-strength pipe to manage the external interference risk. The usual design approach is to provide a 'transition' joint of intermediate grade and thickness that have been selected to achieve compliance with the requirements of Fig.1. Unfortunately these joints are often not purchased,

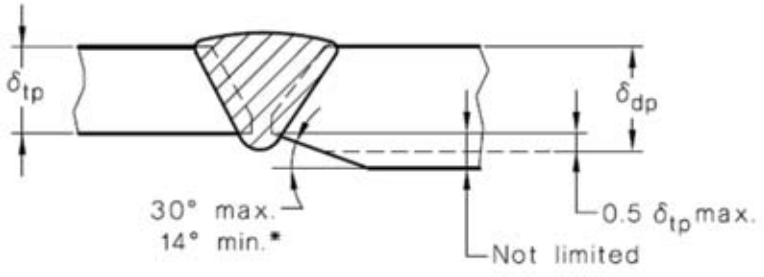

Figure 1 Weld preparation from AS2885.2-2007

- δ_{tp} = *nominal wall thickness of thin pipe*
- δ_{dp} = *thickness for design internal pressure.*

	Thick pipe or fitting grade							
Thin pipe grade	B	X42	X46	X52	X56	X60	X65	X70
X80	2.28	1.90	1.73	1.54	1.42	1.34	1.23	1.14
X70	2.00	1.67	1.52	1.35	1.25	1.17	1.07	
X65	1.86	1.55	1.41	1.25	1.16	1.09		
X60	1.71	1.42	1.29	1.15	1.06			
X56	1.60	1.33	1.22	1.08				
X52	1.49	1.24	1.13					
X46	1.31	1.10						
X42	1.20							

Table 1. Yield-strength ratio of SMYS for various pipe combinations.

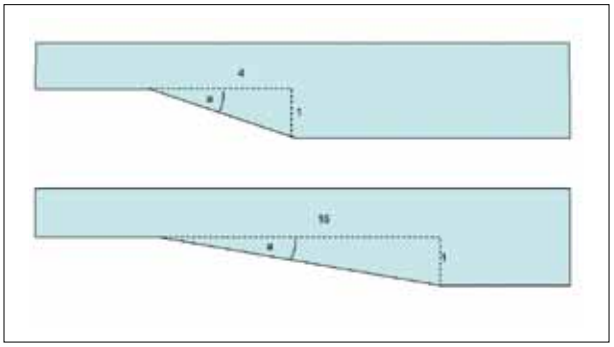

Fig.2. (Top) steep 4:1 taper with a = 14°; (Bottom) gentle 8:1 taper with a = 7°.

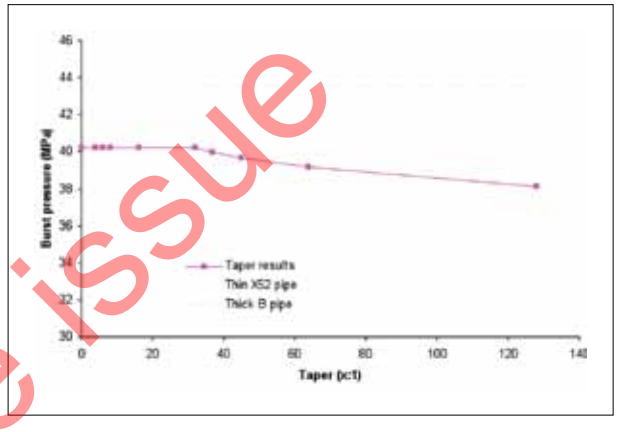

Fig.3. Burst pressure and taper ratio.

or are too difficult to locate, and a crisis occurs at a critical time in the construction schedule.

The frequency of this problem prompted a research project to re-assess this limitation using FEA techniques, and if required, with experimental validation.

AS 2885.2 (Welding) has the following requirements (illustrated in Fig.1) for the design of welded joints between pipes having different pressure-design thicknesses: "In the case of the thicker component, the thickness for design internal pressure shall not be greater than 1.5 times the nominal thickness of the thinner component."

The maximum thickness of the thicker pipe is not limited; however, the pressure design thickness is limited, and depends on its strength. (Note: throughout the remainder of the paper, the material strength is referred to by its API 5L grade, and its associated specified minimum yield strength). Thus, the grade ratio between the thin and the thick pipe is limited to 1.5:1. If the grade ratio can be safely increased, then it will save both time and cost in completing many pipeline projects. Pipe grade combinations which cannot currently be joined are termed 'non-complying' and are noted with grey highlight (Table 1).

Tapers can be defined as sharp, or gentle (Fig.2), with gentle tapers having a lower slope and longer length for the same section change.

Previous work

George and Rodabaugh [1] introduced the concept of the bridging effect, where the stronger or thicker material on either side of the taper supports the under-strength material in the taper. Testing involved an end-capped vessel made from X52 and B grade (a grade ratio of 1.49) pipe with tapers of 4, 8, and 16:1.

The testing was inconclusive because none of the transitions failed. The paper recommended a taper of 4:1 based on measured strains in the tapers during testing. The recommended minimum allowable slope of the taper was 16:1; no specific recommendation of grade ratios are included in this paper. Zhu and Leis [2] ignored the taper and looked at failure in the thick and thin pipe only, proposing that failure would occur in the thin pipe when: UTS2/UTS1 > t1/t2. Based on this criterion, if the thick and thin pipe were designed to the same pressure and design factor, failure will always occur in

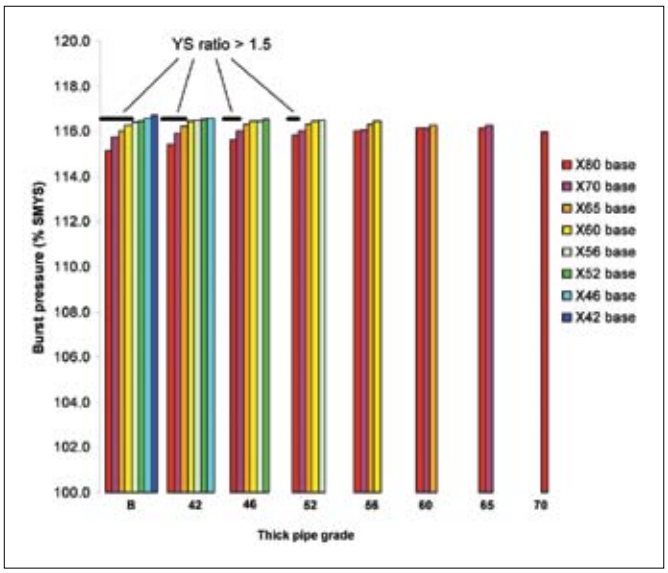

Fig.4. Burst pressure (%SMYS of the thin pipe), with non-complying joints marked.

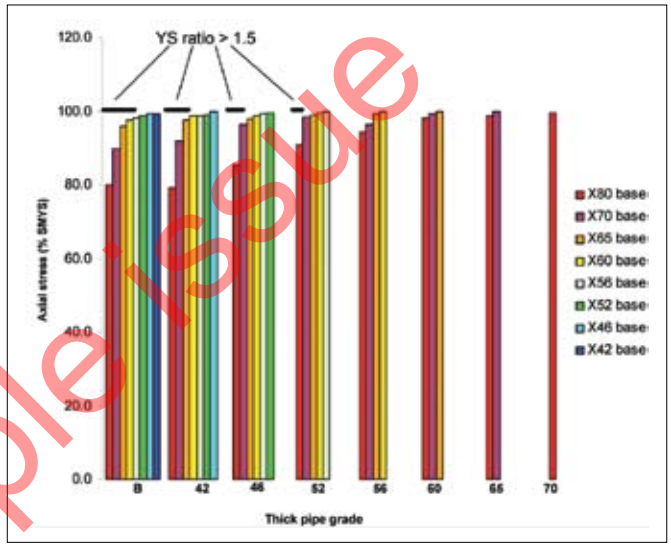

Fig.5. Axial failure stress (%SMYS of the thin pipe) with non-complying joints marked; D/t = 55.

Table 2. Burst pressure comparison (% SMYS).

	Complying YS ratio < 1.5	Non-complying YS ratio > 1.5
Maximum	117	116
Minimum	116	115

the thicker pipe unless it exceeds the design thickness. This paper does not take the bridging effect, discussed above, into account.

Finite-element analysis of George and Rodabaugh pressure vessel testing

As an initial check for this research, an FEA model of the test vessel used in the George and Rodabaugh work, using true-stress/true-strain data based on the published material properties, predicted failure at 41.3MPa (161% SMYS) in the 16:1 taper.

In George and Rodabaugh's testing, the X52 pipe burst at 40.2 MPa (157% SMYS) in a section of pipe wall approximately 230mm from the nearest taper. Failure in the pipe wall rather than in the taper indicates that, singly or combined, a defect, material-property variation, or wall-thickness variation may have occurred in the test, and caused the difference between the FEA model and the reported test result.

The transition joints were also modelled (by FEA) with the tapers used in the test (4:1, 8:1, 16:1), and also with additional tapers of 32, 64 and 128:1.

The FEA modelling (Fig.3) demonstrated that the taper did not affect the burst pressure – for tapers gentler than

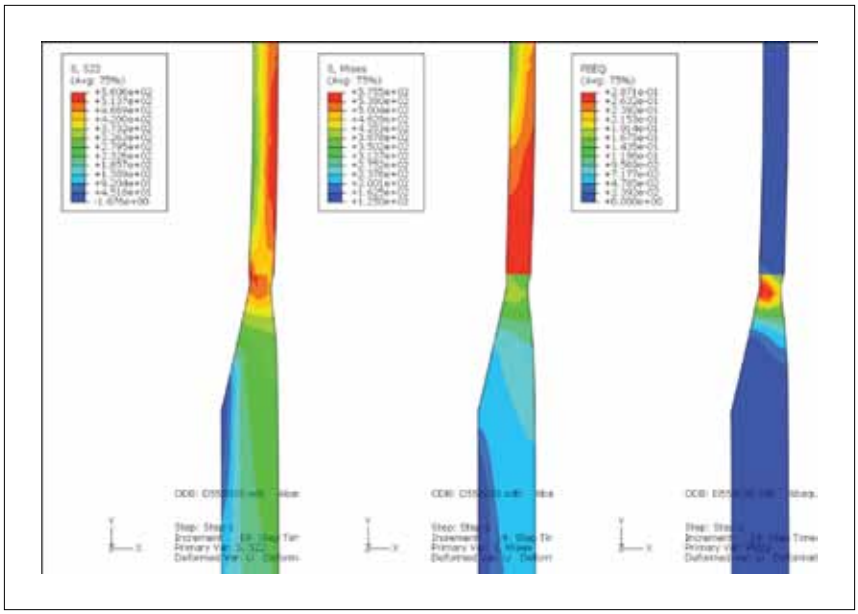

Fig.6. X80 – grade-B transition at 79.9% SMYS axial load showing (left) axial stress, (centre) von Mises' stress, and (right) plastic strain.

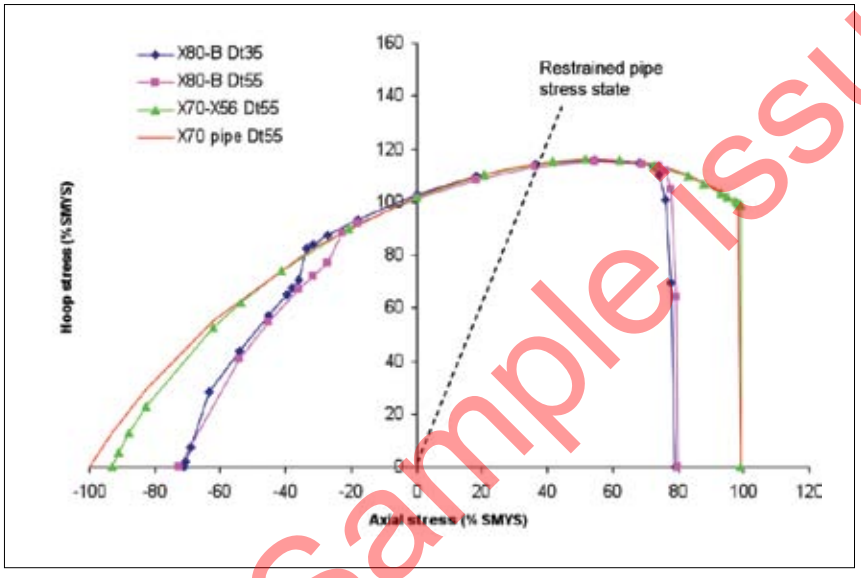

Fig.7. Failure envelopes in terms of SMYS of the thin pipe.

approximately 32:1 – for the material properties used here. This implies that the commonly-used taper of 4:1 does not reduce transition strength.

FEA modelling

Having calibrated the FEA model against the George and Rodabaugh test, axisymmetric modelling was undertaken on all grade combinations with D/t ratios (for the thin pipe) of 35, 55, and 100. In the following sections, only results for a D/t ratio of 55 are presented, other D/t ratio results followed similar trends. The SMYS and SMTS for the grades were used as standardized material properties.

FEA modelling: pressure loading only

All the grade combinations shown in Table 1 were modelled with a D/t ratio of 55 for the thin pipe; in Fig.4, the SMYS is with respect to the thin pipe, and the taper was 4:1.

All the grade combinations had burst pressures of between 115 and 117% SMYS. The differences between grade combinations allowable under AS2885.2, and those not allowed, are small (Table 2). The lowest failure pressure in all cases was with grade-B material in the thicker pipe, due to the increased length of the taper giving a greater length of under-strength lower-grade pipe.

FEA modelling: axial loading only

All the joints were subject to axial loading with no internal pressure (as the unpressurized pipes give the lowest failure strains). As shown in Fig.5, all the pipes failed in the taper at between 79% and 100% SMYS axial stress (of the thin pipe), at an average strain > 0.14% strain. This axial stress may occur as pure tension or, as the tension component of bending. There is only minimal support from the stronger sections (unlike in the pressure case), and thus the failure stresses are below SMYS.

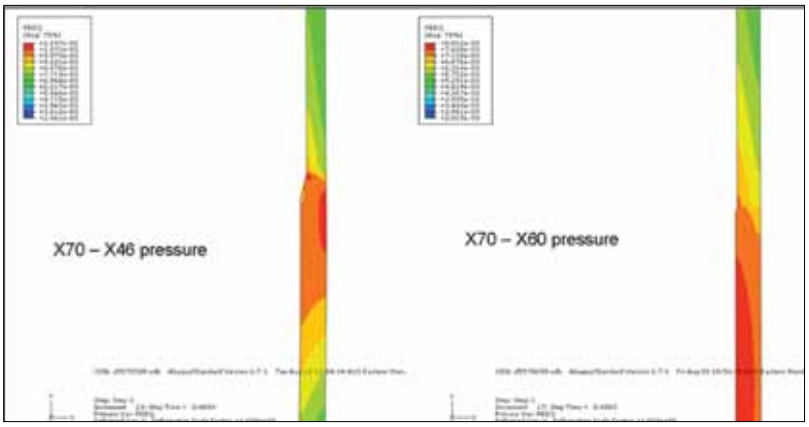

Fig.8.The failure position under pressure in the X70-X46 joint is in the taper; in the X70-X60 joint, the failure is in the thick X60 pipe.

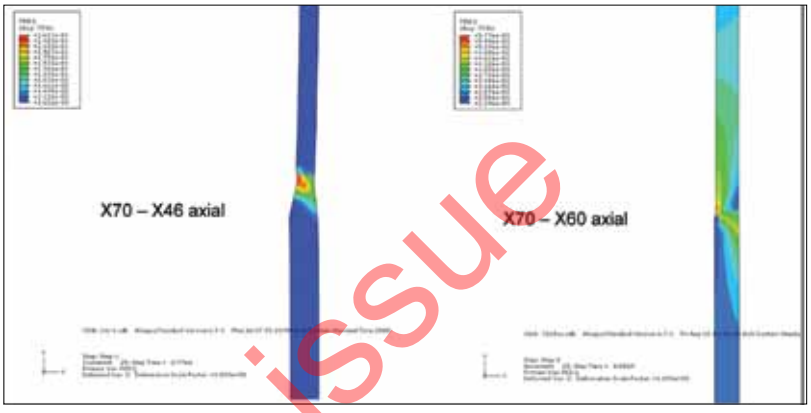

Fig.9.The failure position under axial tension is in the taper for both X70-X46 and X70-X60 joints.

Though failure occurs below the SMYS of the thin pipe, the axial stresses are high compared to the thick pipe. Figure 6 shows that an X80 to grade-B joint fails at 79.9% SMYS of the X80, equivalent to an average of 442MPa, well above the UTS of 414MPa for the grade-B material. In fact, the axial stress is locally as high as 510MPa in the grade-B material transition. As the material fails by plastic collapse, this is driven by the von Mises' stress.

The hoop stress is tensile, which reduces the von Mises' stress to below the value of the axial stress. In the taper, made of grade-B material, the von-Mises' stress is a maximum of around 360MPa which it can withstand, though there is considerable localized plastic strain. The non-complying joints showed lower failure stresses under axial load, and the lowest average axial failure strains were in the complying X42 to grade-B combination (Table 3).

FEA modelling: combined axial plus pressure loading for restrained pipe

Models of X80 – grade-B transitions with D/t ratios of 35 and 55, an X70-X56 transition (with D/t of 55), and a length of plain X70 pipe (also with D/t 55) were subject to a range of axial stresses and internal pressures. All transitions were made with a 4:1 taper.

The failure envelopes (Fig.7) show typical features of the transition-joint behaviour. The dotted line shows the condition in a restrained pipe where the axial stress equals the hoop stress times a Poisson's ratio of 0.3. In a restrained pipeline, the transitions can withstand very high hoop stresses (> 114% SMYS) due to the support of the stronger sections (the bridging effect), while compressive axial stresses significantly reduce the burst pressure.

In non-complying joints (i.e. X80 – grade-B) buckling initiates at approximately 20% SMYS compression (depending on the D/t ratio), as seen by a step in the failure envelope. The buckling is initiated by an offset between the pipe centrelines. For example, in an X80 – grade-B joint at a D/t of 55 and a diameter of 457mm, the design wall thicknesses are 8.3mm for the X80 and 19.03mm for the grade B pipe, and the mid-walls are 4.15mm and 9.51mm from the outside surfaces, respectively. The offset between these mid-walls is 5.36mm, or 64% of the run pipe thickness. In complying joints (i.e. X70 - X56) buckling is not seen.

The X70 pipe (red line) envelopes all other joint behaviour. The X70-X56 joint is almost identical under axial tension, and shows a slightly lower failure pressure under axial compression. The X80 – grade-B joints are similar at axial loadings from -20% SMYS to +75% SMYS. The typical von

Table 3. FEA results for all joints at a D/t of 55, with 'non-complying' joints shown with a shaded background.

Main pipe grade	Thick pipe Grade	YS ratio	Burst pressure (% SMYS)	Axial stress (% SMYS)	Average axial strain (%)
X80	B	2.29	115.1	79.9	0.22
X80	X42	1.90	115.4	79.2	0.22
X80	X46	1.74	115.6	85.6	0.24
X80	X52	1.54	115.8	91.0	0.25
X80	X56	1.43	116.0	94.3	0.26
X80	X60	1.33	116.1	98.0	0.27
X80	X65	1.23	116.1	98.7	0.27
X80	X70	1.14	116.0	99.5	0.28
X70	B	2.00	115.8	89.8	0.22
X70	X42	1.67	115.9	91.7	0.22
X70	X46	1.52	116.0	96.5	0.23
X70	X52	1.35	116.0	98.4	0.24
X70	X56	1.25	116.0	98.5	0.23
X70	X60	1.17	116.2	99.4	0.24
X70	X65	1.08	116.3	99.7	0.24
X65	B	1.86	116.0	95.9	0.22
X65	X42	1.55	116.2	97.5	0.22
X65	X46	1.41	116.3	98.0	0.22
X65	X52	1.25	116.3	99.1	0.22
X65	X56	1.16	116.3	99.4	0.22
X65	X60	1.08	116.3	99.8	0.22
X60	B	1.71	116.3	97.6	0.20
X60	X42	1.43	116.5	98.6	0.20
X60	X46	1.30	116.5	98.7	0.20
X60	X52	1.15	116.5	99.6	0.21
X60	X56	1.07	116.5	99.8	0.21
X56	B	1.60	116.4	98.1	0.19
X56	X42	1.33	116.5	98.8	0.19
X56	X46	1.22	116.5	99.3	0.19
X56	X52	1.08	116.5	99.9	0.19
X52	B	1.49	116.4	98.7	0.18
X52	X42	1.24	116.5	99.1	0.18
X52	X46	1.13	116.5	99.6	0.18
X46	B	1.31	116.6	99.2	0.16
X46	X42	1.10	116.6	99.9	0.16
X42	B	1.20	116.7	99.2	0.14

Mises' yield envelope is truncated at high axial loads by the axial failure load in tension of approx. 80% SMYS.

FEA modelling: failure position

In complying joints under internal pressure in a restrained pipeline, failure generally initiates in the weaker pipe. In non-complying joints, the length of under-strength material becomes significant, and the failure location switches to the taper, with little change in the burst pressure (Fig.8). Under axial tension, failure initiates in the taper for all cases (Fig.9).

FEA modelling: other results

Full three-dimensional models generally replicate the axisymmetric results, with more variable results in terms of buckling. Materials with pronounced yield plateaux may initiate buckling at low bending strains. In some cases, under displacement-controlled loading, stable high bending strains may be achieved: this condition would need to be demonstrated by project-specific materials' testing and modelling.

Other axisymmetric modelling was undertaken to produce the following results:

- weld metal strength has little effect on the strength of the transition;
- yield strengths above SMYS for either pipe result in small increases in the failure stress; thus, assuming minimum material properties is conservative.

Conclusions

- Pressurized bend testing of pipes is required to validate this modelling.
- Because it is difficult to demonstrate that a pipe in service will never be exposed to axial or bending loads, the current grade ratio limits should not be relaxed unless these loads can be ruled out.
- As premature failure may be caused by compression/bending loads, restrictions must exist on any bending or additional axial stress (including temperature effects). It may be possible for a Standard to permit the limit to be relaxed where load combinations at a specific location are 'safe'. However this may be impractical.
- Transitions can withstand high pressures (> 114% SMYS of the strong thin pipe material) with all grade combinations.
- Under internal pressure, the failure location in complying joints is in the thick pipe, and moves to the taper as the yield strength exceeds 1.5, with little change in burst pressure.
- Though bridging is significant under pressure loadings, the same joint under axial load gets little support and fails below the SMYS of the thin pipe.
- Non-complying joints under AS2885.2 have the lowest axial failure stress.
- In all axial cases, failure is in the taper.
- Compressive loading (or the compression component of a bending load) significantly reduces the pressure capacity.
- The use of the 1:4 taper is satisfactory; more gentle tapers produce longer sections of lower-strength material, while shorter tapers may affect fatigue, and the ability to pig and inspect the pipeline.
- Because this analysis is model-based, it is suggested that testing of pressurized, end-capped, pipes under pressure and combined pressure-bending be undertaken to validate this work.

Acknowledgments

The work reported herein was sponsored by the Australian Pipeline Industry Association (APIA).

References

1. H.George and E.Rodabaugh, 1959. Tests of pups support 'bridging effect'. Pipe Line Industry, October, pp 40-45.
2. X.Zhu and B.Leis, 2005. Plastic collapse assessment method for unequal wall transition joints in transmission pipelines. J. Pressure Vessel Technology, November, 127, pp449-456.

PPIM

Pipeline Pigging and Integrity Management

23rd YEAR

Houston, February 14-17, 2011

Courses

Conference

Exhibition

Houston, Texas, USA

Now entering it 23rd year, the PPIM Conference is recognized as the foremost international forum for sharing and learning about best practices in lifetime maintenance and condition-monitoring technology for natural gas, crude oil and product pipelines.

Plan to be there: www.clarion.org
or call us at +1 713 521 5929

The international gathering of the global pigging industry!

Conference Organizers

CLARION TECHNICAL CONFERENCES

TIRATSOO TECHNICAL

Augmenting ILI tools to assess external coatings

by Dr J Bruce Nestleroth[1]* and Jason K Van Velsor[2]

1 Energy Systems, Battelle Memorial Institute, Columbus, OH, USA
2 FBS, Inc., State College, PA, USA

Introduction

THE COATINGS USED TO protect oil and natural gas pipelines can degrade over time, enabling corrosion and stress-corrosion cracks to initiate and grow. Pipeline companies use in-line inspection (ILI) tools to detect these anomalies, and repair methods to mitigate the result of a failed coating. This project developed inspection sensors that could prevent these anomalies from occurring in the first place by monitoring the integrity of the external protective coating of the pipeline. This coating assessment, which could be performed during a typical ILI, could help pipeline owners assess the general health of the coating protecting their pipeline system. A goal of the design was to keep these sensors simple so that an implementation would not add substantial cost or complexity to a typical magnetic-flux leakage (MFL) or caliper survey.

In this development, a sensor system was designed to generate the proper wave type and modes to assess coating conditions. Non-contact electromagnetic acoustic transducers (EMATs) were designed to send guided waves around the circumference of the pipe. With the use of guided-ultrasonic waves, as opposed to bulk-wave ultrasound, very few ultrasonic sensors were required for implementation. For pipes less than 20in diameter, only two are required: one for sending the wave, and a second for receiving. For larger-diameter pipes, four EMATs were used for 100% circumferential coverage, two EMATs reserved for the excitation of ultrasonic energy and two for receiving the signal. This number of EMATs is an entire order of magnitude less than the number of bulk-wave ultrasonic transducers that would be required to obtain only partial circumferential coverage.

The coating-assessment capability was experimentally demonstrated using a prototype EMAT ILI tool, and all three detection features were shown to perform well in an ILI environment. These demonstrations were carried out in pull rigs at Battelle's Pipeline Simulation Facility and at BJ Inspection Services. Improvement to the prototype were made between each test, the most significant of which was the design and construction of a novel set of thick-trace transmitting and receiving printed-circuit board (PCB) EMAT coils. These coils were designed very specifically to be capable of handling the high current densities created by the 1200-V amplifier. Implementation variables, such as moisture and soil loading, were shown to have a minimal influence on the results.

Coating assessment using ultrasonic waves is not entirely new. Ultrasonic pigs designed to detect stress-corrosion cracks are often influenced by coating condition, and most ultrasonic-based stress-corrosion cracking (SCC) tools are typically good coating-detection tools, and are sometimes marketed for this application. However, the implementation is typically complex, with the number of sensors and wave properties chosen to detect and size small cracks. In contrast, this development was focused on developing a coating-assessment tool, with modelling and experiments to establish an optimal configuration for coating assessment, and the result of this approach was a fundamental improvement over existing methods.

This paper was presented at the 22nd Pipeline Pigging and Integrity Management conference held in Houston in February, 2010, and organized by Clarion Technical Conferences and Tiratsoo Technical (a division of Great Southern Press).

*Author's contact details:
tel: +1 614 424 3181
email: nestlero@battelle.org

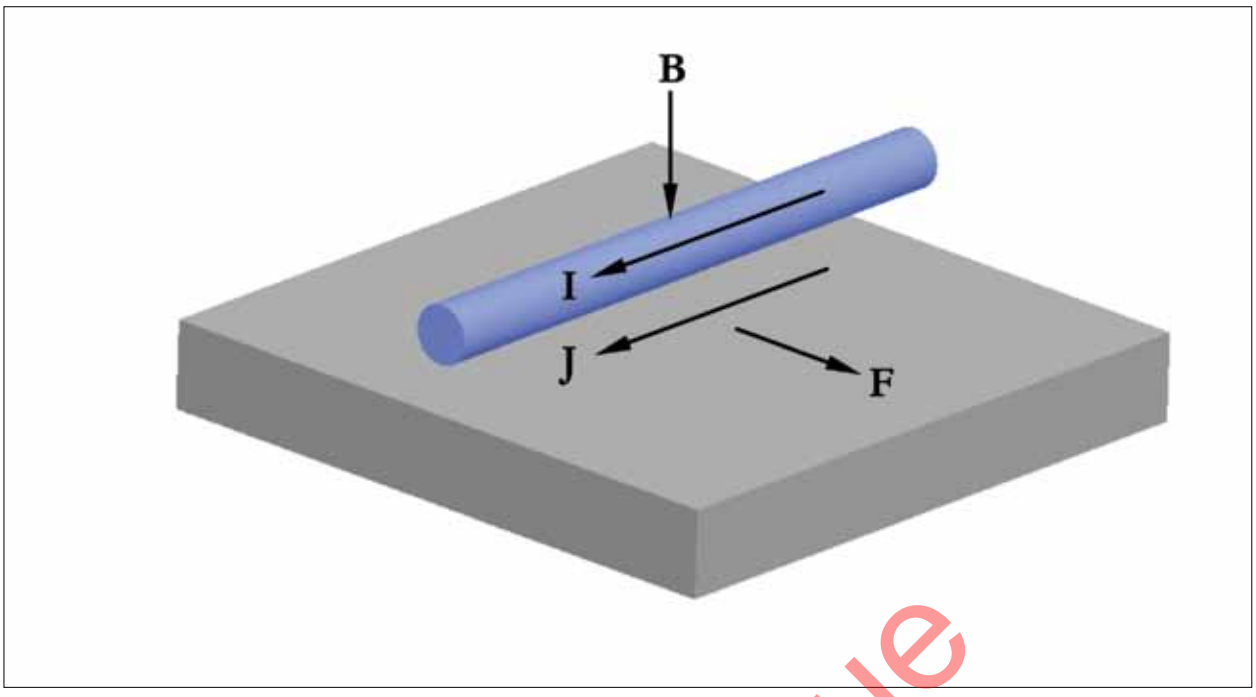

Fig. 1. Lorentz EMAT transducer principle.

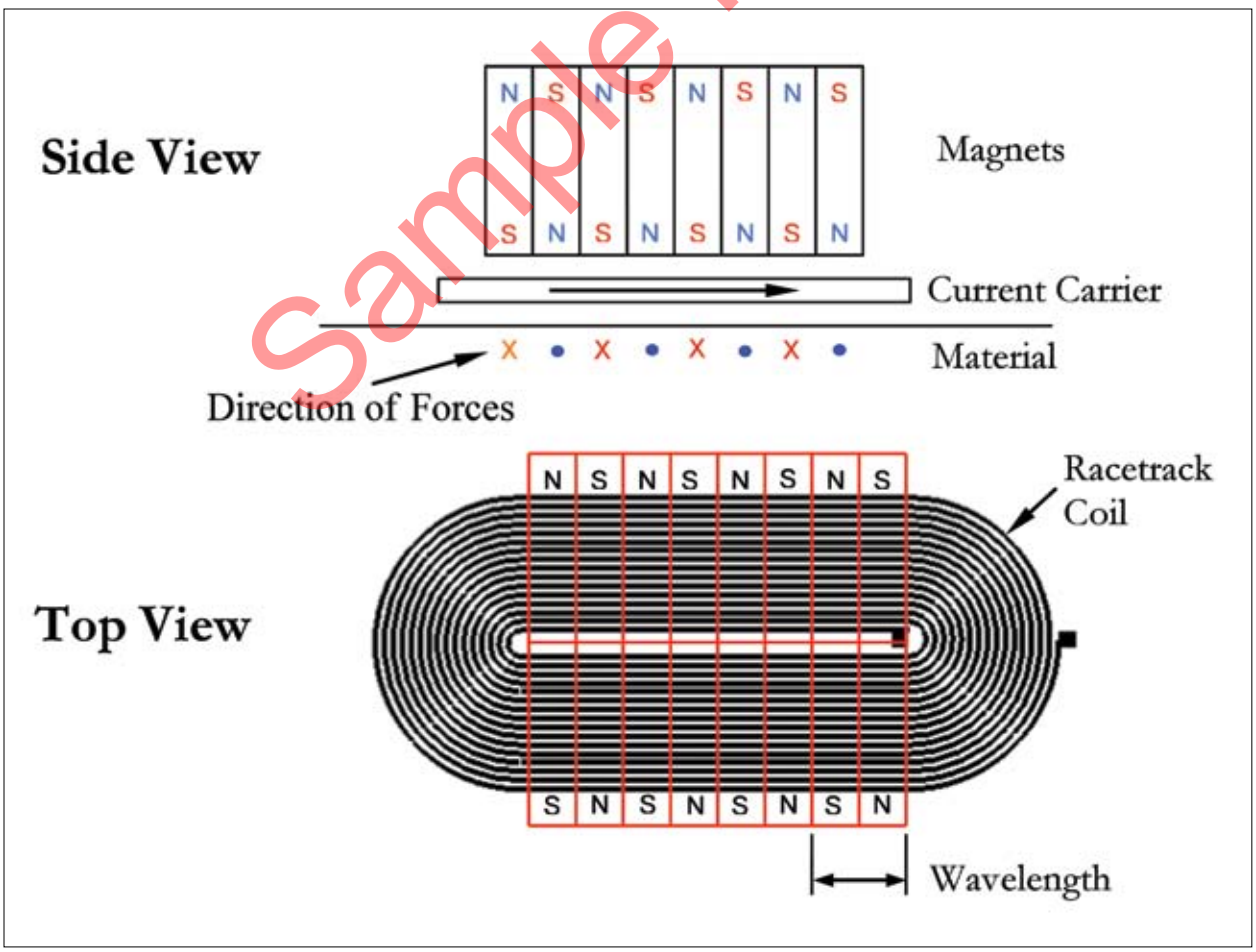

Fig. 2. SH-wave EMAT transducer.

A common approach for assessing coating condition is to assess the amplitude of the received signal; low amplitude means that the coating is good, because the ultrasonic energy went into the coating and was absorbed; while high signal amplitude means that coating was not intact. While this works reasonably well, the pitfall in this approach rests with the fact that the amplitude is affected by many inspection variables including surface roughness, pig speed, and debris. By taking a more fundamental approach to the design in this development, new features for assessing coatings were established, a unique one of which was the arrival time of the ultrasonic wave. For the wave type and frequency selected, the wave velocity is different for bare and coated pipe. Therefore, a disbonded or missing coating can be detected by monitoring the arrival time of the ultrasonic wave, a feature that is amplitude independent. Another feature for assessing coatings, the absorption of selective frequencies, was also demonstrated.

Along with the benefit of knowing a coating's condition, this technology could help justify longer re-inspection intervals for corrosion surveys. For lines with a few manageable corrosion anomalies, as demonstrated by an MFL survey, verifying that the protective coating is intact would help justify that the threat is properly addressed; an additional benefit would be improved assessment of the SCC threat. One method to assess whether SCC is present on a pipeline is to conduct bell-hole excavations, which are sometimes focused by soil modelling to establish that a susceptible environment is present. The coating-assessment results available from this new technology could be used to focus digs at locations with coating faults, and fewer excavations could therefore be performed to establish the viability of the threat.

The project team was comprised members from the US Department of Transportation (DOT), the Pipeline Research Council International (PRCI), BJ Inspection Services, Battelle, and FBS Inc.

Implementation

For a practical ILI implementation, the sensors should not require any type of coupling liquid and should be capable of efficiently generating shear-horizontal (SH) waves in the pipe wall. EMATs were determined to be the most-appropriate sensor type, as they generate and receive ultrasound by coupling magnetic fields to the flow of current within a specimen. EMATs can be non-contact, operate at elevated temperatures, work on rough or oxidized surfaces, and operate at high speeds. Depending on the configuration of the magnetic field and eddy currents, Lamb- and SH-guided waves can be both generated and received.

Fig.3. (a - left) Dual-layer EMAT racetrack coil; (b - right) neodymium rare-earth magnet array.

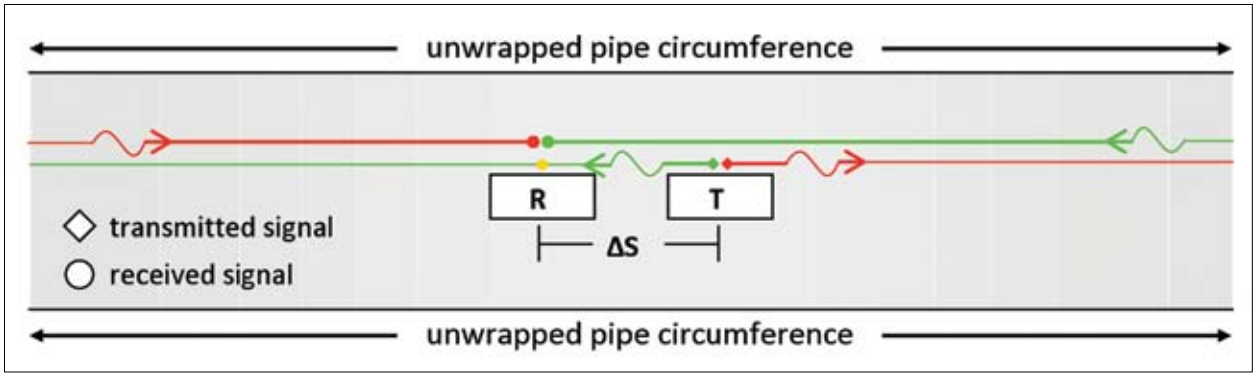

Fig.4. Sensor configuration which allows for the normalization of the received circumferential pulses. The received reference pulse (orange dot) is used to normalize the first complete traverse of the pipe circumference (green dot). Note that the 'red' pulse has not completely traversed the pipe circumference.

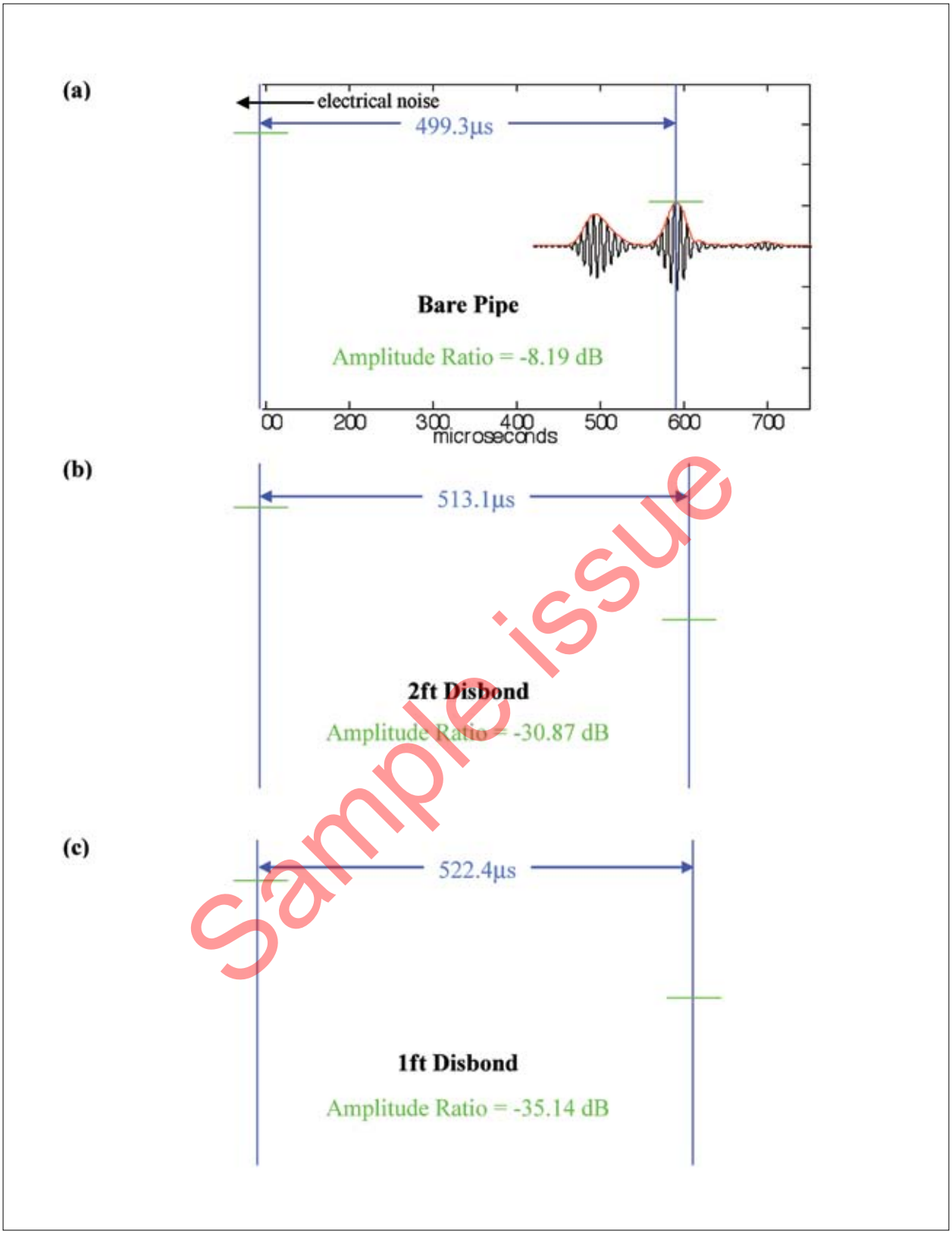

Fig.5. Ultrasonic waveforms obtained from a 20-in diameter schedule 10 pipe with a coal-tar enamel coating with a (a) bare pipe, (b) 2-ft disbonded pipe, (c) 1-ft disbonded pipe.

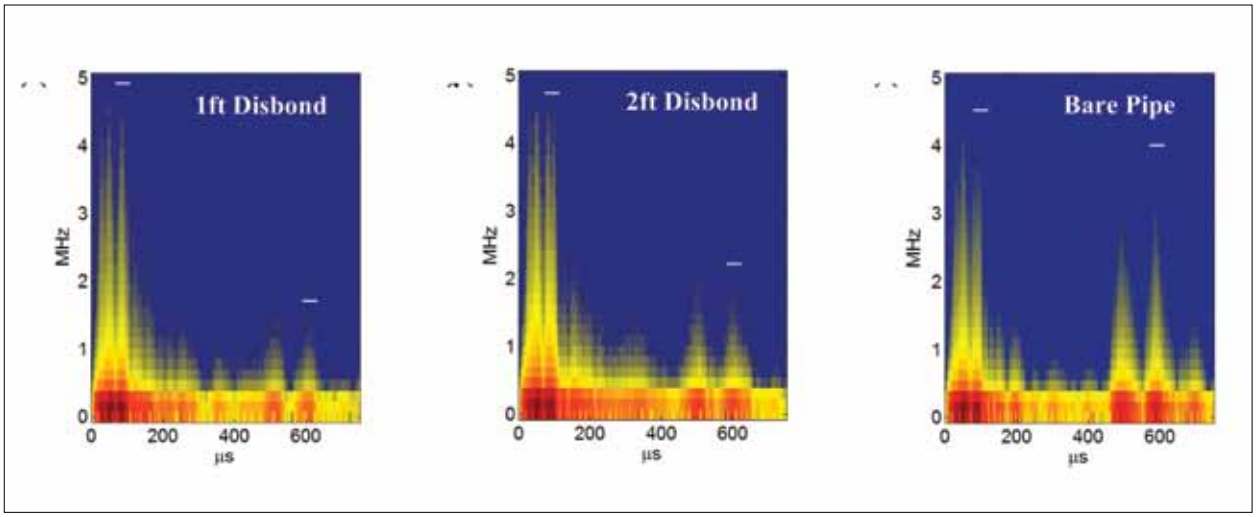

Figure 6. STFTs of RF-waveforms for a (a) 1ft disbond, (b) 2ft disbond, and for a (c) bare pipe. Results obtained using a 64-point Hanning window with 32-point overlap.

The EMATs used in this project are Lorentz-force EMATs, the concept of which is illustrated in Fig.1. The first component in the Lorentz-force transduction mechanism is an eddy current (J) which is induced by passing a current (I) through a wire or trace in close proximity to the specimen. The part to be inspected must be conductive for this to occur. In addition to the eddy current, a static magnetic field (B) must be present; when the current is pulsed in the presence of the magnetic field, a force (F) is induced in the specimen. The direction of the force can be determined by the right-hand rule, and its magnitude and direction are given by Equn 1, where F is the force per unit volume, J is the induced dynamic current density, and B is the static magnetic induction.

$$F = J \times B \quad (1)$$

Figure 2 shows the typical configuration of an SH wave EMAT; the wavelength of the induced wave can be changed by altering the thickness of the magnets. In both the Lamb-wave and SH-wave EMATs, changing the wavelength of the sensor allows the designer to sweep-through the dispersion curve space. A given wavelength activates a line on the dispersion curve that originates at the origin, with a given slope, and the slope of the line can be altered by changing the spacing. A specific mode can then be activated by exciting the transducer at a set frequency.

Table 1 summarizes the desired wavelengths and corresponding magnet sizes for the 130-kHz SH wave that was proposed for detection of disbonded coal-tar enamels. The actual dimensions of the obtained magnets are 12.6mm, resulting in a frequency of 128kHz. Photographs of the core components of the EMAT components are shown in Fig.3: Fig.3a shows the dual-layer EMAT racetrack coil that was designed specifically for the disbonded-coating detection task, while Fig.3(b) shows an array of 80 N-50 grade neodymium rare-earth magnets stacked in ten columns of eight. The individual magnet dimensions are 0.5in×1in × 0.125in, resulting in a total array height of 1in and a sensor wavelength of 25.7mm.

A sensor configuration was adopted that allowed for the normalization of all received pulses to an initial reference pulse, and an illustration of the sensor configuration is seen in Fig.4. In the configuration, the transmitter (T) and receiver (R) are separated by an arc length (ΔS). The reference pulse is the pulse that travels directly from the transmitter to the receiver, and its point of reception is indicated by the orange dot in the figure. The reference pulse can be used to normalize subsequently received signals in the amplitude, time, and frequency domains. Note that in Fig.4, the 'green' signal is the first signal to completely traverse the circumference of the pipe, whereas the 'red' signal never traverses the area in between the transmitter and receiver prior to first reception. For this reason, the received 'green' pulse is the one used to extract information regarding coating integrity.

Figure 5 shows the results from a disbonded-coating detection study that was completed using the initial prototype sensor with the sensor configuration. A 20-in diameter pipe with a coal-tar enamel coating was used for the study, and disbonds were created by removing the coating in fixed-size areas. In the figure, the first pulse to complete one traverse of the pipe circumference is compared to the reference pulse (see the crosshairs). It is seen that a bare pipe (a), a 2-ft disbond (b), and a 1-ft disbond (c), are easily distinguishable. The first pulse seen in all three waveforms is noise from the EMATs and electronics. From this figure it is obvious that the disbonded area's size affects both the received signal amplitude and time-of-flight, as predicted by the theoretical and numerical modelling. There is more than a 20-µs difference between the bare pipe case and the 1-ft disbonded case, and nearly a 10-µs difference between the 1-ft and 2-ft disbonded cases. Accounting for the noise level of the system and experimental error, time-of-flight differences in excess of 2µs can be reliably measured.

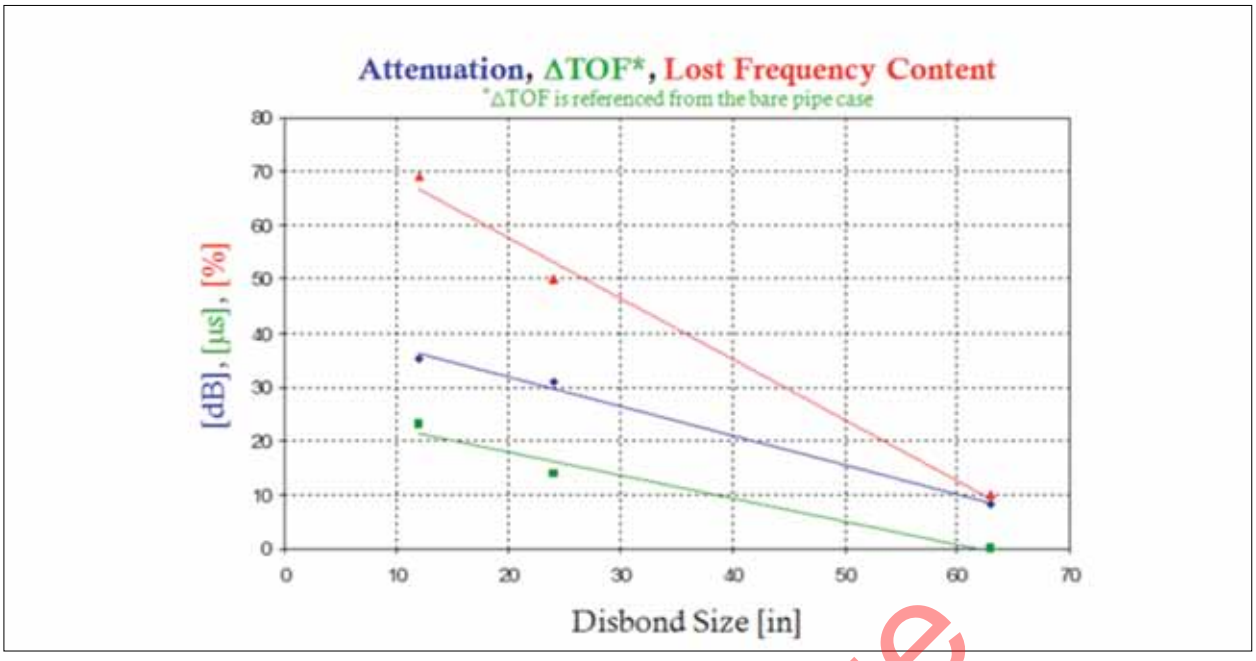

Fig.7. A plot showing the time-, frequency-, and amplitude-disbondment-detection features for three different disbondment sizes in a coal-tar enamel coated pipe.

Fig.8. Scanned images of mylar film (left), thick-trace PCB (centre), and thin-trace PCB (right) coils.

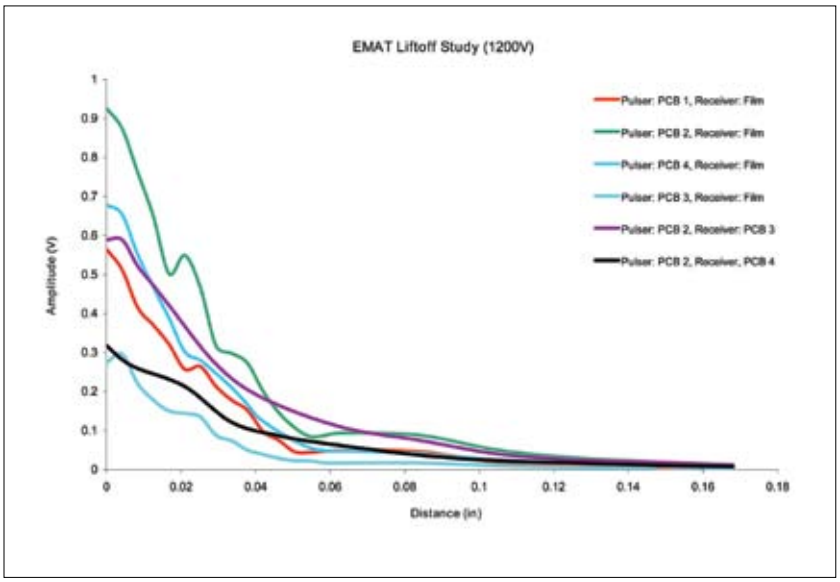

Figure 9. Plot showing the received signal amplitude vs. sensor liftoff for the best pulser/receiver combinations.

Fig. 10. Photograph showing four pipes used for pull testing at the PSF.

The tendency of attenuation to increase with frequency can be used as a disbonded coating detection feature: the absence of coating will result in a frequency spectrum with higher-frequency content. As the amount of well-bonded coating increases, the higher-frequency content will be filtered-out by absorption. An experimental demonstration of this concept is shown in Fig.6, in which the short-time Fourier transforms (STFTs) of the data sets displayed in Fig.5 are plotted. The difference between the two white lines, marking the maximum frequency content of the reference pulse and the first counter clockwise (CCW) traverse, represents the amount of lost frequency content after one complete circumferential traverse of the pipe. Figure 7, in which all three features are plotted on the same scale, summarizes the results of the disbonded coating proof-of-concept study. The sensitivity of the technique can be increased by combining the three features into a single feature, such as through addition or multiplication. It should be noted that no discernable reflections were obtained from the boundaries of the disbonded-coating regions: it is highly likely that they are very small in amplitude and are absorbed or otherwise lost in the noise floor.

Sensor design

One of the most critical design factors in EMAT heads was optimizing penetration power and maximizing sensor liftoff. Table 2 includes the specification of all the coils tested. The coils consisted of one printed on mylar film ('film') and four on printed-circuit boards ('PCB').

Figure 8 shows scanned images of the three primary coil geometries. From Table 2, it can be seen that the primary differences between the PCB coils were the width of the traces, and whether or not the PCB had traces printed on both sides (two-layer). The most significant difference between the film coils and the PCB coils was the trace thickness, with the PCB traces nearly ten times thicker than that of the film coils. By changing the cross-sectional area of the traces, the electrical impedance and current density of the coil are changed.

Sensor lift-off experiments were performed with an arbitrary wave generator connected to a 1200-V amplifier, and it was found that the load applied by the amplifier was very near the operational limit of the film coils. For this reason, the film coils were not used for pulsing in the 1200-V tests. An impedance-matching network was used between the amplifier and pulsing coil in all tests.

Figure 9 shows the results of the sensor lift-off study for several of the best combinations of pulsing and receiving coils. It is seen that the single-layer thick-trace PCB coil, used as a pulser, and the film coil, used as a receiver, are the optimal sensor pair. For nearly all lift-off distances, this combination of coils provided the highest amplitude. Also of interest is the PCB2/PCB3 coil combination: this is because these two coils are very similar in construction and are, in general, slightly more robust than the film coils. From an implementation standpoint, a more-robust coil may be preferred over several decibels of signal amplitude.

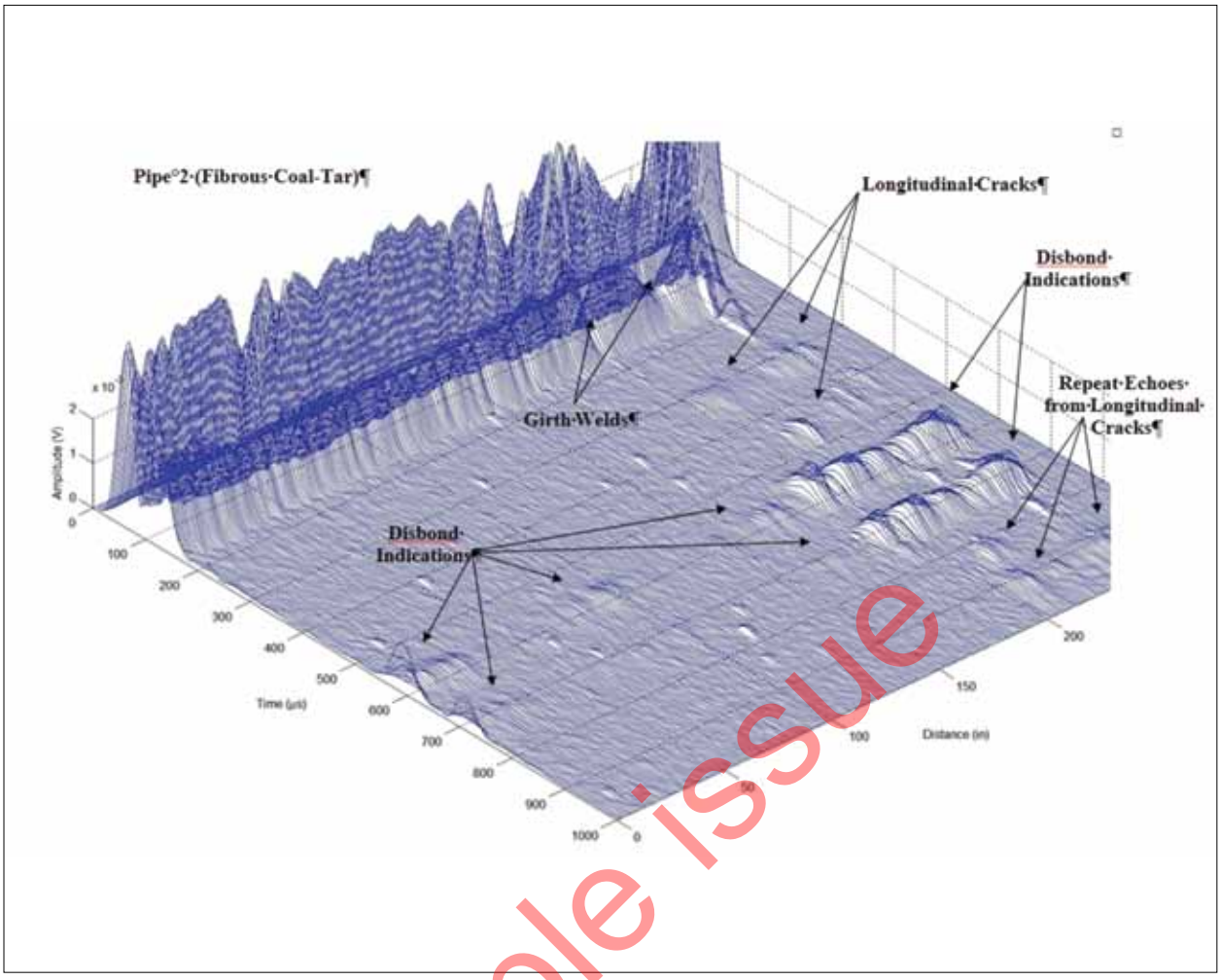

Fig. 11. Three-dimensional plot of analytic envelopes of ultrasonic data acquired on Pipe 2, which is coated with a fibrous coal-tar coating.

A comparison of the PCB2/film coil combination for both the 1000-V and 1200-V systems was also performed, switching between systems resulted in a gain of nearly 8dB in the signal amplitude. This proves that moving from a 1000-V system to a 1200-V system is incredibly advantageous despite the need for a more 'heavy-duty' pulsing coil.

Pull test results

Four pipes were prepared for pull testing at Battelle's pipeline simulation facility. All pipes were 24-in diameter, and three had coatings applied to their outer surfaces. A photograph of the four samples can be seen in Fig.10, and a description of each pipe is given in Table 3. The internal surfaces of all four pipes had been sandblasted and coated with primer to prevent corrosion.

Runs were completed on each of the four pipes. To generate the plots, the analytic envelope of the RF signal was plotted versus the axial location at which it was obtained, and the result serves as a quick reference for the evaluation of each data set. Figures 11, 12, and 13 show the results obtained from Pipe 2, coated with a fibrous coal-tar wrap. Several coating-disbonded regions, as well as other features, can be seen in Fig.11, and Table 4 summarizes these results along with the results for several other axial locations containing disbondments. It is seen from these figures that, though the amplitude is low, the traverse that travels around the full circumference is successfully able to detect all 24-in disbondments using the amplitude-, time-, and frequency-based detection features. An 8-in disbonded area between locations 53in and 92in was not detected because the signal was completely attenuated by the coating that was well bonded. This is an indication that an actual implementation will need at least two sets of sensor heads.

Conclusion and future direction

The primary goal of this research was the development of a more-reliable and robust guided-wave disbonded-coating detection technique than that which is currently available.

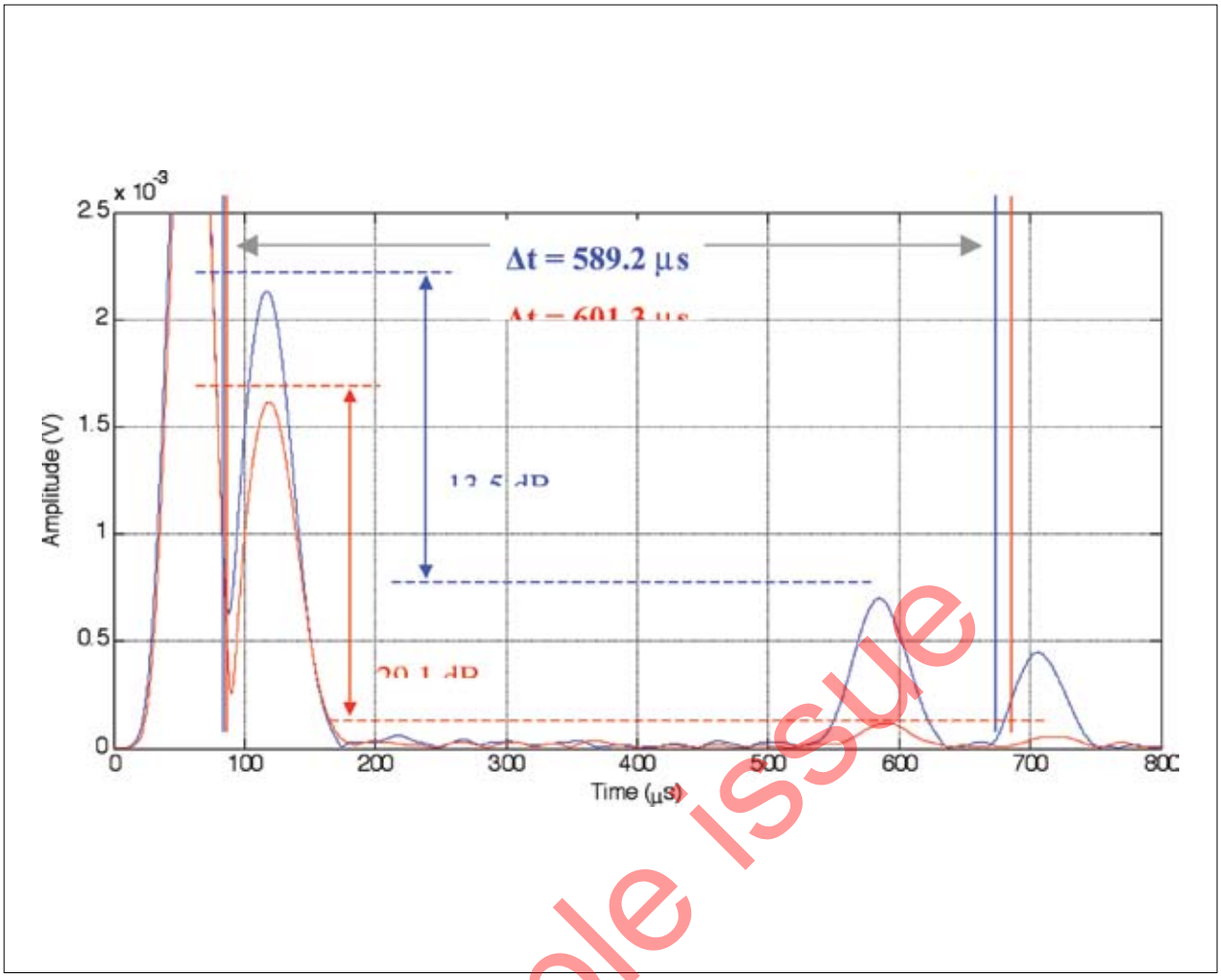

Fig. 12. Two-dimensional plot of analytic envelopes of ultrasonic data acquired on Pipe 2 at 1 in into the pull length (blue) where the pipe was bare, and at 27in into the pull length (red) where an approximate 50% circumference disbondment existed.

Some of the key contributions of this work are outlined as follows:

- Identification and experimental verification of time, frequency-, and amplitude-based disbondment detection features. Prior to this work, the time- and frequency-based features were never used for disbondment detection.

- Development of a sensor arrangement such that all amplitudes can be normalized to some reference pulse, allowing for a more-reliable use of amplitude-based features. This effectively accounts for such things as variation in sensor lift-off.

- Design and construction of a novel set of thick-trace transmitting and receiving PCB EMAT coils. These coils were designed very specially to be capable of handling the high current densities created by the 1200-V amplifier.

- Experimental demonstration of the disbonded-coating detection capability using an actual prototype EMAT ILI tool. All three detection features were shown to perform well in an ILI environment.

- Experimental demonstration of the disbonded-coating detection capability for thin (< 1mm) coatings using a time-based detection. Future work will be needed to optimize this technique through the selection of the ideal wave mode and frequency.

Though a significant contribution toward the reliable detection of disbonded coatings using guided waves has been made, there is always more work to be completed. Because the guided-wave ILI market is still in its early developmental stages, and there are not many competing technologies available, there is significant opportunity to make lasting contributions in this area. It is strongly believed that some of the results of this work will eventually be incorporated into an industrial inspection technology.

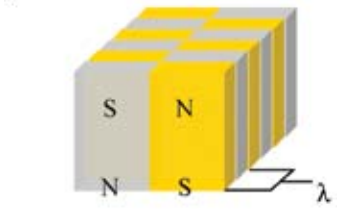

where $\lambda = \frac{c_P}{f}$

EMAT	f (MHz)	c_P (mm/μs)	λ (mm)	Magnet Size (mm)
1	0.13	3.23	24.85	12.42

*Table 1. Illustration and table showing desired wavelength and magnet dimensions to generate a 130-kHz SH0 mode in a bare pipe.**Table 1. Illustration and table showing desired wavelength and magnet dimensions to generate a 130-kHz SH0 mode in a bare pipe.*

	No. of Layers	Turns / in.	Trace Width	Trace Thickness	Substrate Thickness
Film	2	~25	~0.03 in	~0.00125 in	~0.005 in
PCB 1	1	~50	~0.01 in	~0.01 in	~0.03 in
PCB 2	1	~21	~0.035 in	~0.01 in	~0.03 in
PCB 3	2	~50	~0.01 in	~0.01 in	~0.015 in
PCB 4	2	~21	~0.035 in	~0.01 in	~0.015 in

Table 2. Specifications of the different EMAT coils used in performance evaluation

Name	Description	Size (OD, Length, Thickness)
Pipe 1	Bare pipe, free of defects.	24"× 270.75" × 0.300"
Pipe 2	Coated in a fibrous coal-tar wrap with several large disbonded sections, dents, and several simulated and real cracks.	24" × 274" × 0.270"
Pipe 3	Tape wrap with one disbonded section, no defects noted.	24" × 254" × 0.310"
Pipe 4	Fusion-Bonded Epoxy coating with several disbonded regions and simulated defects.	24" × 203.5" × 0.362"

Table 3. Description of pipe samples used for pull tests at the PSF.

Pull Location	Disbond Size	Amplitude Loss	Time-of-Flight	Lost Frequency Content
1 in.	100%	-13.5 dB	589.2 μs	19%
27 in.	~ 30%	-29.1 dB	601.3 μs	46%
99 in.	~ 30%	- 25.9 dB	596.5 μs	41%
170 in.	~ 30%	-27.8 dB	599.9 μs	46%

Table 4. Summary of disbondment-detection results for several pull locations for Pipe 2 (fibrous coal-tar coating).

Multi-diameter, bi-directional pigging for pipeline precommissioning

by Magne Andreas Vik[1], Alf Åge Kristiansen[1], Simon Sykes[2], Steve Hutcheson[3], and Dr Aidan O'Donoghue[4*]

1 StatoilHydro, Haugesund, Norway
2 FTL Seals Technology, Southampton, UK
3 Pipeline Pigging Technology, Chesterfield, UK
4 Pipeline Research Ltd, Glasgow, UK

THIS PAPER EXAMINES the issues associated with multi-diameter, bi-directional pigging specifically for pipeline precommissioning. The technique can be used to flood and subsequently dewater a pipeline without the need for temporary subsea traps. An example is the Alve pipeline in Norway: this 16-km flowline from the Norne platform to the Alve manifold includes 10-in and 12-in pipe sections. The line was flooded from Norne using the pig with oxygen-scavenged seawater and then dewatered using nitrogen and produced gas from the well. The pigs needed to have a high sealing efficiency since very low velocities were used to flood the line, and in order to avoid hydrates on dewatering. Multi-diameter wheel pigs were employed with non-buckling disc-type seals. This paper describes the design of the pigs and the seals to achieve the required functionality. The test facility and testing performed to verify the pig performance is also illustrated. Finally, an overview of the offshore pigging operation is provided.

IN ORDER TO FLOOD and subsequently dewater the Alve flowline, a number of high-seal, multi-diameter and bi-directional pigs were required. The pipeline contains several internal diameters from 10in to 12in: since no pigging from the Alve manifold was possible (no launcher), all operations needed to be performed from Norne FPSO.

Four pigs spaced with MEG were launched from Norne with oxygen-scavenged water, propelled through the pipeline, and then stopped in position just upstream of the manifold. Before start-up of the pipeline and introduction of hydrocarbon gas, the pigs were required to be reversed with nitrogen and travel back through the pipeline, with no gas by-pass, and be received back on Norne. The pressure was first raised to 50bar with nitrogen for pigging and to 80bar with hydrocarbons from topside to give back-pressure for start-up. A field schematic is shown in Fig.1.

Performing this operation without any pigs was initially considered but, after a number of studies, the hydrate risk was considered to be too great. The need for high-seal pigs was identified. A number of additional scenarios for the operation were considered which impacted on pig design:

- Reversal of the pigs from the manifold, just before the inline isolation valve: the risk is that the pig will travel too far and will not be reversible from the 5-in inlet line (pumping into the middle of the pig rather than upstream);

- Reversal of the pigs from before the expansion spool: the implication is that the pig does not need to operate negotiate any bends in the large diameter line.

This paper was presented at the 22nd Pipeline Pigging and Integrity Management conference held in Houston in February, 2010, and organized by Clarion Technical Conferences and Tiratsoo Technical (a division of Great Southern Press).

*Author's contact details:
tel: +44 (0)141 637 8093
email: aidan@pipeline-research.com

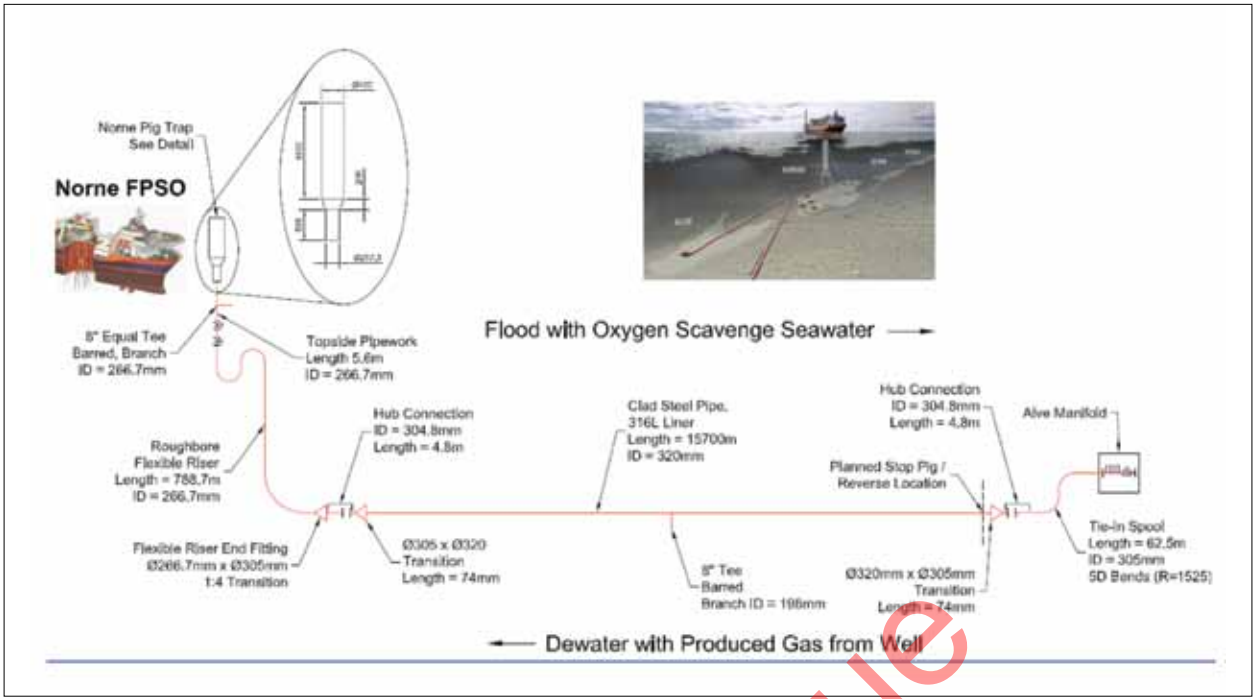

Fig. 1. Field schematic.

Fig. 2. Initial pig concept.

The base case was the second option, but consideration needed to be given to the first option as a potential contingency. Testing would be performed to establish pig efficiency in all components, including the 12-in bends, and to establish if the first pig in the train was reversible from the valve location. If this proved to be difficult then additional procedural steps would be taken to avoid the train reaching the manifold.

A pig train consisting of four pigs with MEG separation was required. The main pipeline features were as follows:

- 10-in vertical launcher
- 10-in topside piping at launcher, with 257mm internal diameter 10-in topside and riser, with 267mm internal diameter
- 12-in pipeline, with 320mm internal diameter, 15.7km in length 12-in tie-in spools and manifold, with 305mm internal diameter with 5-D bends.

The following functional requirements were discussed and agreed with the project:

- the pigs must be fully bi-directional with high sealing ability in both directions; low flow rates were expected, in the region of 300-400l min, resulting in a pig velocity of 0.03 to 0.08m/s. The pig must be able to operate at such low velocities; good seal efficiency and pig support/centralisation were required to ensure safe negotiation with minimum by-pass through all components along the system. The risk of gas by-passing on return to Norne could result in hydrate formation; the ratio between pig-flip differential pressure (pressure to flip the seals forward and cause them to fail) and running differential pressure to be at least 5:1;
- the drive differential pressure in all pipeline components was requested to be less than 7bar;
- the pigs to be fitted with isotope holder for tracking purposes;
- pig handling to be considered for vertical launch and receipt.

The final aspect that needed to be considered as a contingency was the possibility of the pig travelling too far into the manifold, and the provision of a method of reversal from this location. This may mean that the pig straddled the manifold inlet used for driving the pig back to Norne.

Pig selection

The timescales for the project were relatively short, with initial feasibility in August, 2008, and required pig delivery in December, 2008. This only allowed three months to establish concepts, perform detailed engineering, test to verify the pig functionality, and provide four units for the operation.

An initial feasibility study was undertaken with the aim of selecting a single pig type for development for this application. Several different types of multi-diameter pig were considered for this:

- traditional multi-diameter pig with slotted guides and seals of various diameters;
- wheel pig or Varipig from FTL Seals Technology;
- *Paddle Pig* from Pipeline Engineering;
- Other approaches from other suppliers.

It must be stressed that whilst multi-diameter pigs have been successfully developed and used on many occasions, the project team was not aware of any projects which have developed a multi-diameter bi-directional pig and with such a high emphasis on sealing (i.e. no visible leakage in any pipeline component). The pros and cons of each technology were discussed, and it was concluded that – given the timescales – the wheel pig would be the best choice with the highest possibility of success. On the other hand, it is noted that with more time, the other methods could also be made to work.

No other pig was considered for this project from this point onwards. It is considered the best approach to concentrate all efforts on one chosen approach with a high probability of success rather than to dilute the effort by having several different competing pig prototypes which have lower chance of success and take up excessive testing time. Running a competition for pig development is considered inefficient in general, and it is better to establish the base case in a feasibility phase and then develop this further.

Pig design

The pig's mechanical design was performed by FTL Seals Technology with input and guidance from Pipeline Pigging Technology and Pipeline Research Ltd. In addition, StatoilHydro ensured that the requirements from the project were communicated as soon as possible. This is especially important in a tight timescale project and where small changes to the operation philosophy can have significant implications on the pig design. This was managed effectively throughout the development.

The outline concept pig design is shown in Fig.2. The pig consists of two wheel modules with interlinked suspension arms. The pig travels on the centreline of the pipe and so it is easier to specify seals that will provide a good sealing action. The spring force in the suspension units is greater than the weight of the pig and so if the pig drops below the

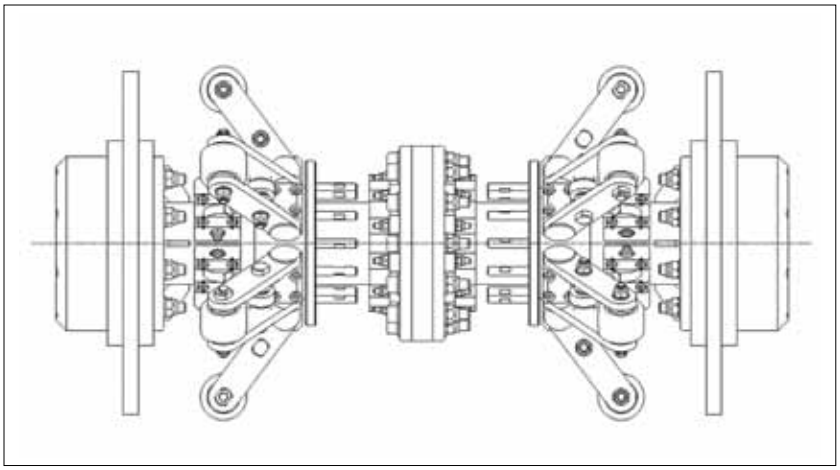

Fig.3. Initial axi-symmetrical design.

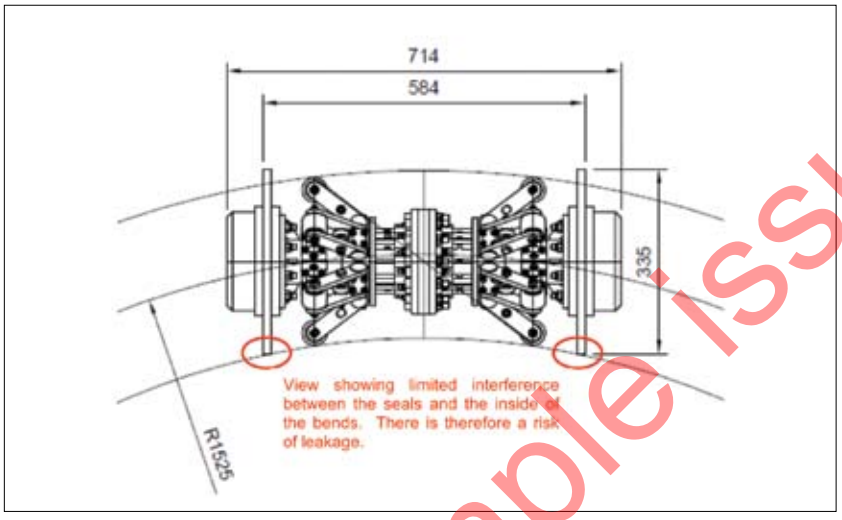

Fig.4. Possible leakage at the bends.

centreline, then the restoring force is greater. The geometry of the wheel arms provides a mechanical advantage which results in a flat force / deflection curve, i.e. the force require to deflect the arms does not increase significantly in smaller diameters. As a result, the load on the wheels and bearings remains at an acceptable and determinable level.

For the Alve pig, these wheel units are facing each other with seals at either end. The pig is axi-symmetrical in design, which guarantees full bi-directionality (Fig.3). It was decided early on that a single, non-buckling seal would be used for both line sizes (10in and 12in). This is discussed in detail below. Detailed engineering of this concept followed, and it became clear that in the event that the pig needed to travel through the 5-D bends at the manifold, then there could be leakage past the pig, and this is demonstrated in Fig.4. This is not acceptable for these functional requirements, and to solve the problem an additional seal was introduced in the centre of the pig – see Fig.5. Other issues associated with the layout of the pig include:

- Installation of an isotope holder: this is shown in Fig.6.
- Provision of a lifting bar at the rear of the pig (see Fig.6): the pig is loaded and removed from Norne as it is not handled subsea.
- The front pig in the train was also a special, known as the Type 1 pig, as this pig could potentially end up in the manifold and come to rest near the ball valve at the end of the manifold straddling the inlet line. This then required a slightly longer bumper nose to ensure that a seal was always downstream of the manifold off-take. The reversal of the pig from the manifold in the event of over-travel was subject to additional testing and modification as described later in this paper.

Seal design

The design of the seals for this pig was critical. One advantage of the wheel pig is that it supports the pig on the pipe centreline with the result that the seal diameter can be set just greater than the internal diameter of the largest bore and still provide a very good wiping action. Coupled with

Test	Description	Parameters
1	**Full facility test** Test pig through the full test facility.	Measure pig velocity over length of test rig, running pressure and flow rate. Observe leakage past the pig.
2	**Reverse in full facility** Reverse the pig through the full test facility.	Measure pig velocity over length of test rig, running pressure, reverse pressure and flow rate. Observe leakage past the pig.
3	**Initial spools test** Launch 257.3mm – 266.7mm – 305mm straight and flip.	Measure running pressure, flow rate and flip pressure. Observe leakage past the pig.
4	**Observation of rear of pig** Stop pig in 266.7-mm section and observe rear of pig for buckling.	Stop the pig in the 266.7-mm section, remove trap, observe rear of pig, try to induce buckle in seal.
5	**Main pipeline test** Launch 257.3mm – 266.7mm – 305mm – 320mm straight and flip. Repeat at very low and low flows.	Measure running pressure, flow rate and flip pressure. Observe leakage past the pig.
6	**Pig to 305-mm section** Launch 257.3mm – 266.7mm – 305mm – 320mm – 305mm straight.	Measure running pressure and flow rate. Observe leakage past the pig.
7	**Bend test** Launch 257.3mm – 266.7mm – 305mm – 320mm – 305mm – 305mm bend	Measure minimum flow in bend before pig stall. Observe leakage past the pig.
8	**Bend test flip** Launch 257.3mm – 266.7mm – 305mm – 320mm – 305mm – 305mm bend and flip.	Measure running pressure, flow rate and flip pressure. Observe leakage past the pig.
9	**Manifold test 1** Launch 257.3mm – 266.7mm – 305mm – 320mm – 305mm – 305mm bend into manifold and dead head.	Measure running pressure, manifold pressure and flow rate. Record position of pig in Manifold. Reverse pig slowly from Manifold. Observe leakage past pig on reverse.
10	**Manifold test 2** Launch 257.3mm – 266.7mm – 305mm – 320mm – 305mm – 305mm bend into manifold and stop at second off-take.	Measure running pressure and flow rate. Record position of pig in Manifold. Reverse pig slowly from Manifold. Observe leakage past pig on reverse.
11	**Permanent set test 1** Leave pig in 257.3mm spool over night (12 hours minimum). Launch into 266.7mm – 305mm – 320mm straight.	Measure running pressure and flow rate. Observe leakage past the pig.
12	**Permanent set test 2** Leave pig in 266.7mm spool over night (12 hours minimum). Launch into 266.7mm – 305mm – 320mm straight.	Measure running pressure and flow rate. Observe leakage past the pig.

Table 1.

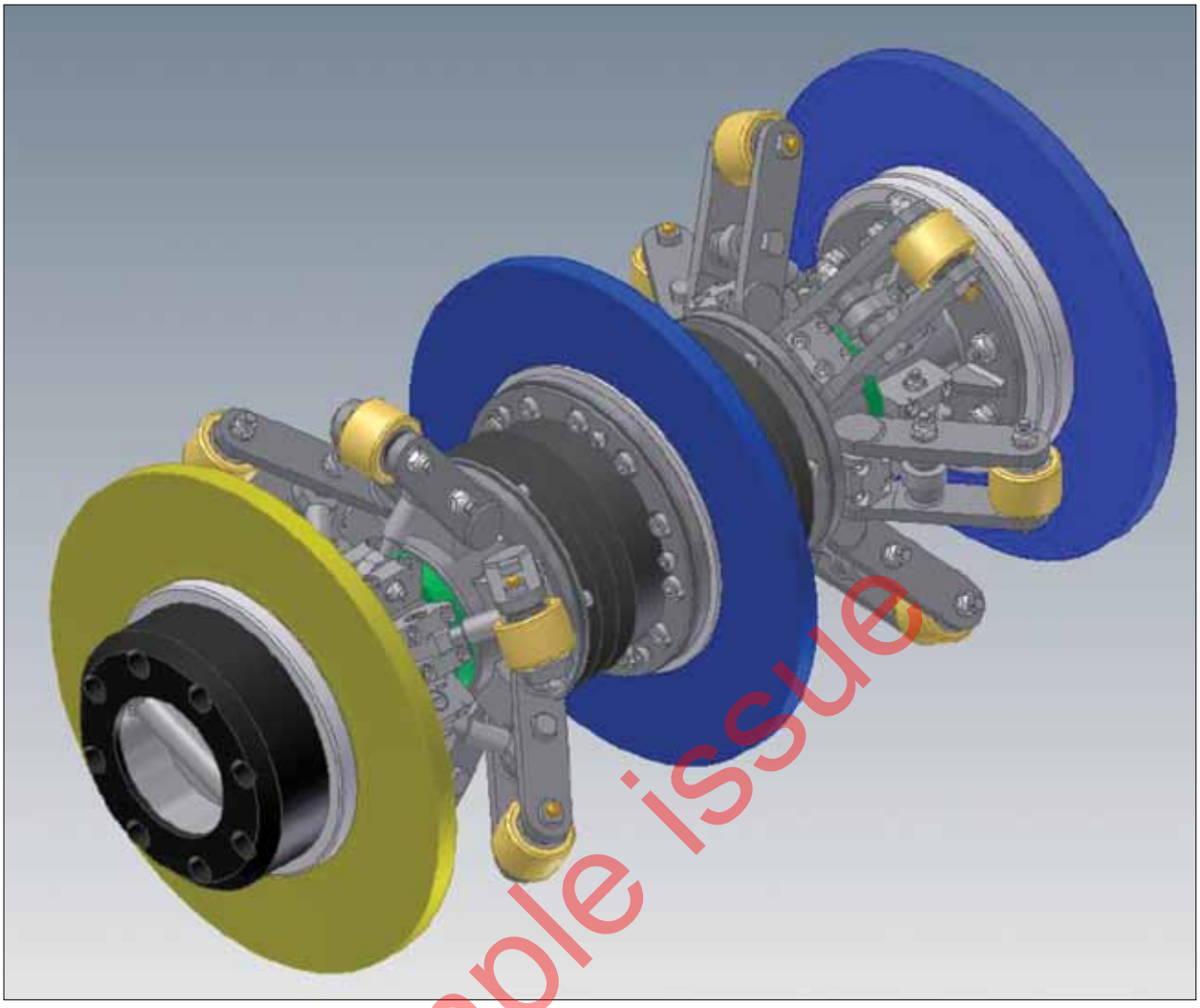

Fig.5. Additional seal at centre of the pig to avoid leakage at bends.

this, there has been good success lately with using a single disc seal to span several line sizes without buckling in the smallest size. This is known as the 'single seal' concept.

The idea is that a single oversized disc has the ability to work and provide a good seal at a range of smaller and smaller diameters before it finally buckles. The following scale of 'buckling' has been investigated previously:

- no buckle
- buckles when forced, but recovers
- buckles when forced, but does not recover
- buckles even when not forced to do so.

To be safe, for this application, it is important that the seal does not buckle or, if forced to do so, it returns to a full seal. Over the years much experience has been gained on buckling and non-buckling of seals for dual- and multi-diameter pigging. Figure 7 shows some examples of where the large-diameter seals are intentionally buckled into the small-diameter line in order to allow smaller-diameter seals to take over. This has been used to good effect in large-diameter change projects where 'buckle inducers' are used to force the seal to fold into the small-diameter line.

The opposite is now proposed: using seals that do not buckle when they enter the small-diameter line. The advantage of using such a seal in this development is that a single seal can be used at the front and the rear of the pig. As a result there is no interference between small-diameter and large-diameter seals over a limited pig length.

A routine has been developed to establish if a seal will buckle or not, and four criteria must be met to ensure that the seal will behave in the required way for different line sizes. This is based on a buckle model of the seal coupled with test and field data, and the output is shown in Fig.8 for this development. Based on this analysis, a number of seal sizes were selected, both for the main seals either end of the pig and also for the central seal positioned to avoid leakage in the 12-in bends. A base-case pig was also established for initial use in testing. The aim is always to arrive on the test site with a base-case design and a number

Parameter	Drive DP (bar)	Flip DP (bar)
257-mm / launch into 10-in	**2.2**	–
267-mm ID straight pipe	**1.8**	7.2
323-mm ID straight pipe	**0.1**	1.2
305-mm ID straight pipe	**0.3**	1.6
305-mm ID bend	**0.5**	1.3

Table 2.

of spares and alternatives to help solve any problems with the pig during verification testing.

Testing

The tests were performed at K-Lab at Kårstø in Norway, the test facility at which is shown in Fig.9. The facility consisted of the main components in the Alve flowline:

- launcher (horizontal, for test purposes)
- tight 10-in section at the beginning, 257mm ID
- 10-in topside and riser piping, 267mm ID
- 10-in x 12-in transition
- 12-in spool with 12-in equal tee, 307mm ID
- 12-in pipeline, 323mm ID (320-mm ID test pipe was unavailable)
- 12-in manifold pipe, 305mm ID
- 12-in bend, 305mm ID.

A manifold spool with two 6-in tees was also included for reversal tests.

All the testing was performed open-ended to allow the pigging to be observed. This is for assurance that the pig was not visibly leaking, and that the seal was adequate and fit-for-purpose. Testing in a closed loop hides many problems, and only demonstrates that the pig travels from launch to receipt; it does not establish that it travels reliably from launch to receipt. Proper risk-assessment procedures and testing with water drive ensured that the HSE risk was minimal.

Launcher inlet pressure, flow-rate, and pig location using magnetic signallers were recorded during all tests. The set of tests shown in Table 1 was performed: each test was repeated if required, and to verify pig parameters. Any problems with the pig during the test were discussed in the light of data output and drawings of the pigs in the various features of concern. A clear line of communication was

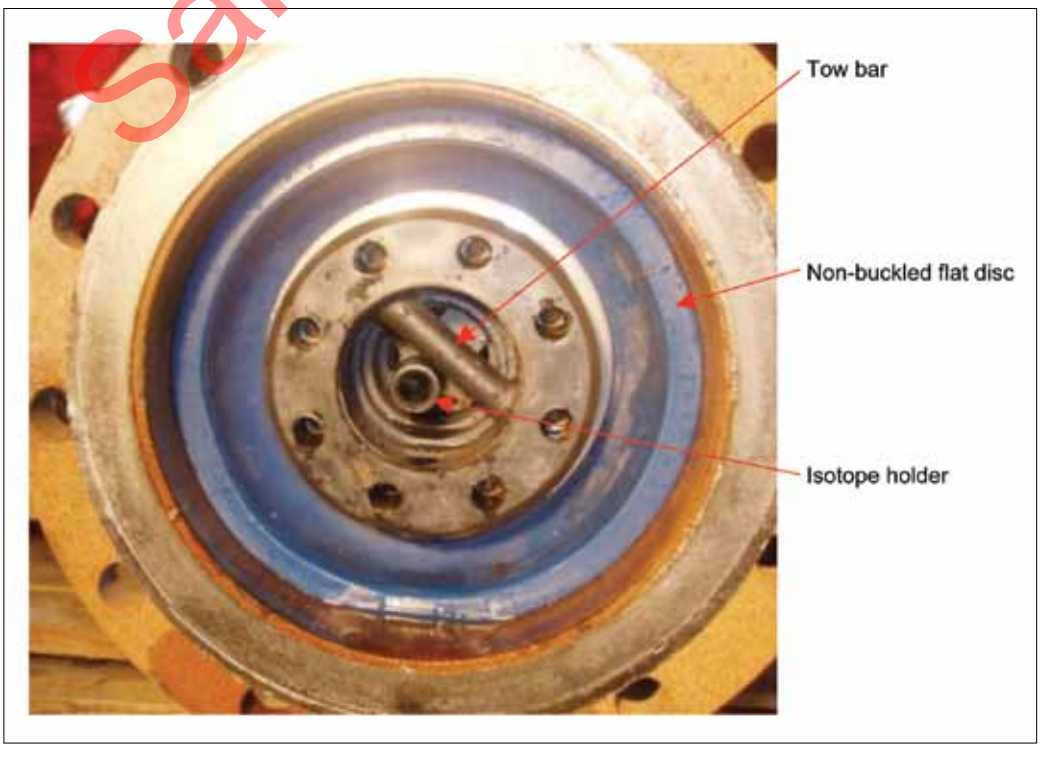

Fig.6. Isotope holder and towing arm.

Fig.7. Examples of buckled seals.

Three buckle inducers used on SVAN project. Buckle inducers are used to force the seals to buckle.

Four buckle inducers used on Norne Heidrun project.

View on large diameter seal which has been allowed to buckle naturally into the small diameter line. This leads to high friction and damage to the seal.

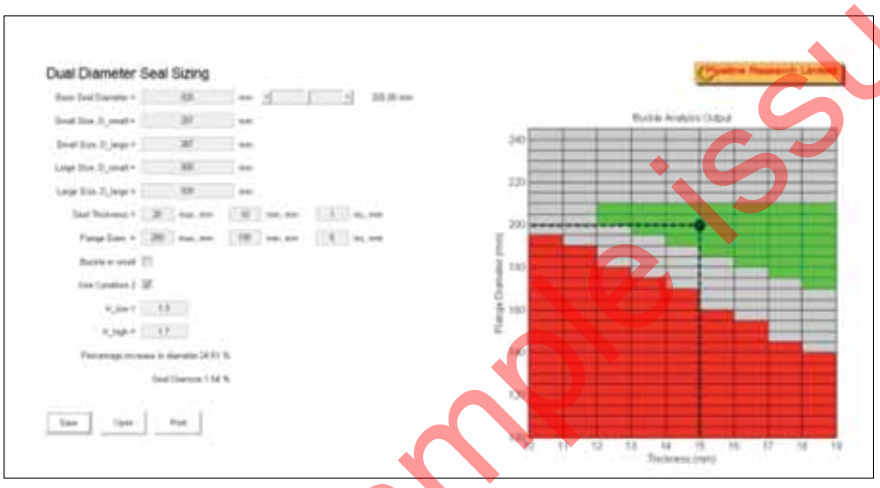

Fig.8. Seal sizing for buckling or non-buckling.

The green area shows the area where non-buckling can be expected for given seal thickness and flange diameter. The grey area is where buckling may occur. The red area is where buckling will most definitely occur.

Fig.9. Test facility.

Fig.10. Buckle test.

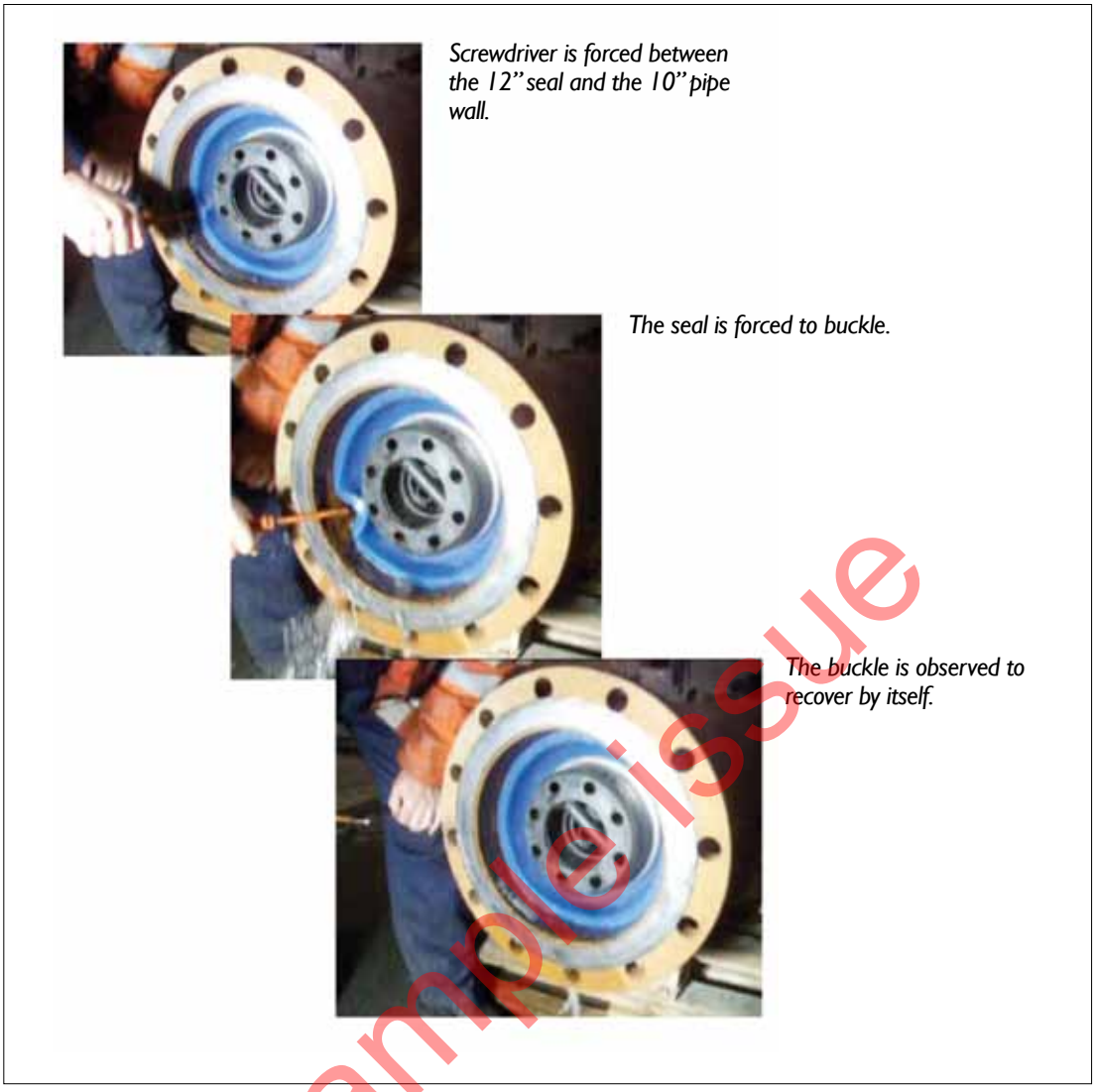

maintained with the project to understand any changes in the precommissioning / RFO procedure which might impact on the pig design.

The buckle test on the seal is highlighted in Fig.10 with stills taken from a video of the test. A screwdriver was forced into the seal and levered to make the seal buckle, and water was shown coming from the buckle. On withdrawal of the screwdriver, the seal recovered unaided. Figure 11 shows a close-up of the 325-mm diameter disc seal in the small, 257-mm, diameter line. The disc seal takes on a cup-like shape.

Table 2 summarizes the basic pig parameters. No visible leakage was observed coming from the seals during the tests, which were performed at very low velocity to replicate the actual scenario offshore – around 0.03m/s. The pig was also fully reversible and the flip capacity of the discs deemed to be adequate to make pigging acceptable and safe.

The final test undertaken was to see if the pig would reverse when positioned against the manifold ball valve, a position which meant that the pig would straddle the inlet as shown in Fig.12. To allow the pig to reverse from this position, by-pass ports were opened in front of this pig which allowed pressure to be transferred from between the pig seals to the ball valve, to allow the pig to move backwards (the net force on the pig pushing it in reverse). The size of the ports was critical as the flow needed to generate the necessary reversal pressure must be able to pass through them. It was anticipated that this would prove to be difficult, given the limitations on by-pass size and also on available flow into the off-take.

The problem is outlined in Fig.12: there is a trade-off between the ability to get the flow through the by-pass ports to displace the pig and the ability of the rear seal to hold this pressure without leakage. This has been achieved in other projects, but on those occasions the balance was easier to achieve. Sleeper discs were used to attempt to increase the pressure capacity of the rear seal but this was ineffective. The final position, where some degree of reversal was possible at the ball valve or straddling the off-take, was where the rear two

Flat 325 mm sealing disc outside the pipe.

Same disc in 257 mm pipe takes on a cup shape but does not buckle.

Fig. 11. Flat disc seal in small diameter.

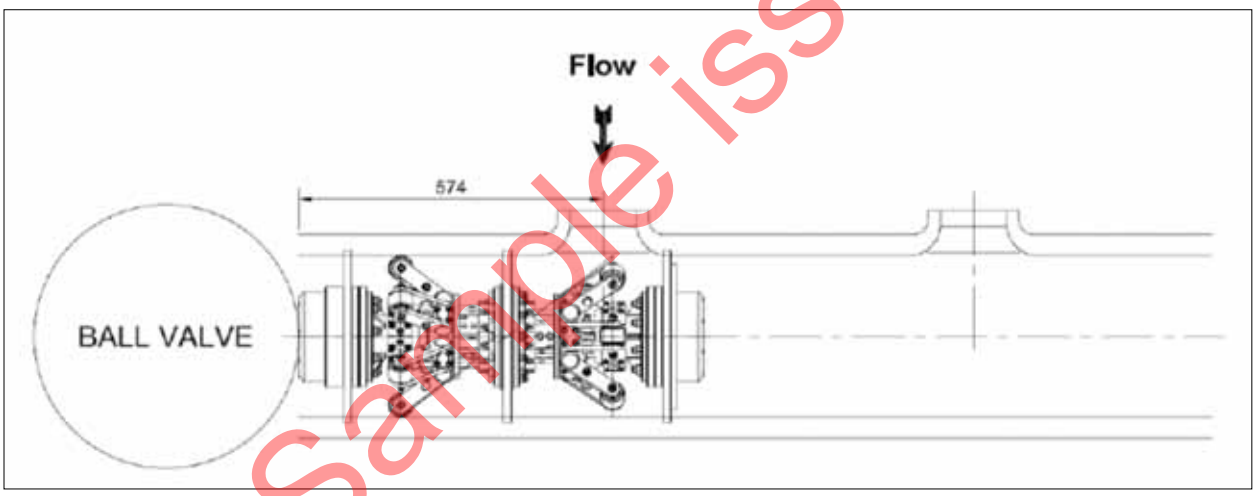

Fig. 12. Reversal position at valve.

seals were upstream of this off-take (Fig.13). This could not be guaranteed, as the front of the pig would have to be extended, resulting in an unwieldy design and problems negotiating the bends. As a result, the emphasis was put back on the operation to avoid the pig reaching this position in the first place, and this was ensured by increasing the tracking effort subsea.

Offshore operation

The operation took place in March, 2009; it was a success, and the pigs performed well and no gas by-pass was observed.

Four pigs were launched from a temporary vertical pig launcher at the topside on Norne. Before the first pig entered the expansion spool at the manifold, the pig train was planned to be stopped. Due to a delay in communication and the short distance from detection to spool, the first pig finally stopped inside the spool, having passed the first 5-D bend.

After all the pigs had been located using isotope tracking, the pig train was reversed and discs flipped with MEG before being returned with nitrogen.

For both outbound flooding with water and return pigging with nitrogen, the pressures experienced were consistent with the pigging trials that had been performed.

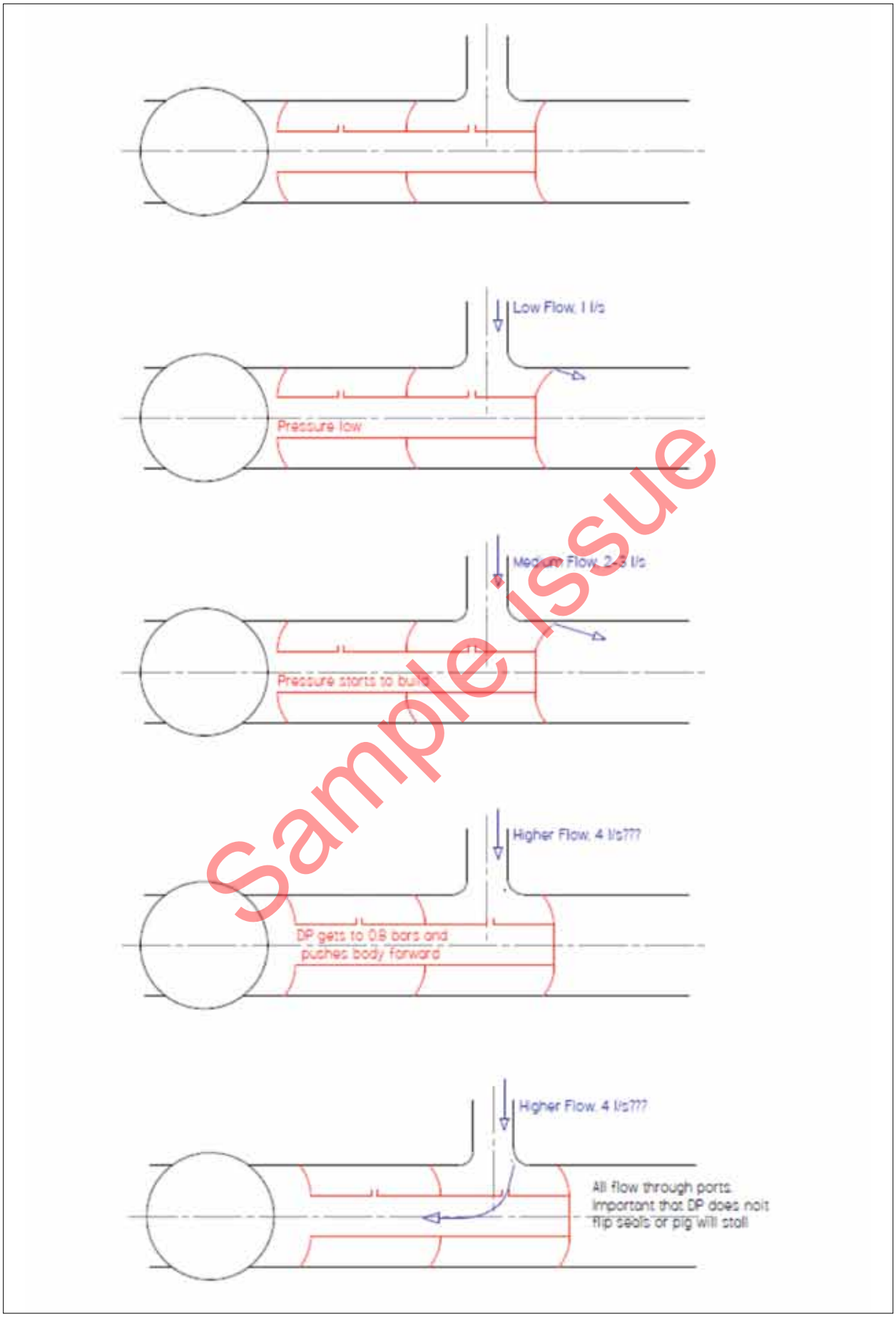

Fig. 13. Reversal at the ball valve – story board.

Conclusion

The multi-diameter bi-directional approach to precommissioning RFO ('ready for operation') is being looked at in more detail, as it potentially rules-out the need for a subsea receiver or launcher and an extra support vessel. The ability to make a single-disc seal work over a wide range of diameters is key to this development, as is the wheel pig to allow the pig to be maintained on the centreline. The Alve pipeline has an approximately 25% increase in diameter. StatoilHydro is now examining a 12-in x 16-in case with a 41% change in diameter, where a similar approach is being adopted with further work on the single seal concept being examined.

Acknowledgement

The authors thank Olaf Erland and Tor Grindheim at K-Lab in Kårstø for their assistance in this development.

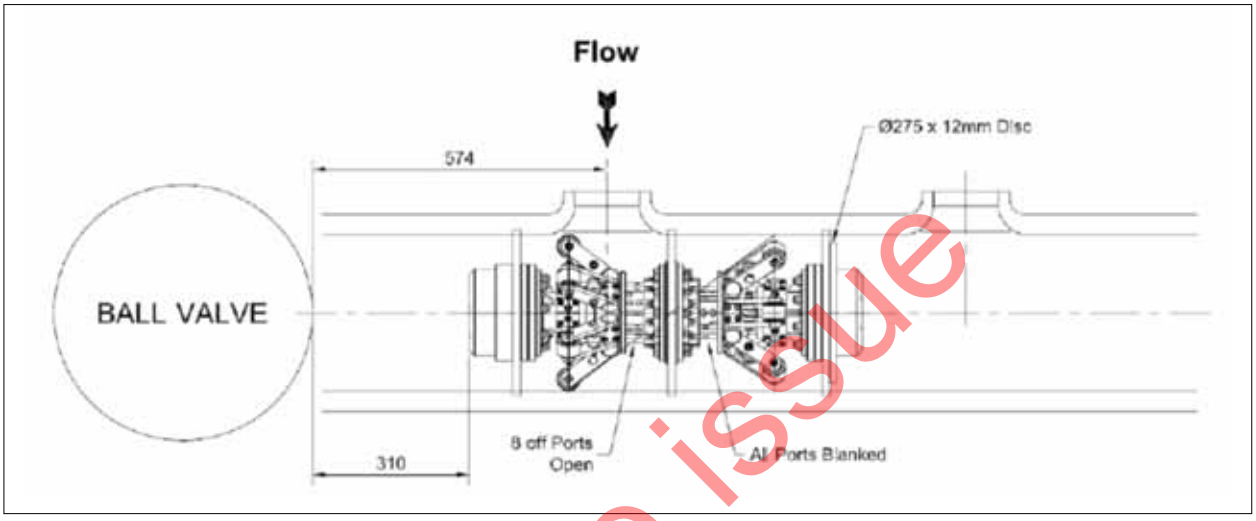

Fig. 14. Reversal position at valve.

Fig. 15. Final pig design.

Continued from page 68.

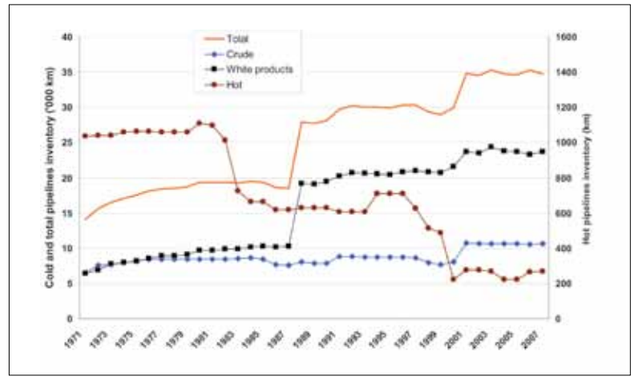

Fig.1. CONCAWE members' oil pipelines and categories (courtesy of CONCAWE).

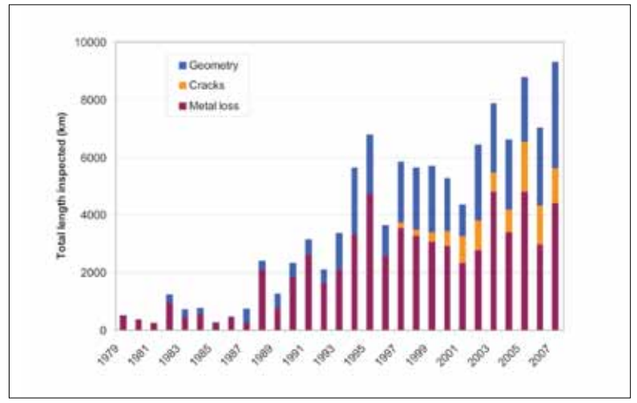

Fig.2. Annual inspections by intelligent pigs 1979-2007 (courtesy of CONCAWE).

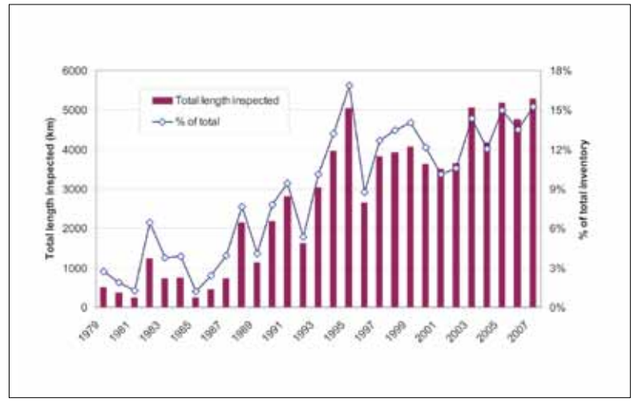

Fig.3. The total proportion of the pipeline network inspected by intelligent pigs 1979-2007 (courtesy of CONCAWE).

	Underground pipe			Above-ground pipe			Pump station pipework		
	No	*%*	*Average spill (m3)*	*No*	*%*	*Average spill (m3)*	*No*	*%*	*Average spill (m3)*
Surveillance by pipeline staff	31	8	234	3	9	53	0	0	0
Routine monitoring by operator	81	22	315	14	41	97	35	61	85
Automatic detection system	37	10	156	2	6	43	9	16	55

Table 2. Spillage discovery statistics, 2007.